

From Vertex Detectors to Inner Trackers with CMOS Pixel Sensors

Alejandro Pérez Pérez
IPHC – CNRS Strasbourg



Outline

- **Introduction to CMOS Pixel Sensors (CPS)**
- **CPS adapted to an inner tracker: ALICE-ITS Upgrade**
- **Next R&D challenges**
- **Summary**

Introduction to CPS

CPS: Development motivation

- **CPS triggered by the need of very granular and low material budget sensors**

- **CPS applications exhibit milder running conditions than at pp/LHC**

- Relaxed readout (r.o.) speed & rad. tolerance

- **Application domain widens continuously (existing/foreseen/potential)**

- **Heavy-ion collisions**

- STAR-PXL, ALICE-ITS, CBM-MVD, NA61...

- **e^+e^- collisions**

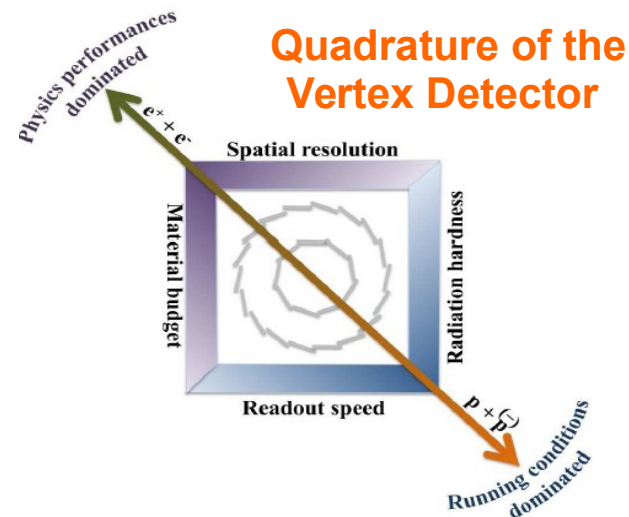
- BES-III, ILC, Belle II (BEAST II)

- **Non-collider experiments**

- FIRST, NA63, Mu2e, PANDA, ...

- **High-precision beam-telescopes** (adapted to medium/low energy e^+ beams)

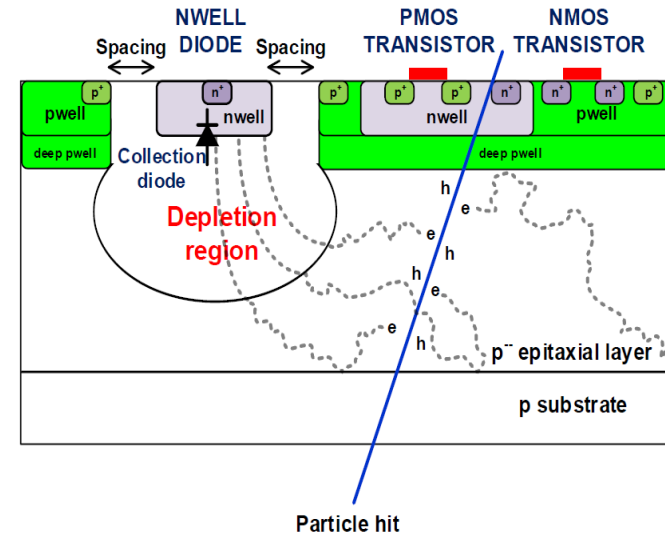
- Few μm resolution @ DUT achievable with EUDET-BT (DESY), BTF-BT (Frascati)



CPS: Main features

The basic working principle

- Secondary charges generated in epi-layer by ionization
 - Signal proportional to epi-thickness
- Charges transport driven by 3 potentials
 - P-well/coll. node/P++ (usually GND/few volts/GND)
- Epi-layer not fully depleted: $d_{\text{dep}} \sim 0.3 \sqrt{\rho_{\text{sub}} \times U_{\text{bias}}}$
⇒ transport is mix of thermal diffusion & drift



Prominent features

- Signal processing integrated on sensor substrate ⇒ downstream electronics & syst. integration
- High granularity ⇒ excellent spatial resolution ($O(\mu\text{m})$)
- Signal generated in thin ($10\text{-}40\mu\text{m}$) epi-layer ⇒ usual thinning up to $50\mu\text{m}$ total thickness
- Standard fabrication process ⇒ low cost & easy prototyping, many vendors, ...

CPS technology potential

- Mainly driven by commercial applications ⇒ Not fully optimized for particle detection
- R&D largely consists in exploiting as much as possible the potential of the accessible industrial processes

CPS @ PICSEL - IPHC: A long term R&D

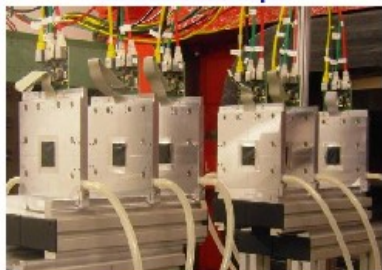
■ Ultimate objective: ILC, with staged performances

↳ CPS applied to other experiments with intermediate requirements

running

EUDET 2006/2010

Beam Telescope



ILC > 2020

International Linear Collider



On-going R&D

HR-CMOS for
X-rays (2018)



EUDET (R&D for ILC, EU project)

STAR (Heavy Ion physics)

CBM (Heavy Ion physics)

ILC (Particle physics)

HadronPhysics2 (generic R&D, EU project)

AIDA (generic R&D, EU project)

FIRST (Hadron therapy)

ALICE/LHC (Heavy Ion physics)

EIC (Hadron physics)

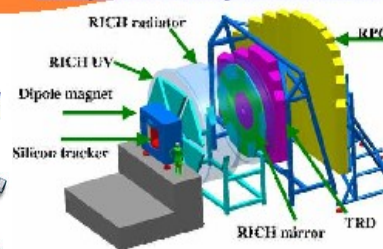
CLIC (Particle physics)

BESIII (Particle physics)

...

CBM > 2018

Compressed Baryonic Matter



On-going R&D

running

STAR 2013

Solenoidal Tracker at RHIC



ALICE 2018

A Large Ion Collider Experiment

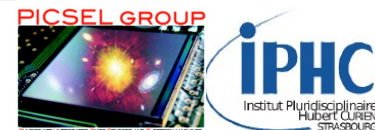


On-going R&D

CPS State-of-the-Art in operation: STAR-PXL sensor

ULTIMATE main characteristics

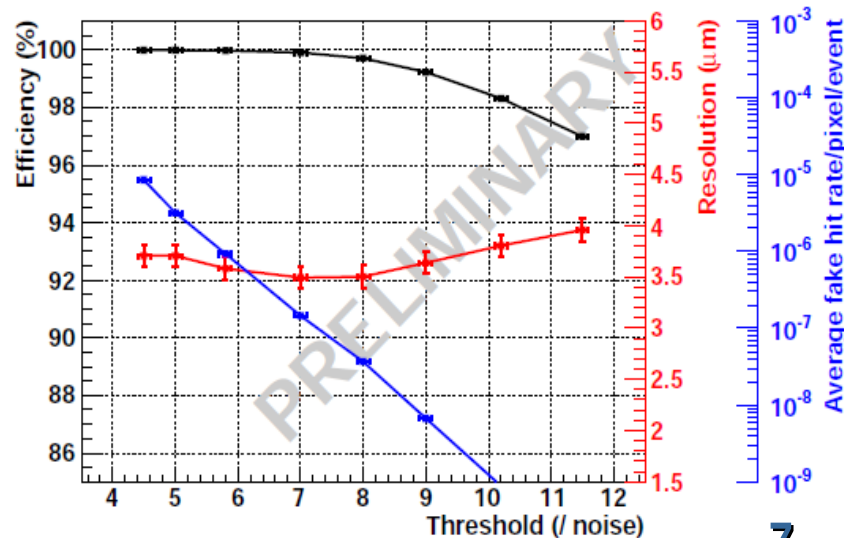
- CMOS sensor (0.35 μm AMS twin-well) high-p epi-layer 15 μm
- Sensor thinned to 50 μm (total thickness $\Rightarrow 0.05\% X_0$)
- || column (rolling shutter) r.o. with in-pixel CDS & amplification
- End-of-column discriminator (1-bit) followed by \emptyset -suppression
- 960 x 928 (columns x rows) pixels of 20.7 μm pitch
 $\Rightarrow 19.9 \times 19.2 \text{ mm}^2$ sensitive area
- $t_{\text{r.o.}} \lesssim 200 \mu\text{s}$ ($\sim 5 \times 10^3$ frames/s) \Rightarrow suited for $> 10^6 \text{ part./cm}^2/\text{s}$
- 2 outputs @ 160 MHz
- Operation @ $T \sim 30^\circ\text{C}$ & $W \lesssim 150 \text{ mW/cm}^2$



ULTIMATE Performances

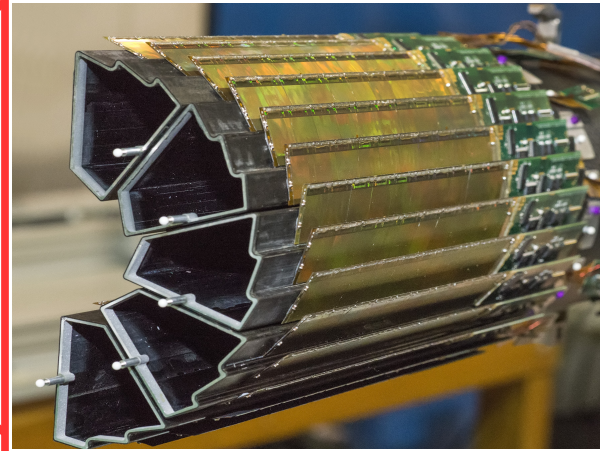
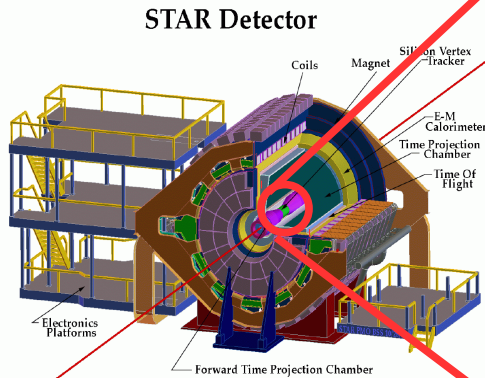
- Noise $\lesssim 15 \text{ e}^- \text{ ENC}$ @ 30-35 $^\circ\text{C}$
- $\varepsilon_{\text{det}} \gtrsim 99.9\%$, $\sigma_{\text{sp}} \gtrsim 3.5 \mu\text{m}$, Fake rate $\lesssim 10^{-5}$
- Rad. hardness validated @ 30 $^\circ\text{C}$
(150 kRad $\oplus 3 \times 10^{12} \text{ n}_{\text{eq}}/\text{cm}^2$)

MIMOSA 28 - epi 15 μm



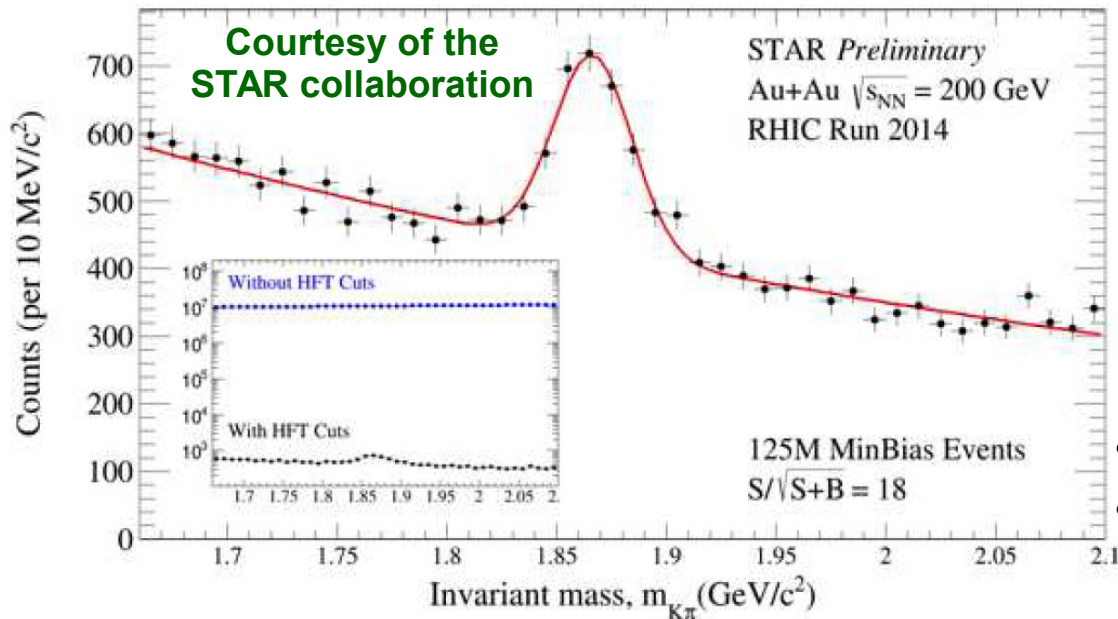
CPS State-of-the-Art in operation: STAR-PXL detector

STAR-PXL @ RHIC: 1st CPS @ a collider experiment !



STAR-PXL HALF-BARREL

- 2 layers @ $r = 2.8, 8$ cm
- 20 ladders (10 sensors) ($0.37\% X_0$)
 $\Rightarrow 180M$ pixels
- Air flow cooling: $T < 35^\circ\text{C}$



Several Physics-runs

- 1st /2nd run in 2014 & 2015
- Preparation for 3rd run (Jan. 2016)
- $\sigma_{ip}(p_T)$ matching requirements
 $\sim 40 \mu\text{m}$ @ 600 MeV/c for π^\pm/K^\pm

Observation of D^0 production

- **STAR:** peak significance = 18
- **ALICE:** peak significance = 5

CPS performances: Spatial Resolution (σ_{sp})

Several parameters govern σ_{sp}

- **Pixel pitch**
- **Epi-layer:** thickness & ρ
- **Sensing node:** geometry & electrical properties
- **Signal-encoding resolution:** Nb of bits
- σ_{sp} function of:
pitch \oplus SNR \oplus charge-sharing \oplus ADCu \oplus ...

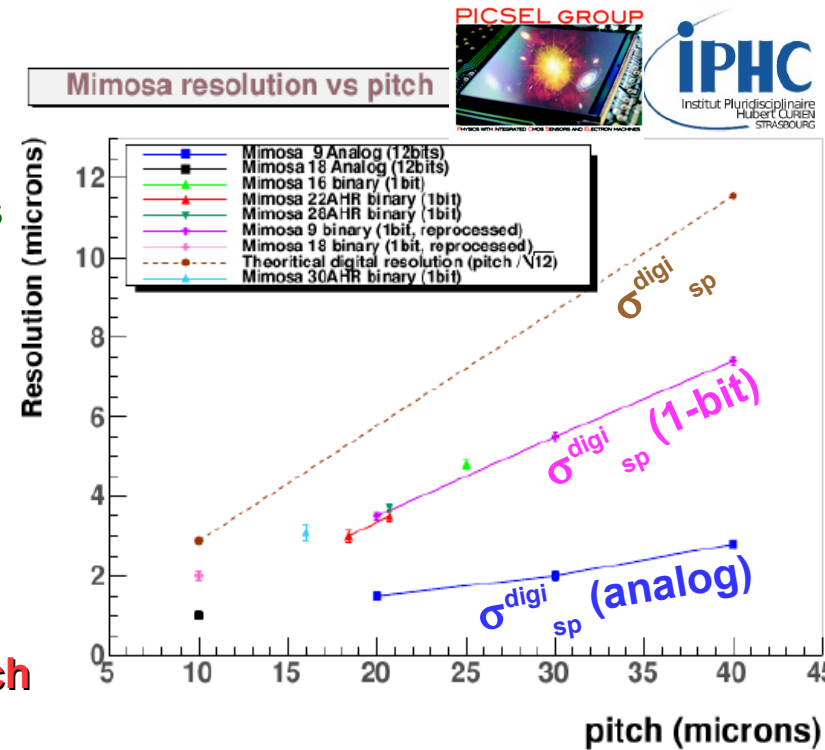
Pixel-pitch impact (analogue output)

- Pitch = 10 (40) $\mu\text{m} \Rightarrow \sigma_{sp} \sim 1 \mu\text{m} (\lesssim 3 \mu\text{m})$
- **Nearly linear improvement in σ_{sp} vs pixel pitch**

Signal-encoding impact (digital output)

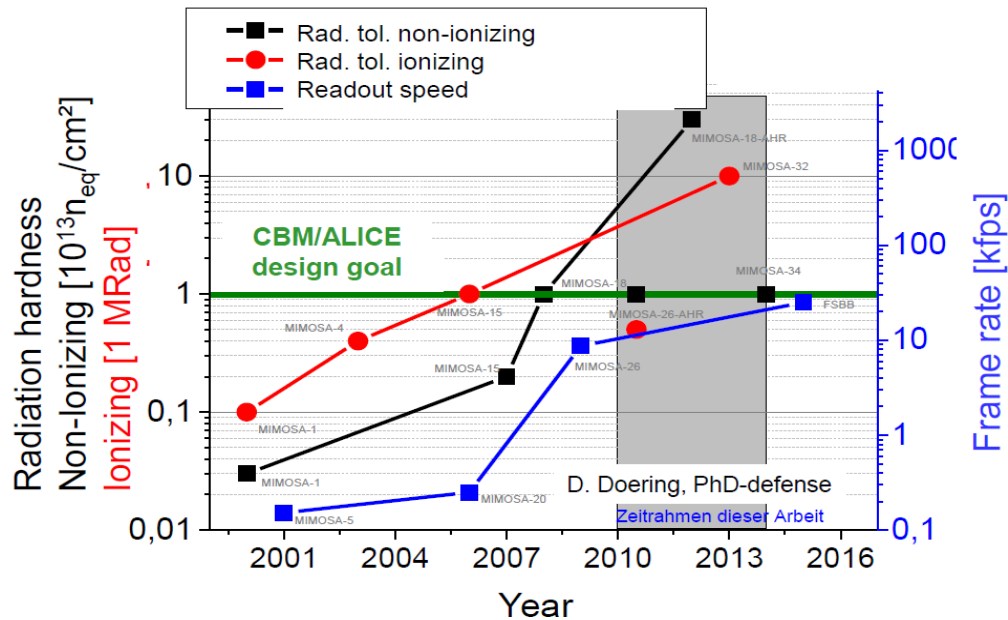
- $\sigma_{sp}^{\text{digi}} = \text{pitch}/(12)^{1/2}$
 \Rightarrow e.g. $\sigma_{sp}^{\text{digi}} \sim 5.7 \mu\text{m}$ for 20 μm pitch

- **Significant improvement in σ_{sp} by increasing signal encoding resolution**



Nb of bits	12	3-4	1
Data	<i>measured</i>	<i>reprocessed</i>	<i>measured</i>
σ_{sp}	$\lesssim 1.5\mu\text{m}$	$\lesssim 2\mu\text{m}$	$\lesssim 3.5\mu\text{m}$

CPS performances: r.o. speed & rad. hardness



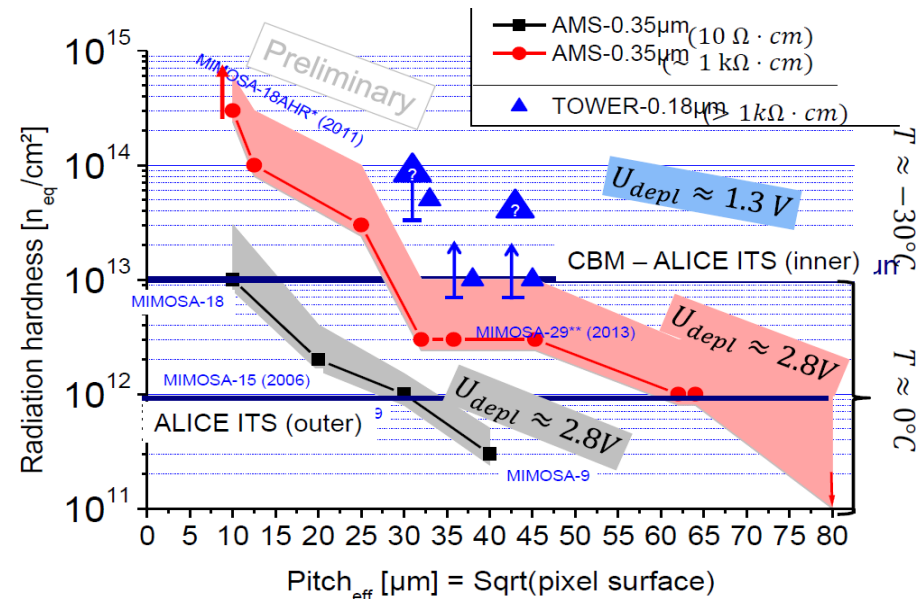
- 15 years of experience of PICSEL group in developing CPS
- Strong collaboration with ADMOS group at Frankfurt

r.o. speed evolution

- Two orders of magnitude improvement in 15 years of research

Radiation tolerance

- Significant improvement with time
- Sensor validation up to $10^{14} n_{eq}/cm^2$
- Adequacy to ALICE-ITS and CBM applications



Sensors: IPhC Strasbourg
M. Deveau, D. Doering, B. Limik, S. Strothauer, CBM/IKF Frankfurt

Development of CPS adapted to Vertex & Tracker detector

Next challenge: ALICE-ITS upgrade

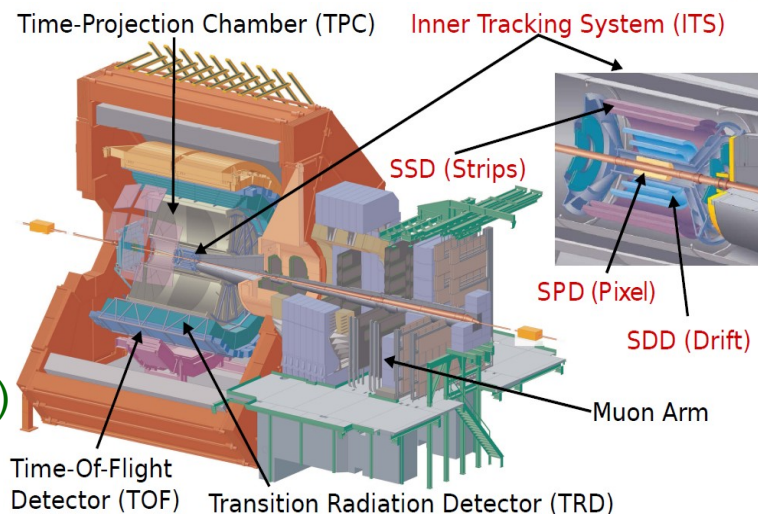


ALICE goals

- Study quark gluon plasma in heavy-ion collisions
- High precision measurements @ low- p_T

Upgraded ITS entirely based on CPS

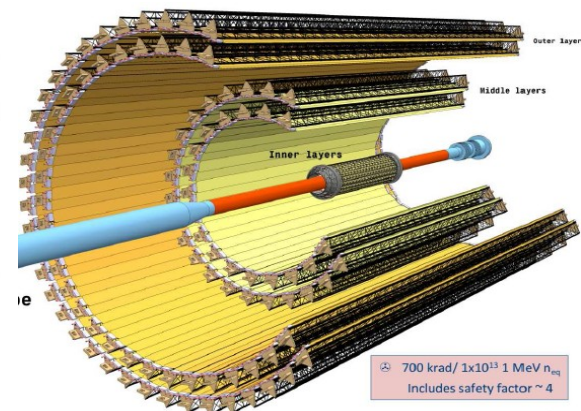
- **Present detector:** 2xHPD/2xDrift-Si/2xSi-strips
- **Future detector:** 7-layers with CPS (25-30k chips)
- ⇒ **1st large tracker (~ 10 m²) using CPS**
- ITS-TDR approved on March 2014 (Pub. In J.Phys. G41 (2014) 087002)



New ALICE-ITS requirements

	σ_{sp}	$t_{r.o.}$	Dose	Fluency	T_{op}	Power	Active area
STAR-PXL	$< 4 \mu m$	$< 200 \mu s$	150 kRad	$3 \cdot 10^{12} n_{eq}/cm^2$	30-35°C	160 mW/cm ²	0.15 m ²
ITS-in	$\lesssim 5 \mu m$	$\lesssim 30 \mu s$	2.7 MRad	$1.7 \cdot 10^{13} n_{eq}/cm^2$	30°C	$< 300 mW/cm^2$	0.17 m ²
ITS-out	$\lesssim 10 \mu m$	$\lesssim 30 \mu s$	100 kRad	$1 \cdot 10^{12} n_{eq}/cm^2$	30°C	$< 100 mW/cm^2$	$\sim 10 m^2$

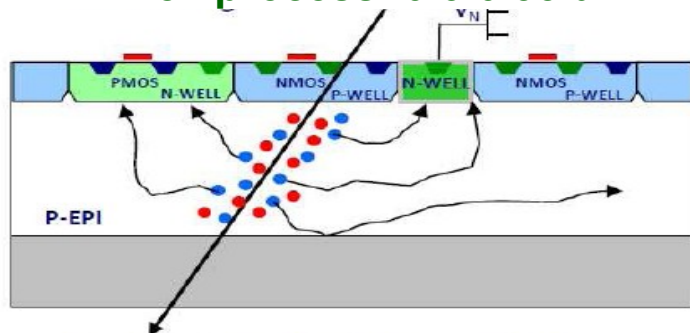
- **Different requirements on inner & outer layers calls for different chips designs!**



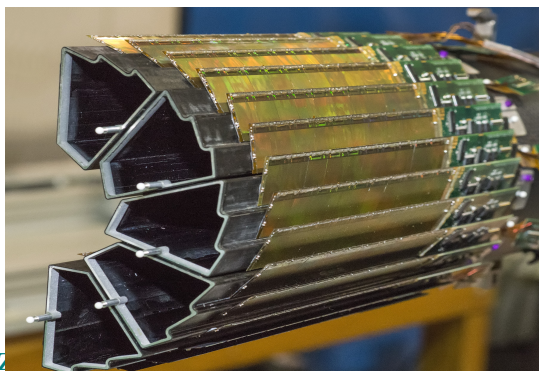
⇒ **0.35 μm CMOS process (STAR-PXL) marginally suited to this r.o. speed & rad. hardness**

CMOS Process Transition: STAR-PXL → ALICE-ITS

Twin well process: 0.6-0.35 μm

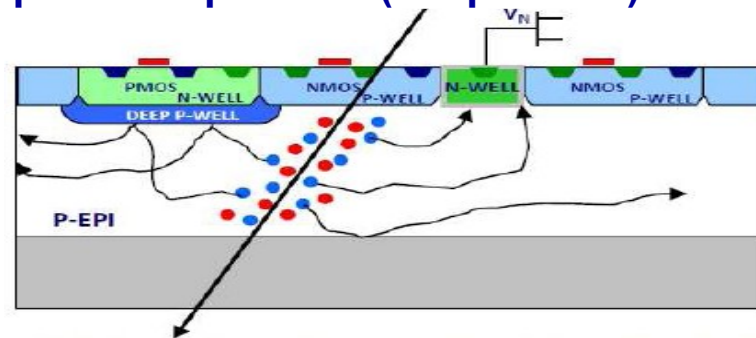


- Use of PMOS in pixel array not allowed
⇒ parasitic q-collection of additional N-well
- Limits choice of readout architecture strategy
- Already demonstrated excellent performances
 - **STAR-PXL:** Mi-28 (AMS 0.35 μm process)
⇒ $\varepsilon_{\text{det}} > 99.5\%$, $\sigma_{\text{sp}} < 4\mu\text{m}$
 - **1st CPS detector @ collider experiment**

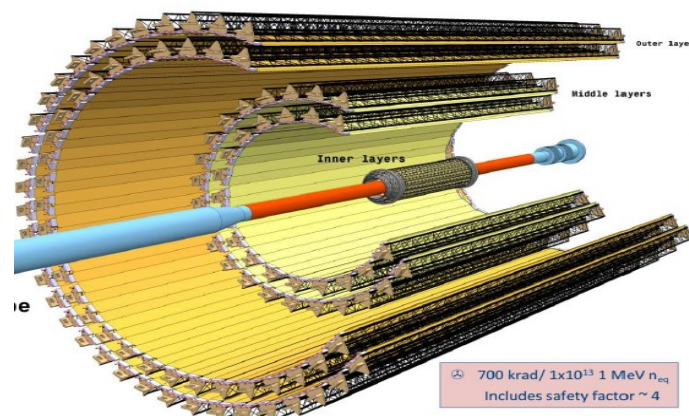


Alejandro Pérez Pérez

Quadrupole well process (deep P-well): 0.18 μm



- N-well of PMOS transistors shielded by deep P-well
⇒ both types of transistors can be used
- Widens choice of readout architecture strategies
 - **New ALICE-ITS:** 2 sensors R&D in || using TowerJazz CIS 0.18 μm process (quadru. well)
 - ➔ **Synchronous Readout R&D:**
proven architecture ⇒ safety
 - ➔ **Asynchronous Readout R&D:** challenging



ALICE

700 krad/ 1×10^{13} 1 MeV n_{eq}
Includes safety factor ~ 4

ALICE-ITS: Boundaries of the CPS Development

New fabrication process (TowerJazz CIS 0.18 μm)

- Expected to be ration tolerant enough
- Expected to allow for fast enough readout
- Larger reticule: $\sim 25 \times 32 \text{ mm}^2$

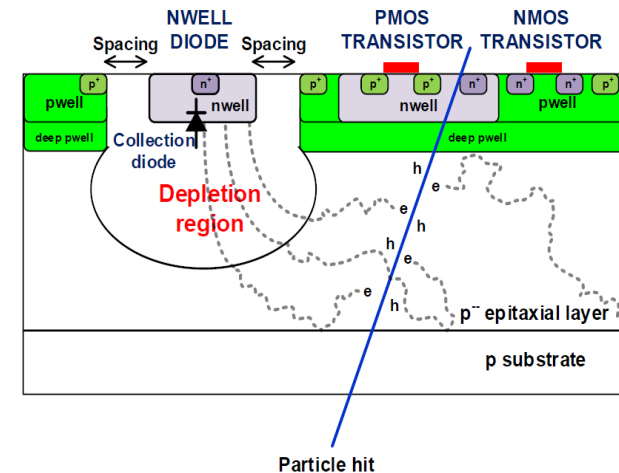
Drawback of smaller feature size

- 1.8 V operative voltage (instead of 3.3 V)
 \Rightarrow reduced dynamics in signal processing circuit and epi-layer depletion voltage
- Increase risk of Random Telegraph Signal (RTS) noise

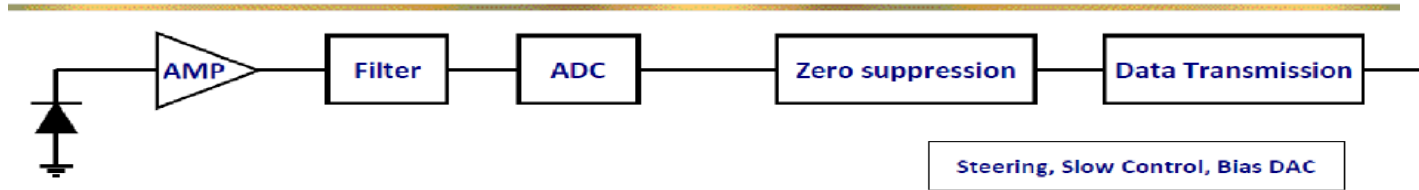
Requirements of the larger surface to cover

- Good fabrication yield \Rightarrow sensor design robustness
- Mitigate noisy pixels
- Sensor operation stable along 1.5 m ladder (voltage drop)
- Material budget
 - Minimize power consumption
 - Minimal connexions to the outside \Rightarrow sensor periphery (slow-control, steering, ...)

STAR-PXL	ALICE-ITS	added-value
0.35 μm	0.18 μm	speed, TID, power
4 ML	6 ML	speed, power
twin-well	quadruple-well	speed, power
EPI 14/20 μm	EPI 18/40 μm	SNR
EPI $\gtrsim 0.4 \text{ k}\Omega \cdot \text{cm}$	EPI $\sim 1 - 8 \text{ k}\Omega \cdot \text{cm}$	SNR, NITD



ALICE-ITS: Readout chain components



■ Typical readout components

- **AMP:** in-pixel low noise pre-amplifier
- **Filter:** in-pixel filter
- **ADC** (1-bit \equiv discriminator): may be implemented at end-of-column or pixel level
- **Zero suppression** (SUZE): only hit pixel info is retained and transferred
 - Implemented at sensor periphery (usual) or inside pixel array
- **Data transmission:** O(Gbps) link implemented at sensor periphery

■ r.o. alternatives

- Rolling shutter (synchronous): || column r.o. reading N-lines at the time (usually $N = 1-2$)
- data-driven (asynchronous): only hit pixels are output upon request (priority encoding)

■ Rolling shutter: best approach for twin-well process

- Trade-off between performance, design complexity, pixel dimensions, power, ...
e.g.: Mimosa-26 (EUDET-BT), Mimosa-28 (STAR-PXL)

ALICE-ITS: Two Architectures for the pixel chip

Pixel pitch: $36 \times 64 \mu\text{m}^2$

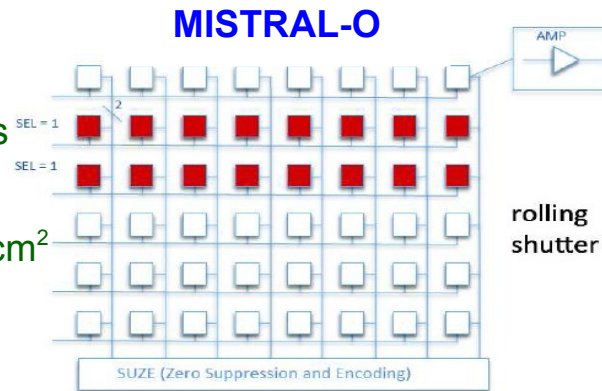
Time resolution: $\sim 20 \mu\text{s}$

W: 80 mW/cm^2

Max hit rate: $\sim 0.8 \text{ MHz/cm}^2$

Dimension: $15 \times 30 \text{ mm}^2$

Dead area: $1.5 \times 30 \text{ mm}^2$

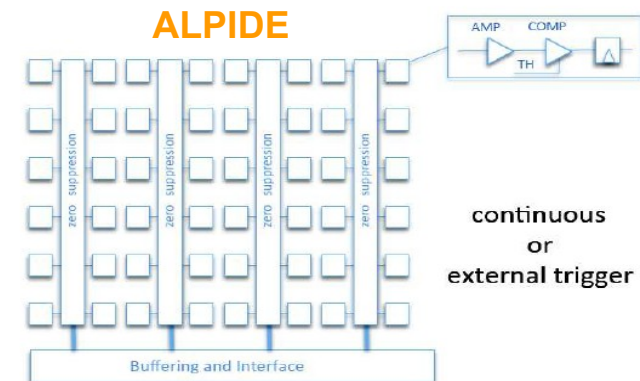
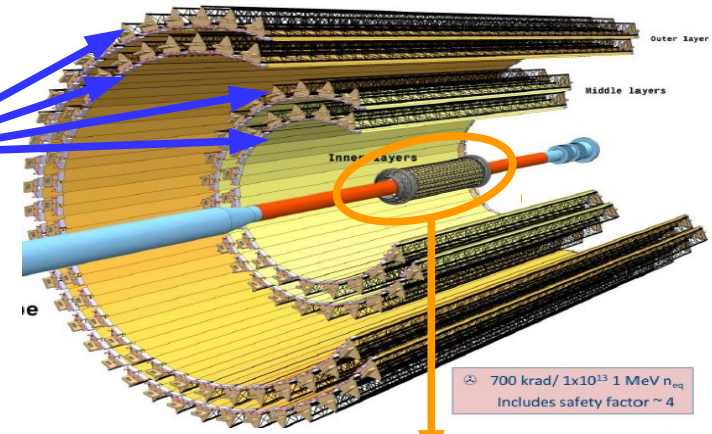


Goal: early available and reliable solution

- **Conservative design based on STAR-PXL**
- Big pixel \Rightarrow low power & high speed
- Moderate rad. hardness & $\sigma_{sp} \sim 10 \mu\text{s} \Rightarrow \text{OK}$

Goal: high performance, accept risks

- **Aggressive design**
- In-pixel discrimination
- Data-driven r.o. (priority encoder)



Pixel pitch: $28 \times 28 \mu\text{m}^2$

Time resolution: $\lesssim 5 \mu\text{s}$

W: 39 mW/cm^2

Max hit rate: $\sim 3 \text{ MHz/cm}^2$

Dimension: $15 \times 30 \text{ mm}^2$

Dead area: $1.1 \times 30 \text{ mm}^2$

- **Both chips have same physical & electrical interfaces**
- **Base-line solution: ALPIDE for all ITS layers**

Exploring the new technology

Technology Exploration & Sensor Performances

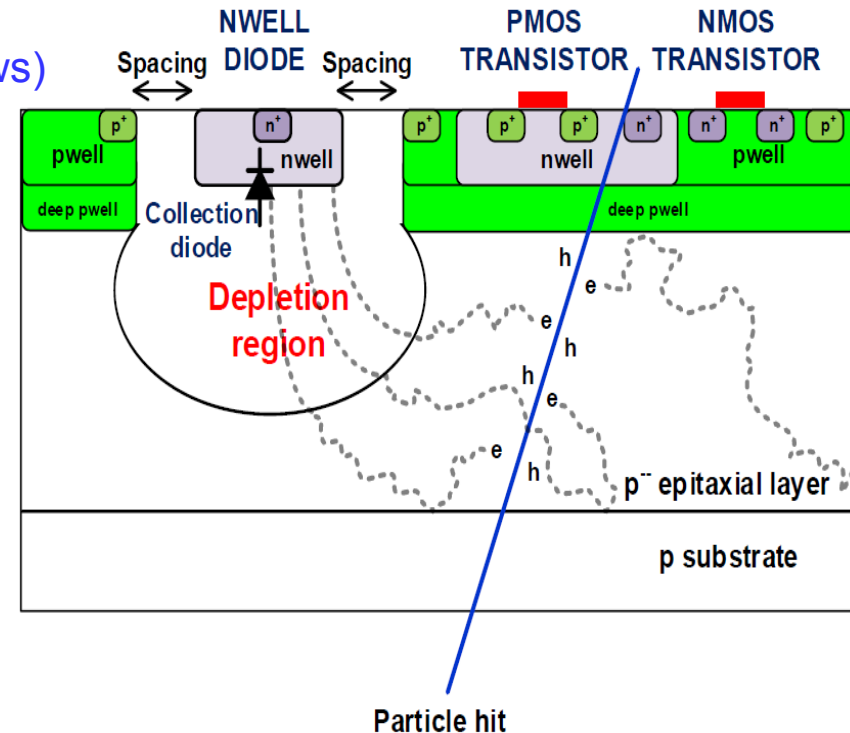
- **Goal:** understand the detection performances in terms of external parameters
⇒ Optimization for ALICE-ITS (and evaluate adequacy for other applications)

External parameters

- Diode and spacing (footprint) size/geometry
- **Pixel size/geometry:** square vs elongated
 - Elongated pixels in row direction (less rows)
⇒ Lower $t_{r.o.}$ of rolling shutter
- **Diode layout of elongated pixels**
 - Staggering ⇒ lower diode inter-distance
- **Epi-layer:** thickness and resistivity (profile)

Performances in terms of

- Noise
- CCE, SNR @ seed pixel
- Hit pixel multiplicity ⇒ data transmission
- ϵ_{det} , σ_{sp} & Fake-rate
- Rad. Tolerance



Exploratory chips: MIMOSA-32ter & MIMOSA-34

■ TowerJazz 0.18um technology validation & performances optimization

■ MIMOSA-32ter

- **Analog-output:** source follower or feedback-loop ($t_{int} \sim 34$ or $12 \mu s$)
- Sub-matrices of 16×64 pixels with different sizes ($20 \times 20, 33, 40, 80 \mu m^2$), diodes geometries (octagonal vs square) and some with deep P-well
- **Epi-layer:** $18 \mu m$ HR ($\rho = 1 \text{ k}\Omega \text{ cm}$)

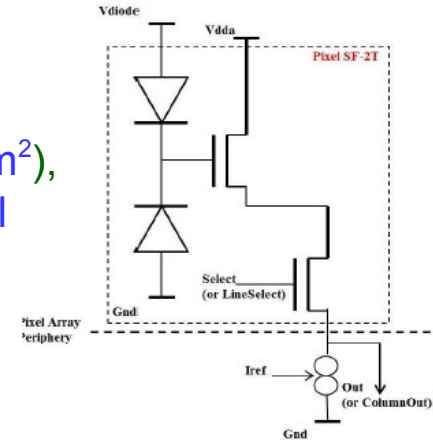
■ MIMOSA-34

- **Analog-output:** source follower ($t_{int} \sim 32 \mu s$)
- 30 sub-matrices with 16×64 staggered pixels
 - **Dimensions:** 22 or $33 \times (27, 30, 33, 44, 66) \mu m^2$
 - **Diode/footprint:** $1+1, 2, 5, 5+5, 8, 11, 15 \mu m^2 / 11, 15 \mu m^2$
- **Epi-layer:** $18, 20, 30 \mu m$ HR ($\rho = 1 - 6 \text{ k}\Omega \text{ cm}$)

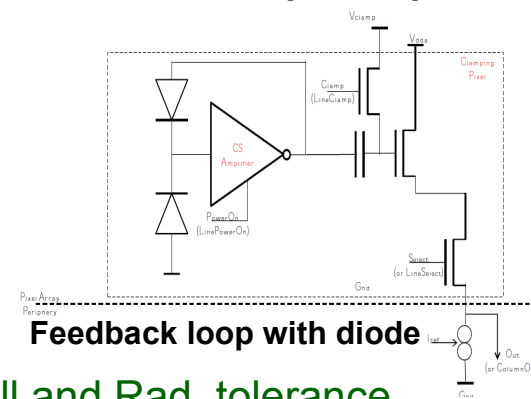
■ Test purposes

- **Validate new technology:** epi-layer characteristics, deep P-well and Rad. tolerance
- **Study:** sensing node charge collection, elongated pixels performances

source follower



Diode & pre-ampli



Feedback loop with diode

MIMOSA-32ter: performances

CERN-SPS BT Set-up

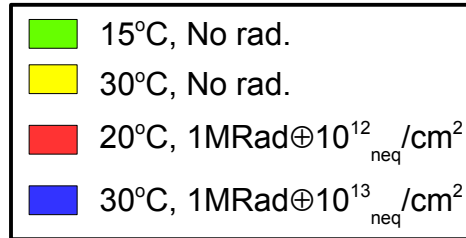
- **Beam:** 60-120 GeV/c π^+
- $T_{\text{cooling}} = 15, 20 \text{ \& } 30^\circ\text{C}$

Main results

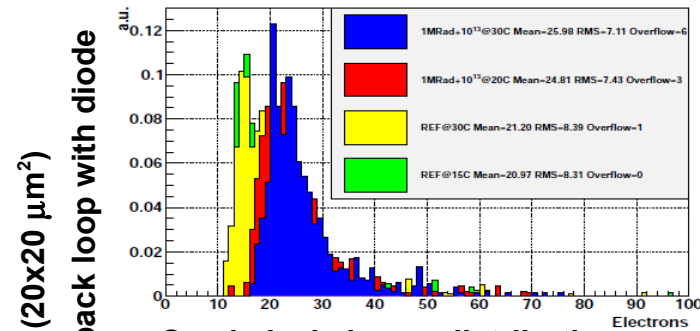
- $20 \times 20 \text{ }\mu\text{m}^2$ pixel (performances vs rad. dose @ 30°C)
 - Small noise increase: $21 \rightarrow 26 \text{ e}^- \text{ ENC}$
 - SNR_{seed} reduction: $26-28 \rightarrow 19$ (30%)
 - $\epsilon_{\text{det}} > 99\%$ for $1\text{MRad} \oplus 10^{13} \text{ n}_{\text{eq}}/\text{cm}^2$
 - $\sigma_{\text{sp}} \sim 3.2 \text{ }\mu\text{m}$
- $20 \times 40 \text{ }\mu\text{m}^2$ pixel (@ 20°C)
 - $\epsilon_{\text{det}} > 99\%$ for $1\text{MRad} \oplus 10^{13} \text{ n}_{\text{eq}}/\text{cm}^2$
 - $\sigma_{\text{sp}} \sim 5.0 \text{ }\mu\text{m}$

Technology validation

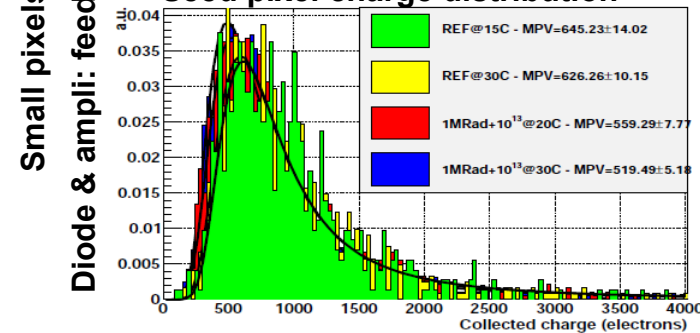
- HR epi-layer ✓
- deep P-well (no parasitic charge coll.) ✓
- Radiation tolerance ✓



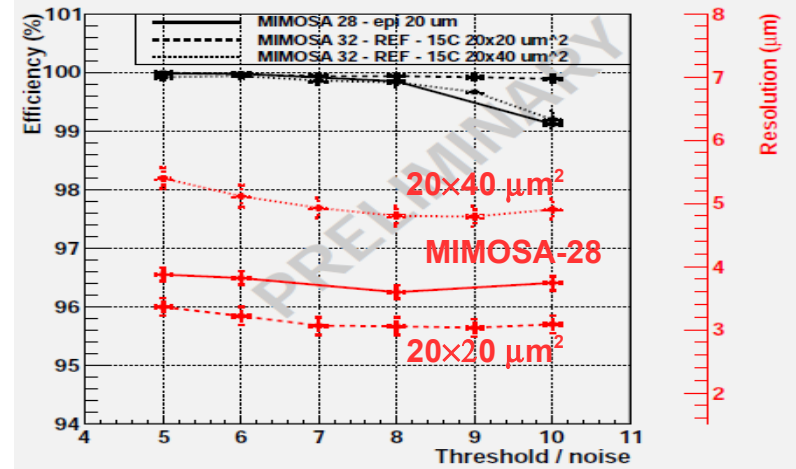
Noise distribution



Seed pixel charge distribution



ϵ_{det} & σ_{sp} vs threshold



MIMOSA-34: performances vs diode & pixels sizes

■ DESY BT Set-up (August 2013):

- 2BT: 8xSi-strips & 6xMIMOSA-26 (120 μm thick)
- $\sim 4.4 \text{ GeV/c } e^-$ beam

■ MIMOSA-34: Various pixels & diode dimensions

- Pixel (22x27,30,33,44,66) & diode (8,11,15) sizes (μm^2)
- Excellent SNR_{seed} for various considered pixels

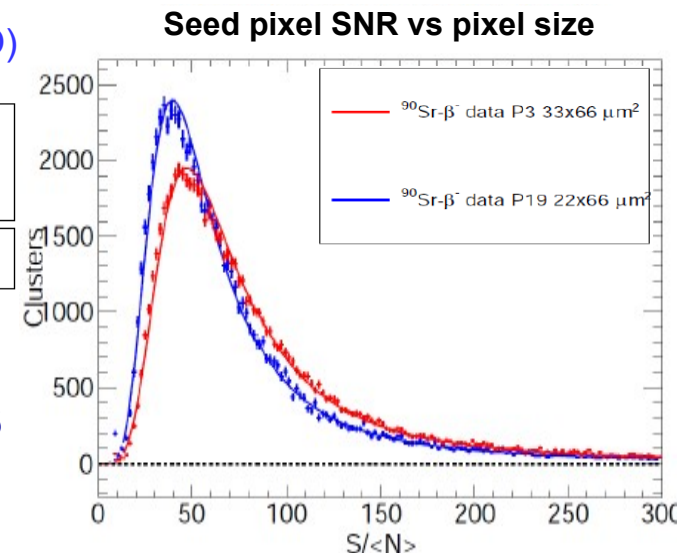
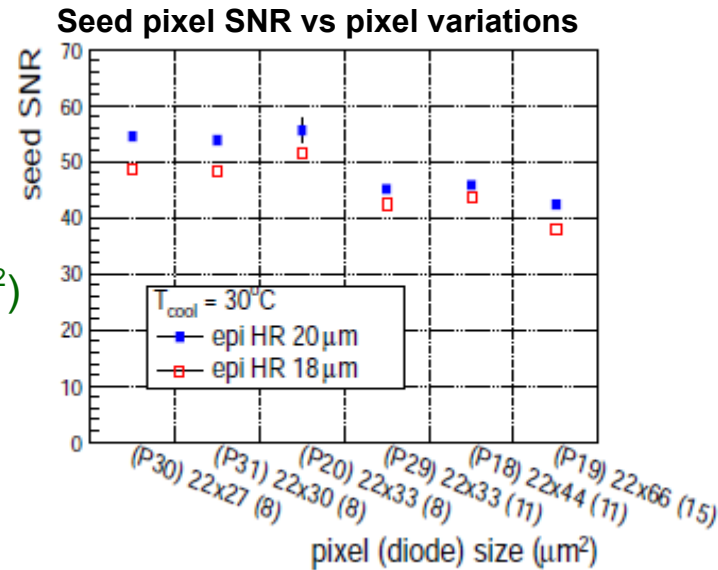
\Rightarrow e.g. MPV > 40 for 22x66 μm^2 pixel $\Rightarrow \epsilon_{\text{det}} \sim 100\%$

- **33x66 μm^2 pixel:** Not tested in BT but with β -source
 - Excellent MPV (> 50) \Rightarrow expects $\epsilon_{\text{det}} \sim 100\%$ & $\sigma_{\text{sp}} \sim 10 \mu\text{m}$
 - Pixel size adapted for ALICE-ITS outer layers (MISTRAL-O)

Process ▷	0.35 μm	0.18 μm				
Pixel Dim. [μm^2]	20.7 × 20.7	20 × 20	22 × 33	20 × 40	22 × 66	33 × 66
$\sigma_{\text{sp}}^{\text{bin}} [\mu\text{m}]$	3.7 ± 0.1	3.2 ± 0.1	~ 5	5.4 ± 0.1	~ 7	$\sim 10 \mu\text{m} ?$

■ Variations showed acceptable degradation of performances for nominal TID + NIEL @ ALICE-ITS

■ Next-step: optimization with pre-ampli scheme

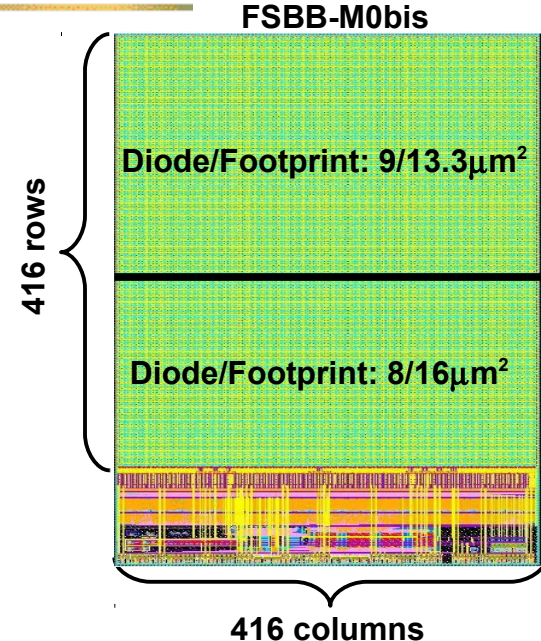


Going MISTRAL-O

Main features of the Sensors Studied on Beam

Full Scale Building Block (FSBB) sensor

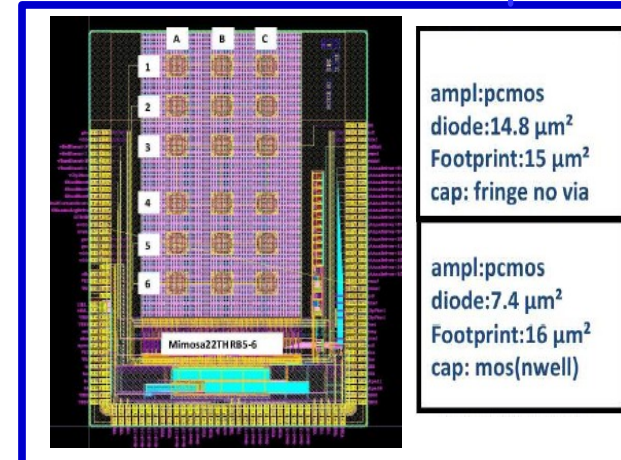
- Complete (fast) chain of double-row r.o. and 2D sparsification (SUZE): $t_{r.o.} = 40 \mu s$
- Sensitive area ($\sim 1 \text{ cm}^2$) \approx area of final building block
- Similar Nb of pixels ($\sim 170k$) than complete final chip (160k)
- Epi-layer: high-p $18 \mu m$ thick
- BUT:** pixels are small ($22 \times 32.5 \mu m^2$ staggered layout) & sparsification circuitry is oversized (power!)



Large-pixel prototype (MIMOSA-22THRb)

- Two slightly different large pixels
 - $36 \times 62.5 \mu m^2$ and $39 \times 50.8 \mu m^2$ (staggered layout)
- Pads over pixel array (3ML used for in-pixel circuitry)
- Double-row r.o. with no-sparsification ($t_{r.o.} \sim 5 \mu s$)
- Epi-layer: high-p $18 \mu m$ thick
- BUT:** only $\lesssim 10 \text{ mm}^2$, 4k pixels & no sparsification

Mi22-THRB6: $36 \times 62.5 \mu m^2$



Main goals of MIMOSA-22THRb & FSBB-M0 Prototyping

Parametres investigated	MIMOSA-22THRb7/6	FSBB-M0bis
Sensing node geometry	X	X
Epitaxial layer parametres	x	X
In-pixel signal processing	X	x
on 3 ML (Pre-Amp, clamping)	X	–
Pads over pixels	X	–
Large pixel detection efficiency	X	–
at 30°C (incl. after OB radiation load)	X	–
Large pixel single point resolution	X	–
Complete signal sensing & processing chain	–	X
Fake rate (160,000 pixels)	x	X
Impact of voltage drop	–	X
Cluster encoding data size	X	x

FSBB BT @ CERN-SPS in Oct. 2015

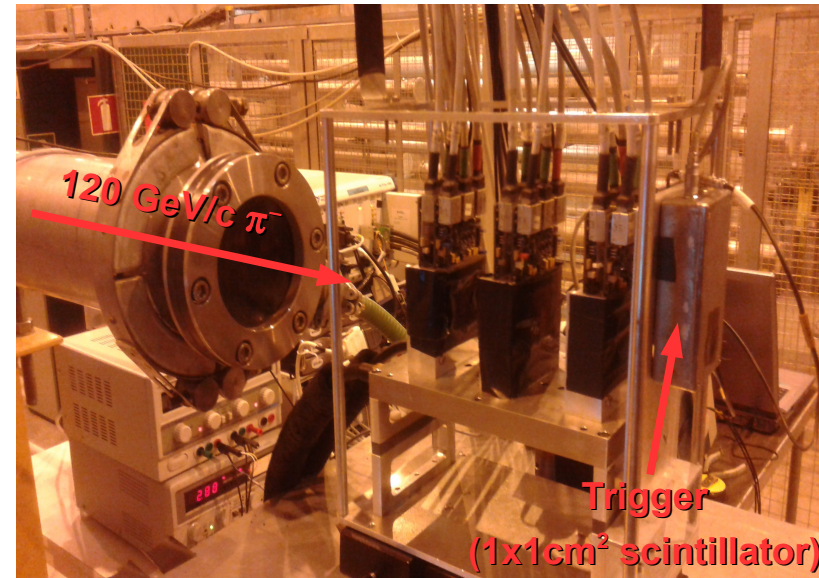
Experimental set-up

- 3 pairs of FSBB planes on T4/H6 (120 GeV/c π^-)
- Particle flux: trigger rate $\sim 4, 25$ & 100 kHz/cm²
- **All measurements performed at $T_{\text{coolant}} = 30$ °C**

Measurements vs discriminator threshold

- Detection efficiency vs fake rate (noisy pixel)
- Spatial resolution associated with binary encoding of 22×32.5 μm^2 pixels
- Radiation tolerance @ $T_{\text{coolant}} = 30$ °C: up to 1.6 MRad $\oplus 1.0 \times 10^{13}$ n_{eq}/cm²
- Studies of the impact of operation parameters on sensor performances
 - e.g. input voltage (VDD), pixel current, ...
- Study of the impact of noisy pixel masking on efficiency and spatial resolution

Main Goal: validation of r.o. architecture and pixel masking in full size chip

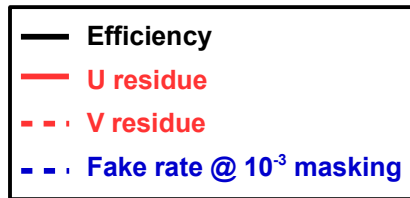


Main FSBB-M0 detection performances (1/3)

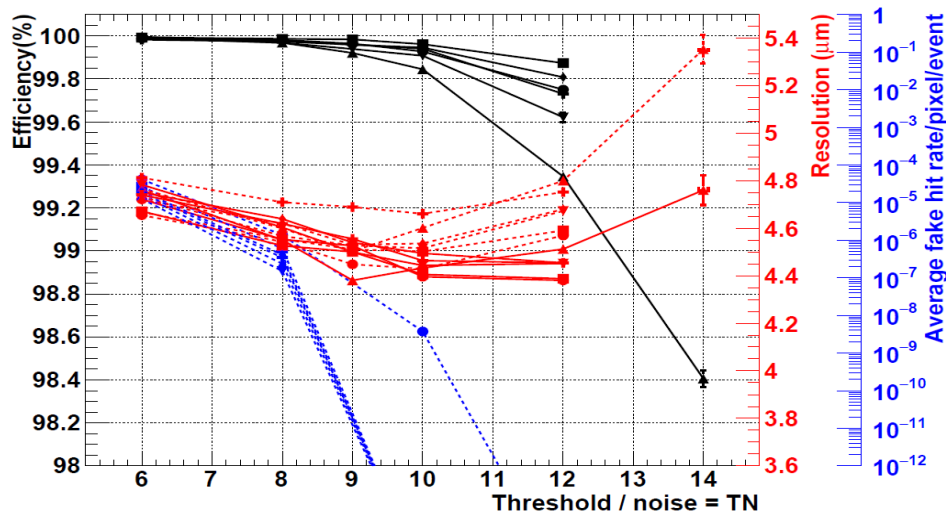
All the 6 sensor performances on the same plot

Excellent and uniform performances among sensors (thr < 10xNoise)

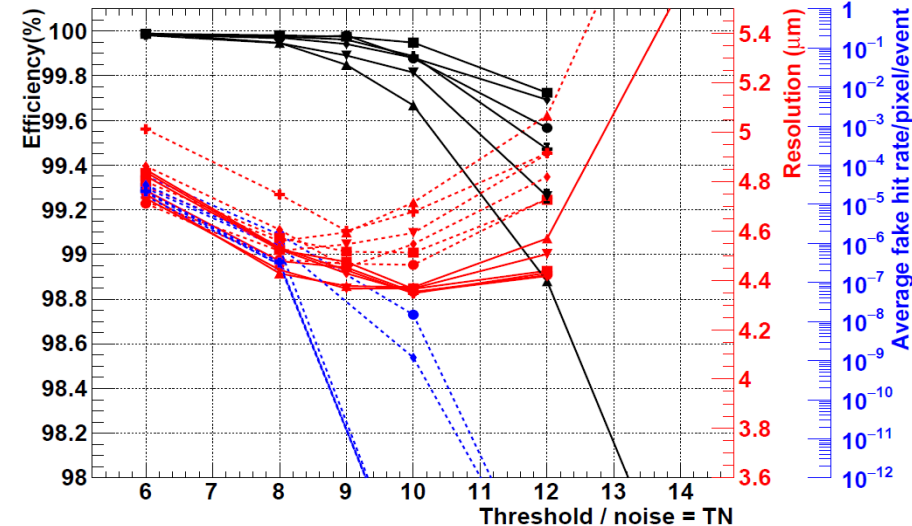
- detection efficiency: > 99%
- spatial resolution: < 5 μm
- Fake rate: < 10^{-6} with moderate (10^{-3}) hot pixels masking



Diode/Footprint: 8/16 μm^2



Diode/Footprint: 9/13.3 μm^2



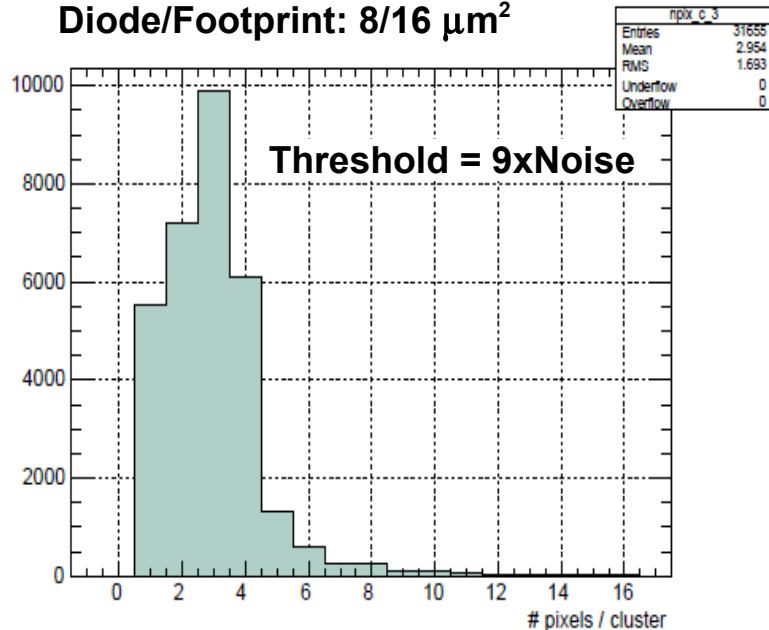
Detection performances stability

- Same results obtained @ DESY (4.5 GeV/c e^-) and CERN-SPS (120 GeV/c π^-)
- Same results for different particles rates: 1 – 25 hits/frame
- Robust performances in terms of operation parameters

Main FSBB-M0 detection performances (2/3)

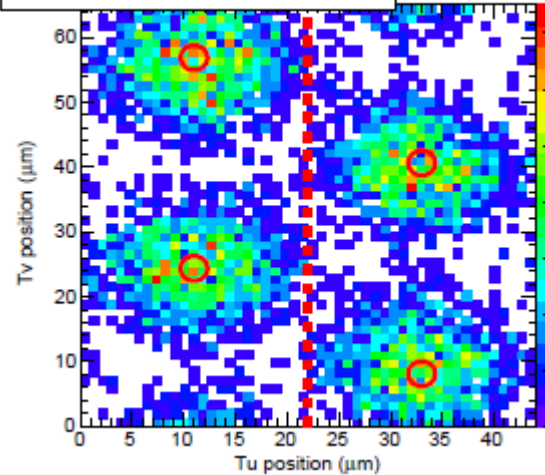
Spatial resolution vs cluster pixel size

Diode/Footprint: 8/16 μm^2

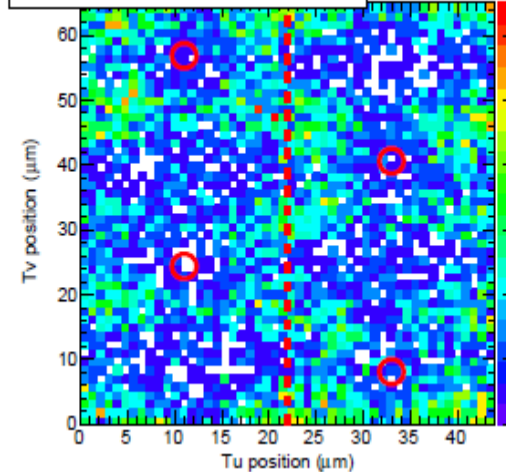


Track position @ DUT w.r.t closest set of collection diodes as a function of cluster pixel multiplicity

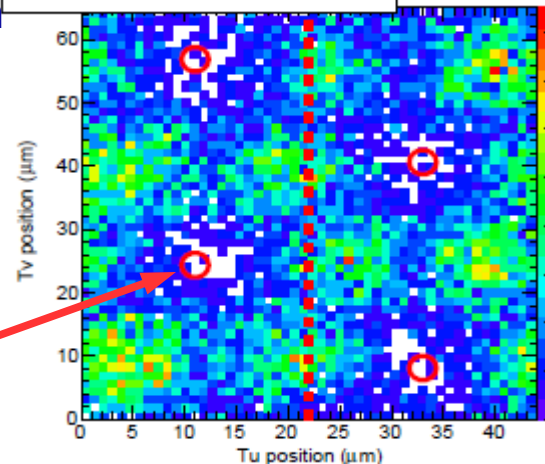
Tu vs Tv on matrix for Mult. = 1



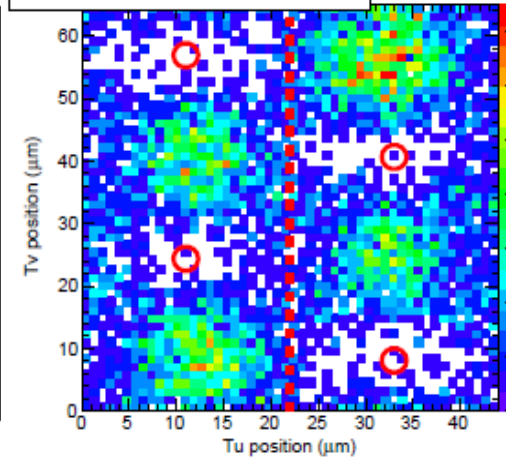
Tu vs Tv on matrix for Mult. = 2



Tu vs Tv on matrix for Mult. = 3



Tu vs Tv on matrix for Mult. = 4



Collection diode

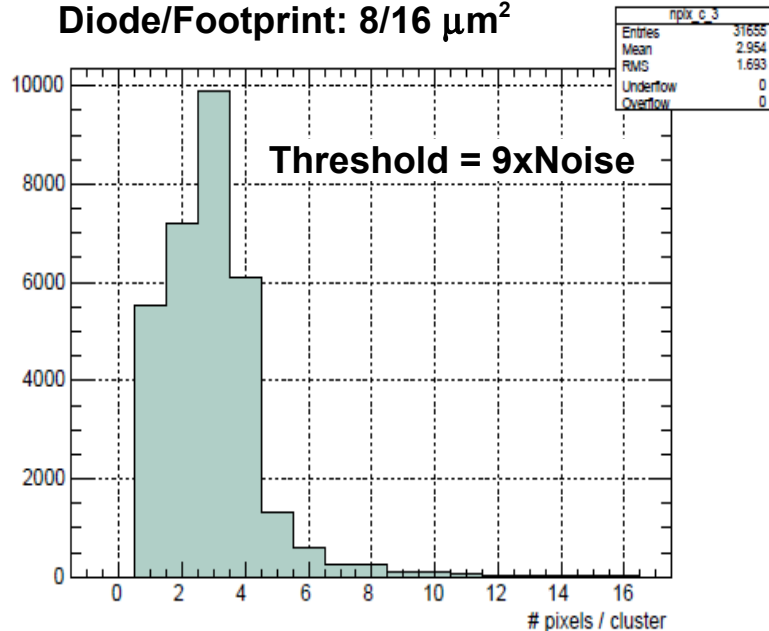
Telescope pointing resolution $\sim 2 \mu\text{m}$

Charge sharing depends on track impinging position w.r.t coll. diode

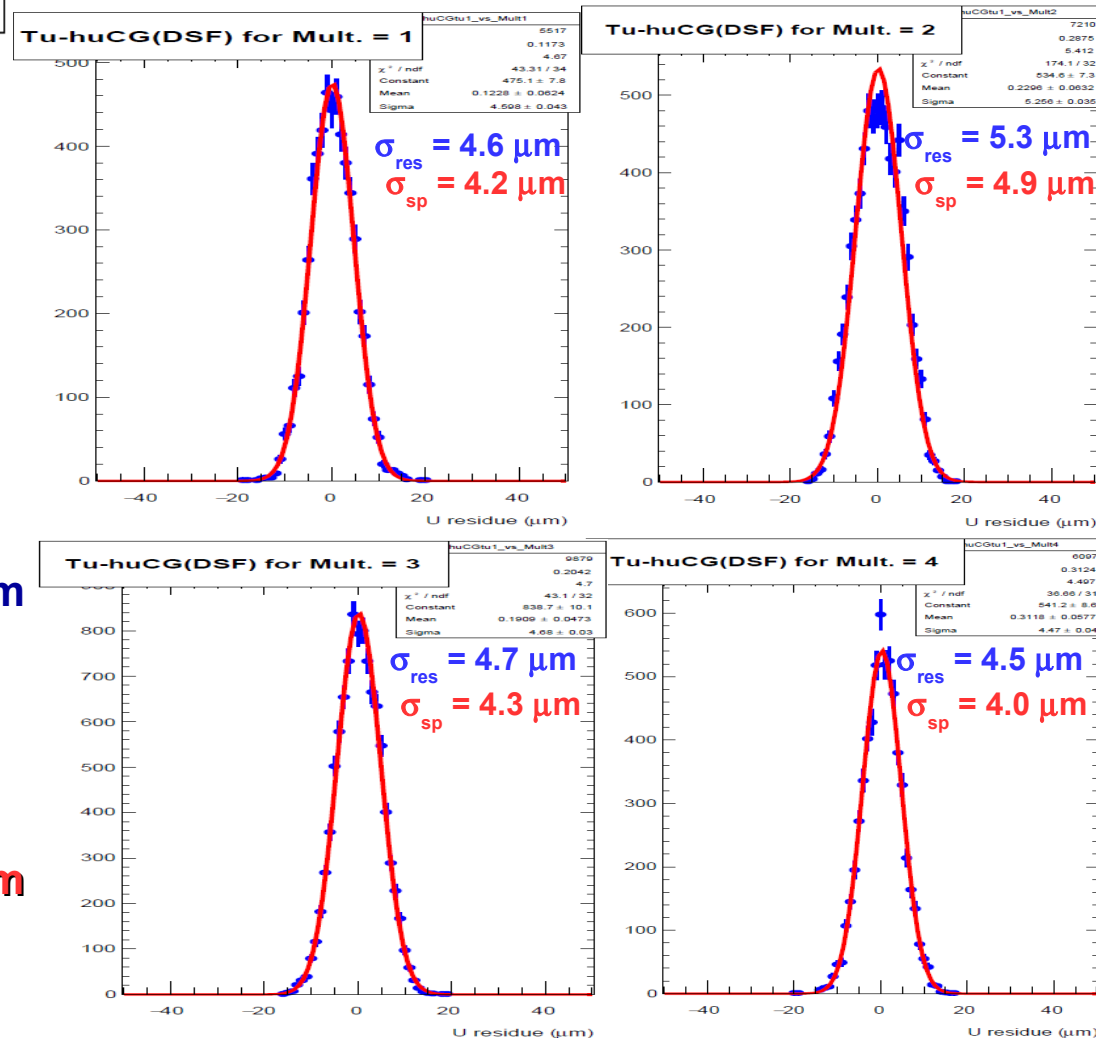
Main FSBB-M0 detection performances (2/3)

Spatial resolution vs cluster pixel size

Diode/Footprint: 8/16 μm^2



Residue distribution in the **raw** parallel direction as a function of cluster pixel multiplicity



Telescope pointing resolution $\sim 2 \mu\text{m}$

Charge sharing depends on track impinging position w.r.t coll. diode

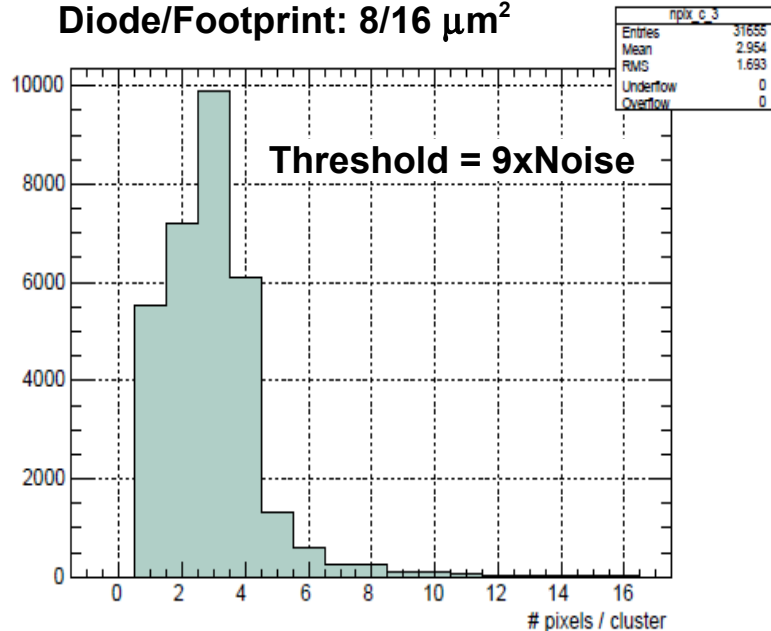
Spatial resolution is mostly dependent on # pixels/cluster

$\sigma_{\text{sp}}(\text{Mult}=1) \sim 4.2 \mu\text{m} < \sigma_{\text{sp}}^{\text{digi}} \sim 7.8 \mu\text{m}$

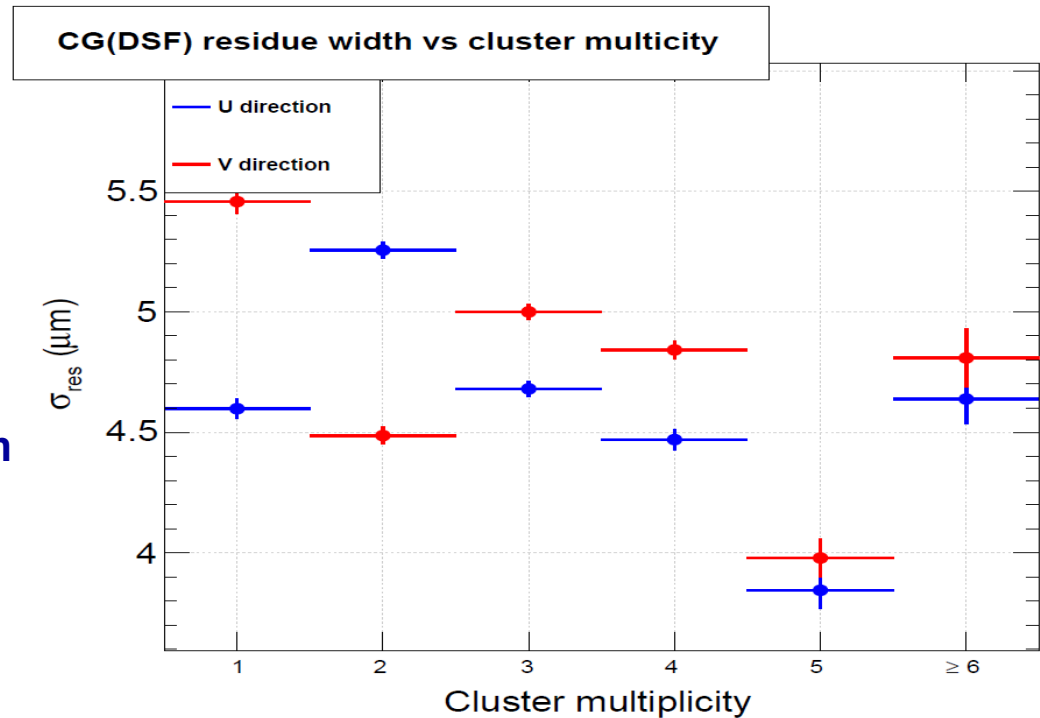
Main FSBB-M0 detection performances (2/3)

Spatial resolution vs cluster pixel size

Diode/Footprint: 8/16 μm^2



Residue RMS in the **raw/column** parallel direction as a function of cluster pixel multiplicity



Telescope pointing resolution $\sim 2 \mu\text{m}$

Charge sharing depends on track impinging position w.r.t coll. diode

Spatial resolution is mostly dependent on # pixels/cluster

$\sigma_{\text{sp}} (\text{Mult}=1) \sim 4.2 \mu\text{m} < \sigma_{\text{sp}}^{\text{digi}} \sim 7.8 \mu\text{m}$

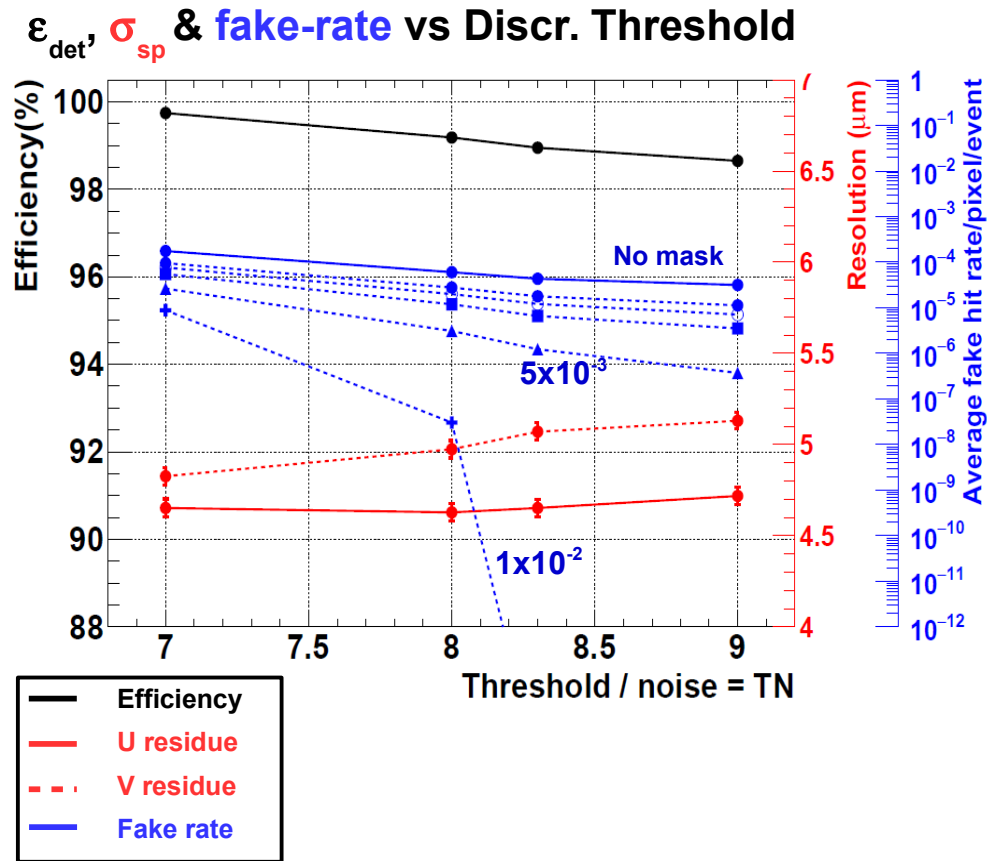
Staggering mitigates σ_{sp} difference in raw/column directions

Main FSBB-M0 detection performances (3/3)

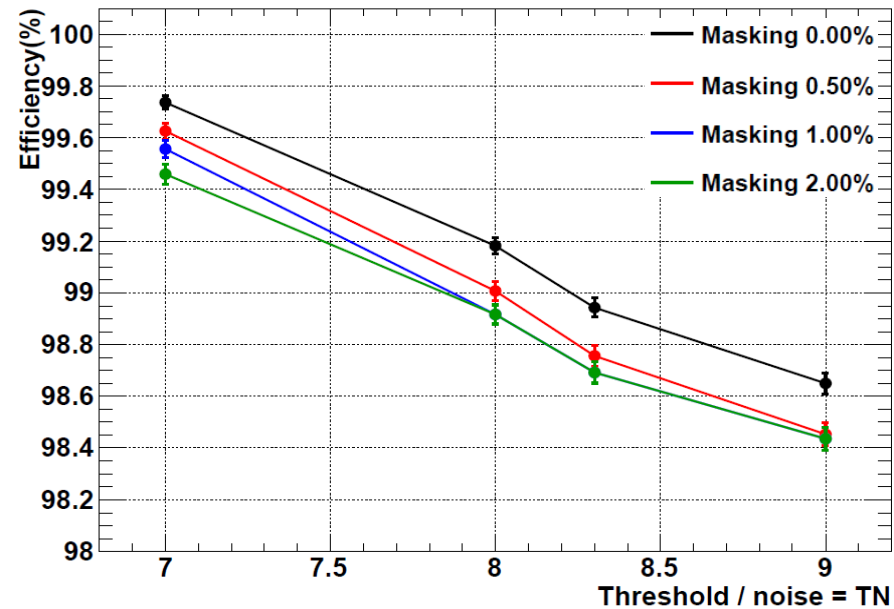
Study of rad. tolerance @ $T \gtrsim 30^\circ\text{C}$: loads relevant to ALICE-ITS inner layers

- Load: $1.6 \text{ MRad} \oplus 10^{13} n_{\text{eq}}/\text{cm}^2$

Diode/Footprint: $9/13.3 \mu\text{m}^2$



ϵ_{det} vs Discr. Threshold vs pixel masking

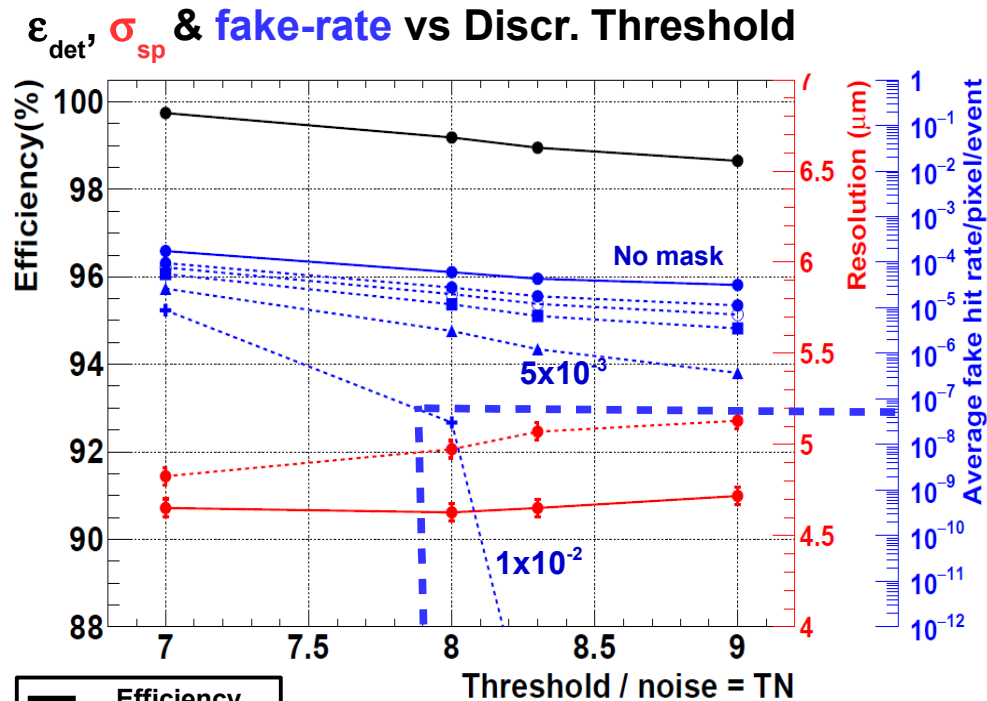


Main FSBB-M0 detection performances (3/3)

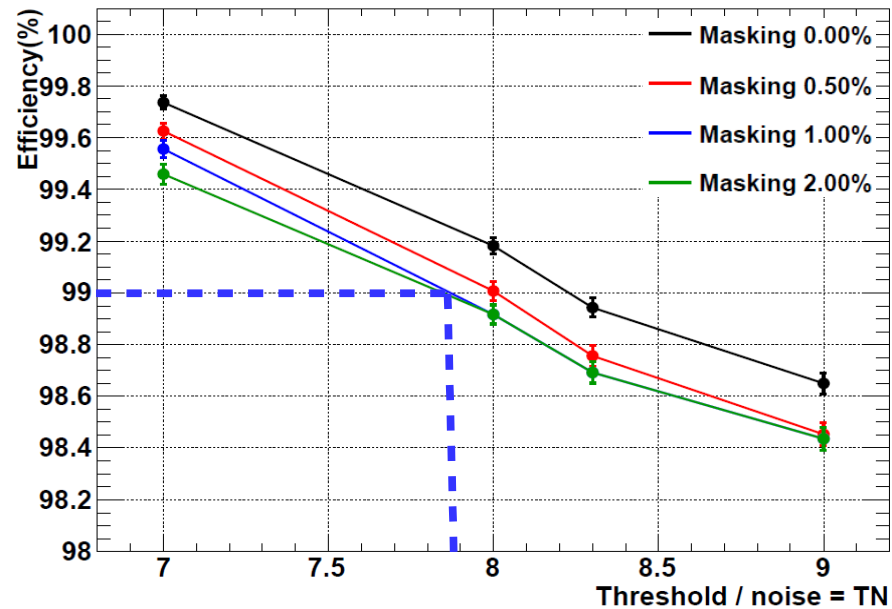
Study of rad. tolerance @ $T \gtrsim 30^\circ\text{C}$: loads relevant to ALICE-ITS inner layers

- Load: $1.6 \text{ MRad} \oplus 10^{13} n_{\text{eq}}/\text{cm}^2$

Diode/Footprint: $9/13.3 \mu\text{m}^2$



ϵ_{det} vs Discr. Threshold vs pixel masking



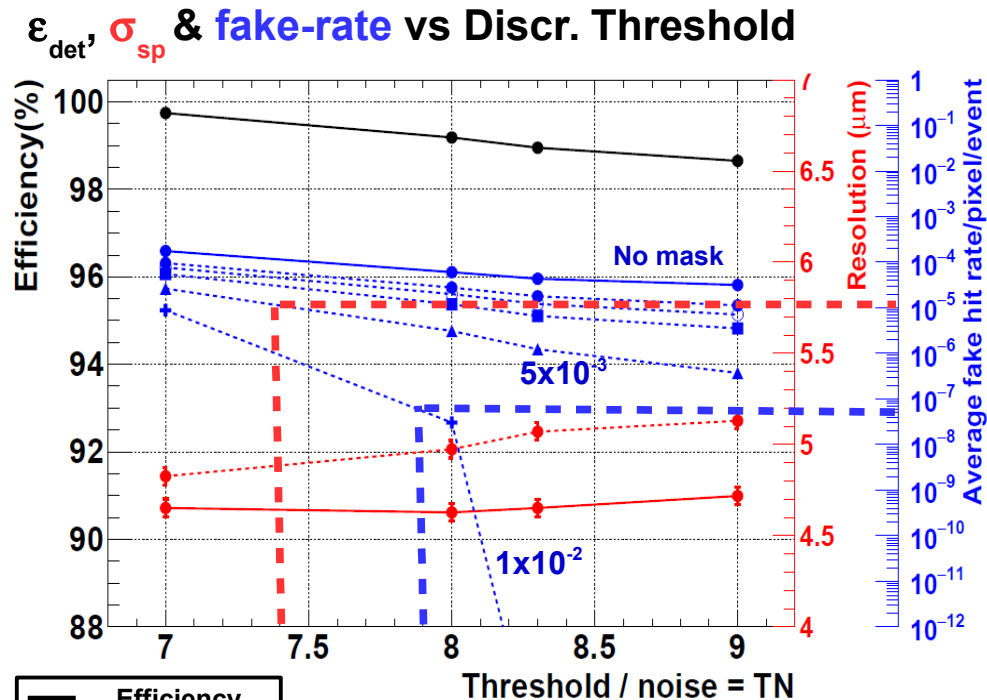
$\epsilon_{\text{det}} \sim 99.0\%$ & $\langle \text{Fake} \rangle \sim 7 \times 10^{-8}$ (1.0% masking) @ Thr = $7.9 \sigma_{\text{TN}}$

Main FSBB-M0 detection performances (3/3)

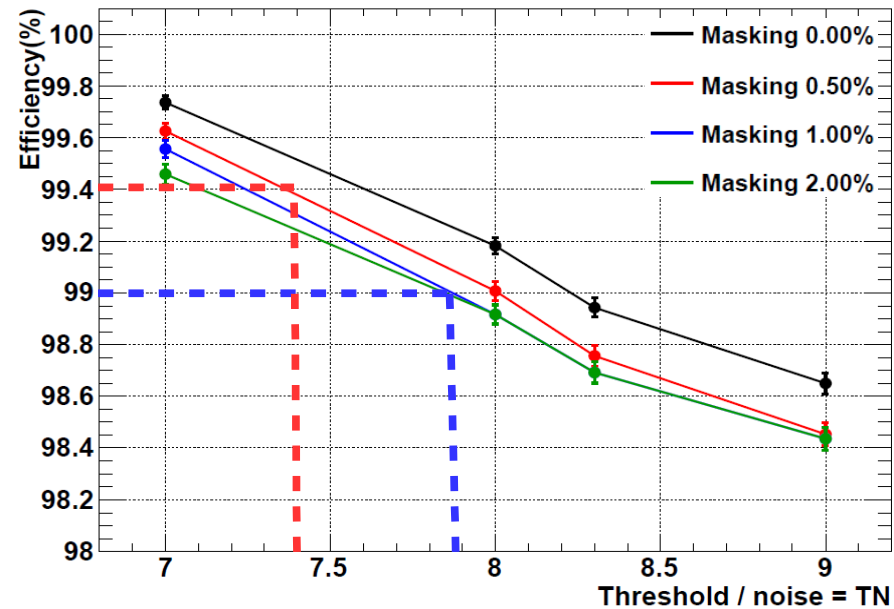
Study of rad. tolerance @ $T \gtrsim 30^\circ\text{C}$: loads relevant to ALICE-ITS inner layers

- Load: $1.6 \text{ MRad} \oplus 10^{13} n_{\text{eq}}/\text{cm}^2$

Diode/Footprint: $9/13.3 \mu\text{m}^2$



ϵ_{det} vs Discr. Threshold vs pixel masking



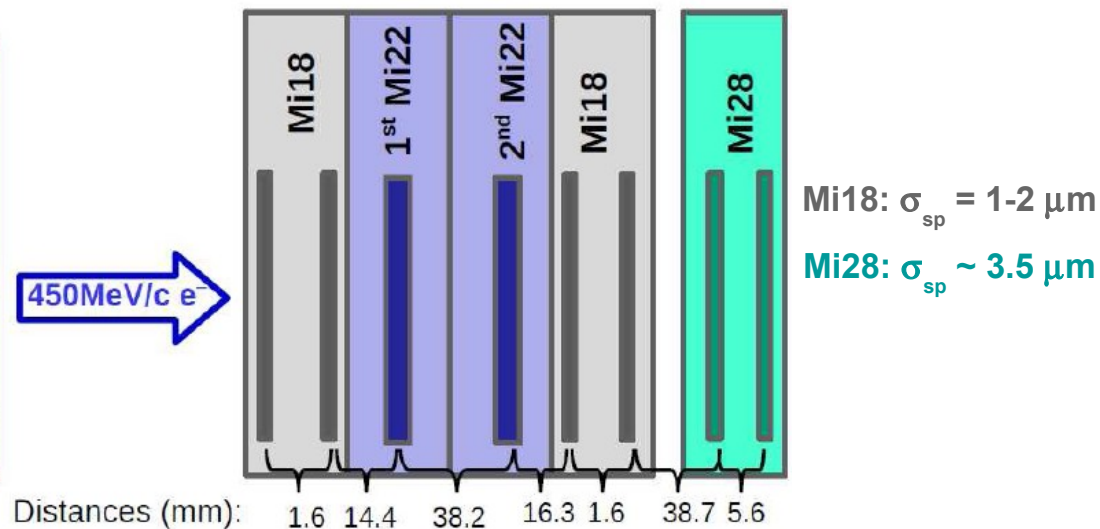
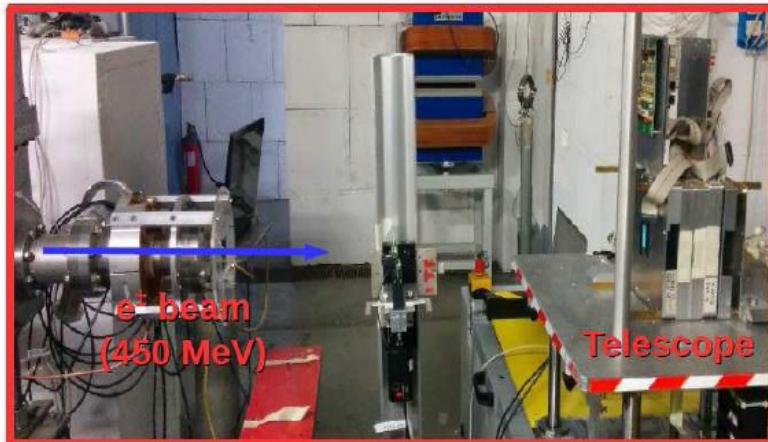
$\epsilon_{\text{det}} \sim 99.0\%$ & $\langle \text{Fake} \rangle \sim 7 \times 10^{-8}$ (1.0% masking) @ Thr = $7.9 \times \sigma_{\text{TN}}$

$\epsilon_{\text{det}} \sim 99.4\%$ & $\langle \text{Fake} \rangle \sim 1 \times 10^{-5}$ (0.5% masking) @ Thr = $7.4 \times \sigma_{\text{TN}}$

MIMOSA-22THRb BT @ Frascati in May 2015

Experimental set-up

- **Beam:** 450 MeV/c e^-
- **Telescope:** 2xMi28 (digital output) and 4xMi18 (analog-output) sensors thinned to 50 μm
- **Trigger:** beam injection signal \Rightarrow synchronisation due to small spill length (few ns)



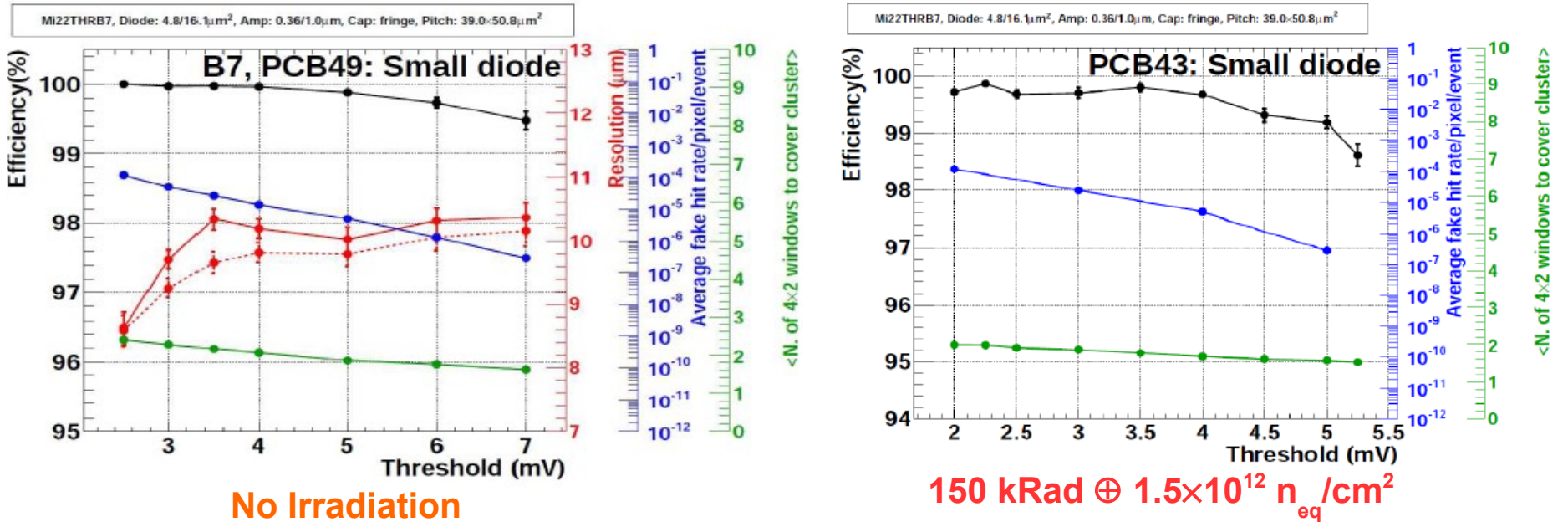
Measurements vs discriminator threshold

- Detection efficiency vs fake rate (noisy pixel)
- Spatial resolution associated with binary encoding of $36 \times 65.2 \mu\text{m}^2$ & $39 \times 50.8 \mu\text{m}^2$ pixels
- Radiation tolerance @ $T_{\text{coolant}} = 30^\circ\text{C}$: up to 150 kRad $\oplus 1.5 \times 10^{12} n_{eq}/\text{cm}^2$

Main Goal: validation of large pixel performances

Main MIMOSA-22THRb detection performances (1/2)

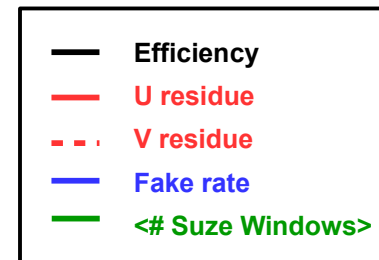
Pixel type	Pixel dim.	Diode/Footprint	Pre-Amp T.	Clamping capa.	Integ. time
MIMOSA-22THR b7	39 μm x 50.8 μm	5/16 μm^2	N-MOS	MOS (N-well)	5 μs



Excellent detection performances

- $\varepsilon_{\text{det}} > 99\%$ & $\sigma_{\text{sp}} \sim 10 \mu\text{m}$ (as expected)
- Good performances for radiation load relevant for outer ALICE-ITS

Validation of large pixel design for the outer layers of the ALICE-ITS!

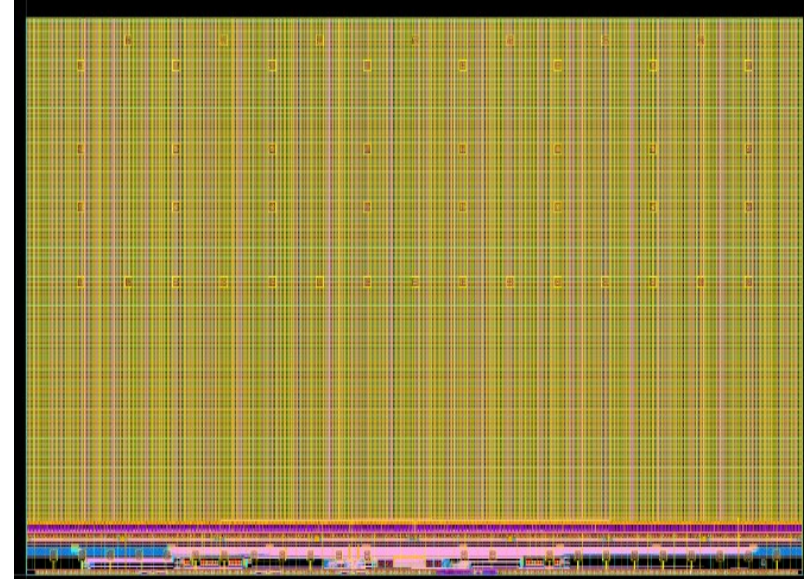


Final Sensor: MISTRAL-O

■ Combination of 4 FSBB-M0 with MIMOSA-22THRb7 pixels

■ Main characteristics

- Chip dimensions: 15 x 30 mm²
- Sensitive area: 13.5 x 29.95 mm²
 - 1.5 mm wide side band (insensitive) (evolving towards 1 mm)
- 832 columns of 208 (160k) pixels
- Pixel dimensions: 36 x 65 μm²
- In-pixel Pre-Amp & clamping (fringe capa)
- End-of-column signal discriminator
- Discriminator's output 2D sparsification (SUZE)
- Fully programmable control circuitry
- Pads over pixel array



■ Typical performances (based on FSBB-M0 & MIMOSA-22THRb tests)

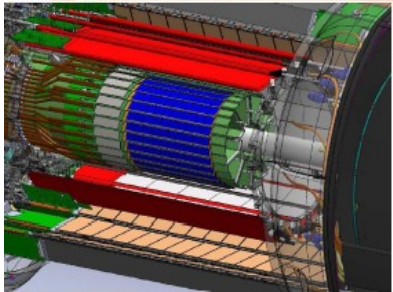
- $t_{r.o.} \sim 20 \mu s$; $\sigma_{sp} \sim 10 \mu m$; Power consumption $\leq 80 \text{ mW/cm}^2$
- Rad. Hardness $> 150 \text{ kRad} \oplus 1.5 \times 10^{12} n_{eq}/\text{cm}^2 @ T \gtrsim 30 \text{ }^\circ\text{C}$

Forthcoming Challenges

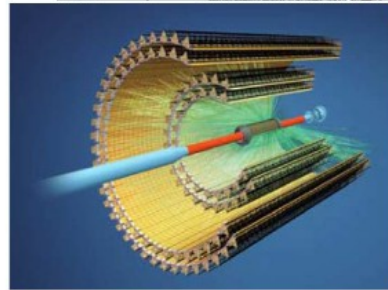
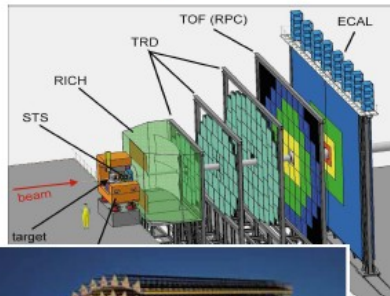
Forthcoming Challenges: R&D @ IPHC

How to improve speed and rad. tolerance while preserving σ_{sp} (3-5 μm) and material budget ($< 0.1\% X_0$)?

$O(10^2) \mu\text{s}$



$O(10) \mu\text{s}$



EUDET/STAR

2010/14



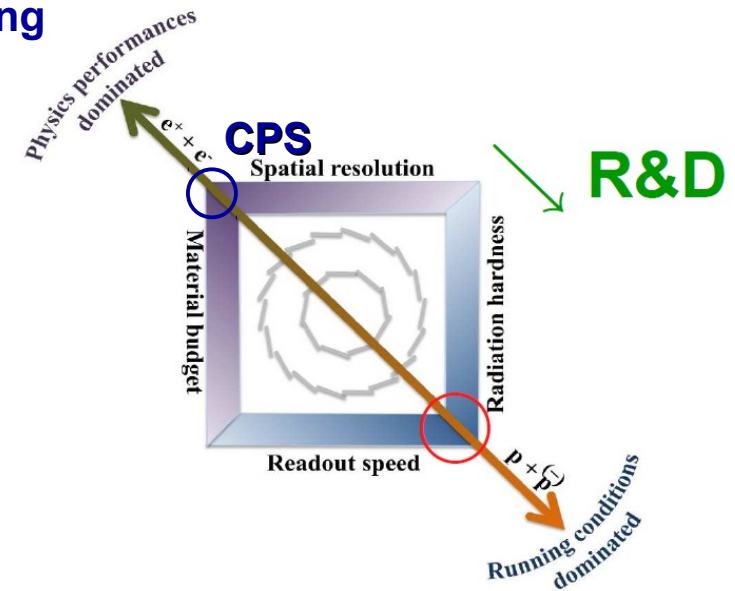
ALICE/CBM

2015/2019

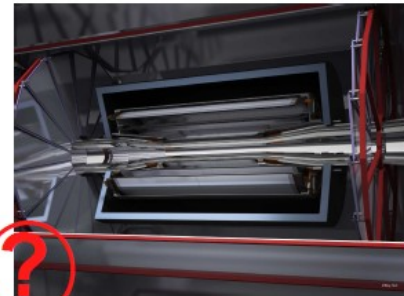


?X?/ILC

$\gtrsim 2020$



$O(1) \mu\text{s}$



Micro Vertex Detector (MDV) of CBM @ SIS100

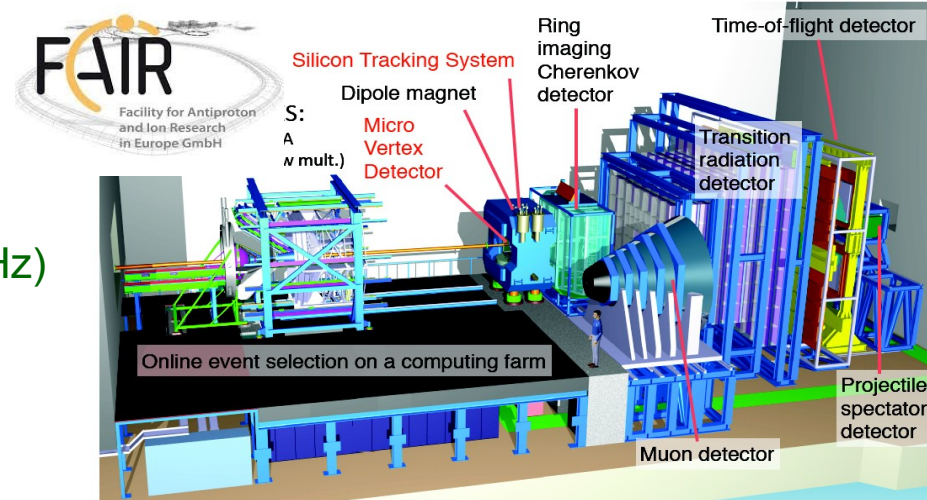
Goals

- Study of super-dense nuclear matter with relativistic ion-collisions
- Open charm from 30 GeV p-Au (10 MHz)
- Low-p tracker: 1-12 GeV Au-Au (30-100 kHz)

Beam on target ≥ 2021

MVD

- 4 planes of pixels sensors
- Sensor requirements

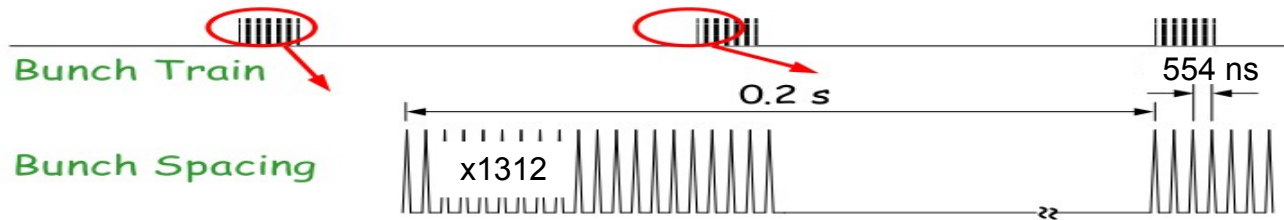


Sensor properties	MISTRAL - O	MIMOSIS-100 (preliminary)
Active surface	13.5 x 29.95 mm ²	~ 10 x 30 mm ²
Pixels	832 colls x 208 pixels	~ 1500 colls x 300 pixels
Pixel pitch	36 x 65 μm ²	22x33 μm ²
Integration time	20.8 μs	30 μs
Data rate	320 Mbps	> 6x 320 Mbps
Rad tol. (non-io)	>10 ¹² n _{eq} /cm ²	>3 x 10 ¹³ n _{eq} /cm ²
Rad tol (io)	> 100 kRad	> 3 MRad
Operation Temperature	+30°C	-20°C in vacuum

In reach with lightly modified APIDE (FSBB?)

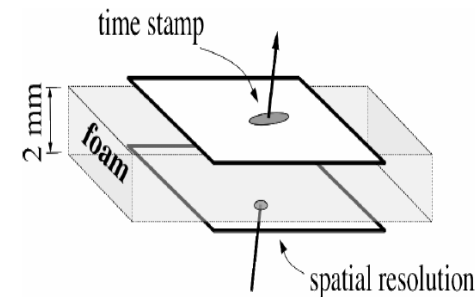
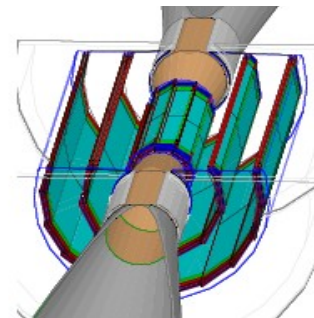
Towards ILC vertex detector

ILC collision scheme



Vertex detector (VXD) layout: 3 layers of double-sided CPS

- **Mini-vectors:** associate hits in double-sided layers (track seeding in VXD)
- Different optimization approaches for the different layers
 - **Innermost layers:** low surface & larger occupancy
 - ➔ Workout σ_{time} (reduce pile-up) & σ_{sp} (impact parameter)
 - **Outer layers:** larger surface & lower occupancy
 - ➔ Can deal with degraded σ_{time} & σ_{sp}
 - ➔ Minimize power consumption \Rightarrow material budget



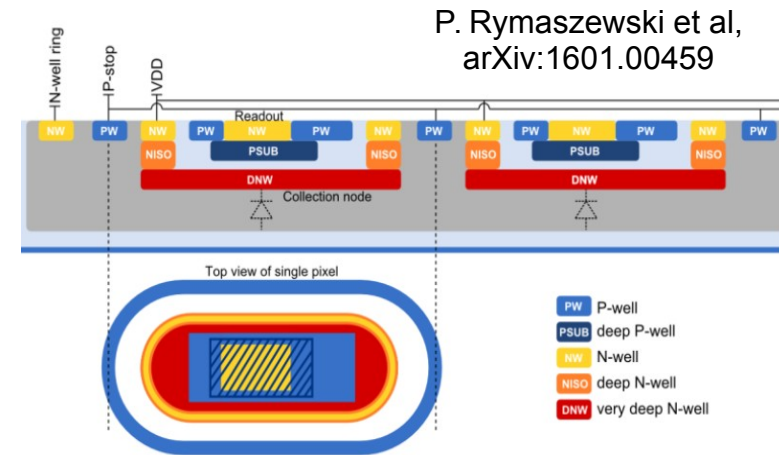
R&D ideas (So far a concept, design being started)

- **Innermost layer:** two digital output sensors with $\sigma_{\text{time}} \sim 1 \mu\text{s}$ (~2 bunches pile-up) in one side and $\sigma_{\text{sp}} \lesssim 3 \mu\text{m}$ on the other \Rightarrow Combine asynchr. (σ_{time}) and synchr. (σ_{sp}) readouts
- **Outer layers:** larger pixels with higher signal-charge-encoding resolution (3-4 bits)

Technology Perspectives for Performance Improvements

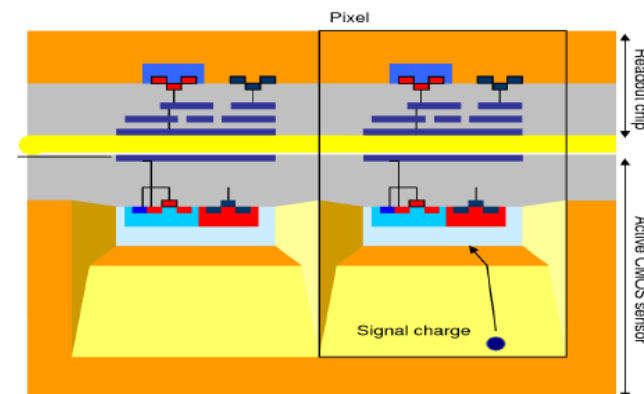
HV/HR-CMOS sensors: $d_{\text{dep}} \sim 0.3 \sqrt{\rho_{\text{sub}} \times U_{\text{bias}}}$

- Extend sensitive volume & improved q-collection
⇒ Faster signal & stronger rad. tolerance
- Not bound to CMOS processes using epi-layers
 - Easier access to VDSM (< 100 nm) process
 - Higher in-pixel μ -circuitry density
- Unanswered questions
 - Minimal pixel dimensions (σ_{sp}) ?
 - Uniformity over large sensitive area & production yield?



2-tiers chips

- Signal sensing (front-end) & processing (r.o.) parts distributed over two interconnected tiers (AC coupling)
- Smart sensor ⇒ 1 r.o. pixel addressing N pixel-front-ends
⇒ Reduce density of interconnections
- Can combine 2 diff. CMOS processes: front-end/r.o.
- Benefits:** small pixels ⇒ resolution, speed, data-compression and robustness
- Challenges:** interconnection technology (reliability & cost)



Ivan Peric: CPIX14, Bonn, 2014

Summary

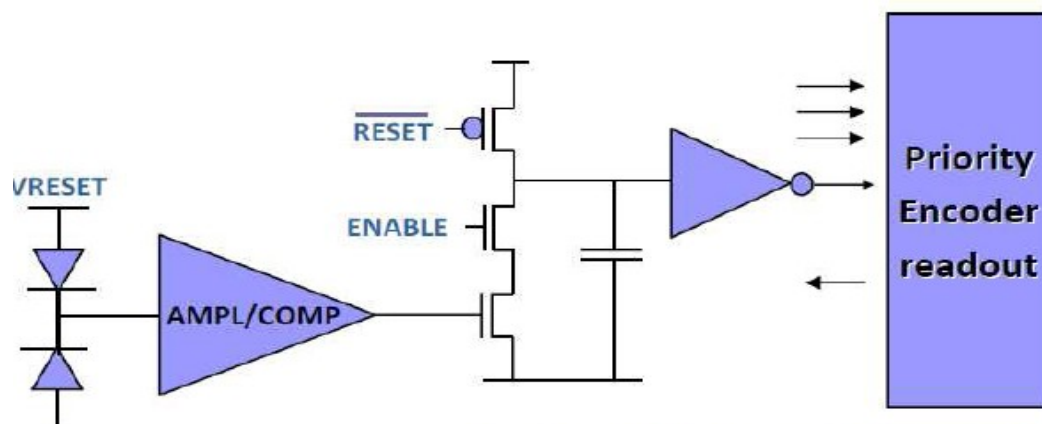
Summary

- **Substantial experience has been collected with running STAR-PXL proving added value of CPS to physics**
 - Demonstrated that CPS can provide spatial resolution and material budget required for numerous applications
- **CPS are suited for vertex detectors ($\ll 1 \text{ m}^2$) and have attractive features for tracking devices ($\gg 1 \text{ m}^2$)**
- **Forthcoming Challenges**
 - **CPS for inner trackers:** ALICE-ITS \Rightarrow large area (10 m^2) to cover with 20-30k sensors
 - **Improve rad. tolerance:** CBM experiment @ FAIR/GSI $\Rightarrow \gtrsim 10 \text{ MRad} \oplus \gtrsim 10^{14} n_{\text{eq}}/\text{cm}^2$
 - **Improve readout speed:** ILC vertex detector $\Rightarrow \lesssim 1 \mu\text{s}$
- **Perspectives for technological advances**
 - **HV/HR-CMOS sensors:** improvement on charge collection
 \Rightarrow faster signal and stronger rad. tolerance
 - **2-tier sensors:** combine of 2 CMOS processes for sensing & r.o. parts
 \Rightarrow more in-pixel intelligence

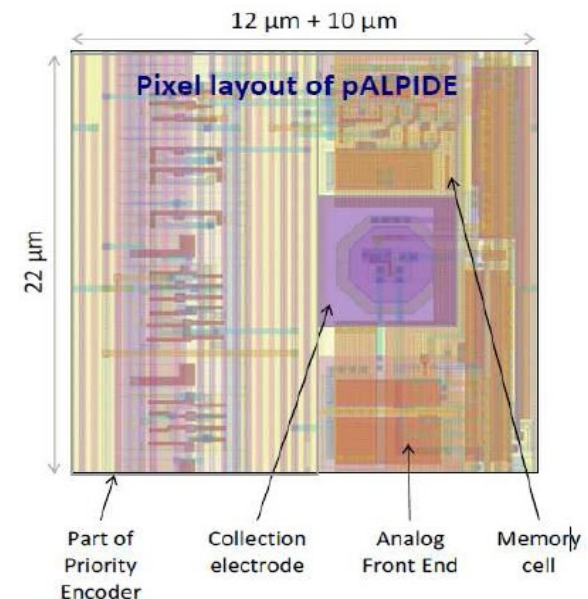
Backup

ALPIDE (ALice Pixel DEtector): readout architecture

- **Concept similar to hybrid pixel readout architecture**
 - TowerJazz CIS quadrupole well process: both N & P MOS can be used
- **Continuously power active in each pixel**
 - Low power consumption analogue front-end ($< 50\text{nW/pixel}$) based on single stage amplifier with shaping
 - High gain ~ 100
 - Shaping time few μs
 - In-pixel discriminator
 - Binary output stored into multi-event buffer awaiting for external readout
- **Only zero-suppressed data transferred to periphery \Rightarrow priority encoder readout**



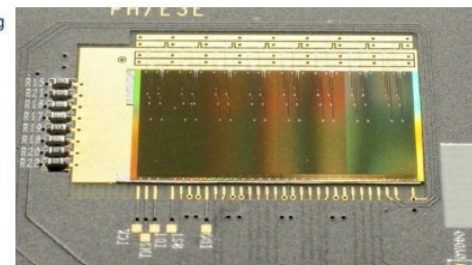
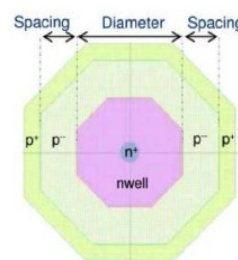
Courtesy of W. Snoeys / TWEPP-2013



ALPIDE: performances assessment

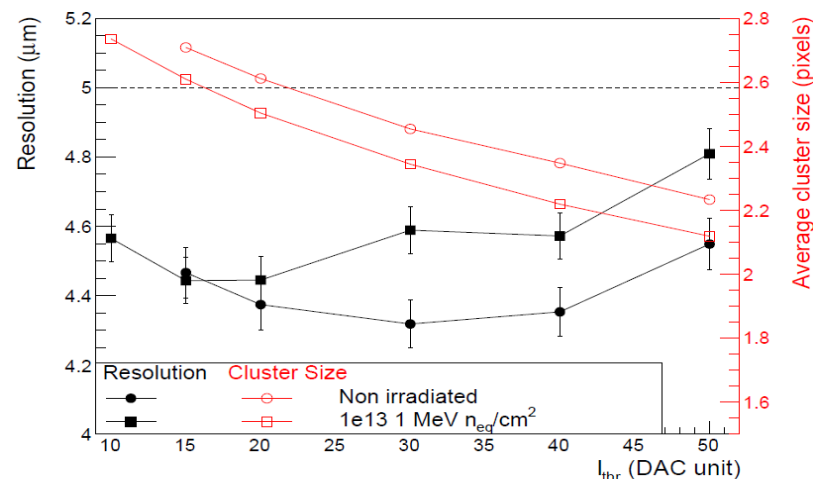
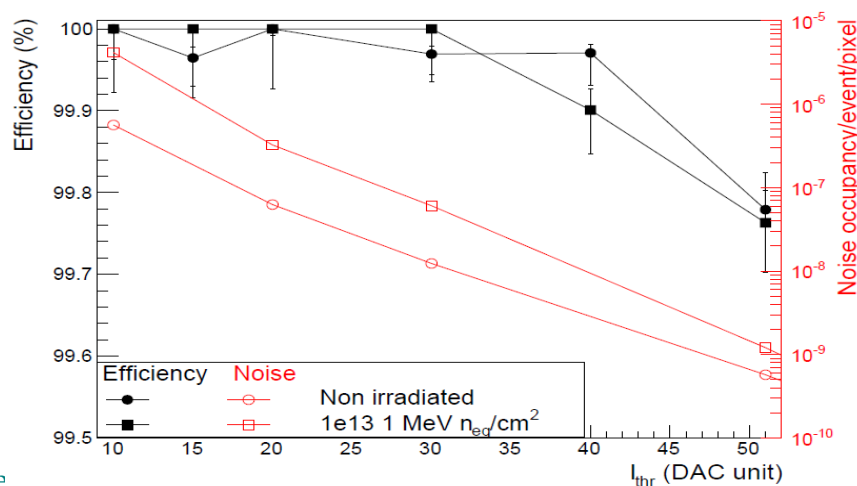
APIDE-1 beam test @ DESY (5-7 pions)

- Final sensor dimensions: 15x30 mm²
- ~0.5M pixels of 28x28 μm²
- 4 different sensing node geometries
- Possibility of reverse biasing the substrate
⇒ default is -3 V (better epi-layer depletion)
- Possibility to mask pixels (fake-rate mitigation)
⇒ default is O(10⁻³) pixels



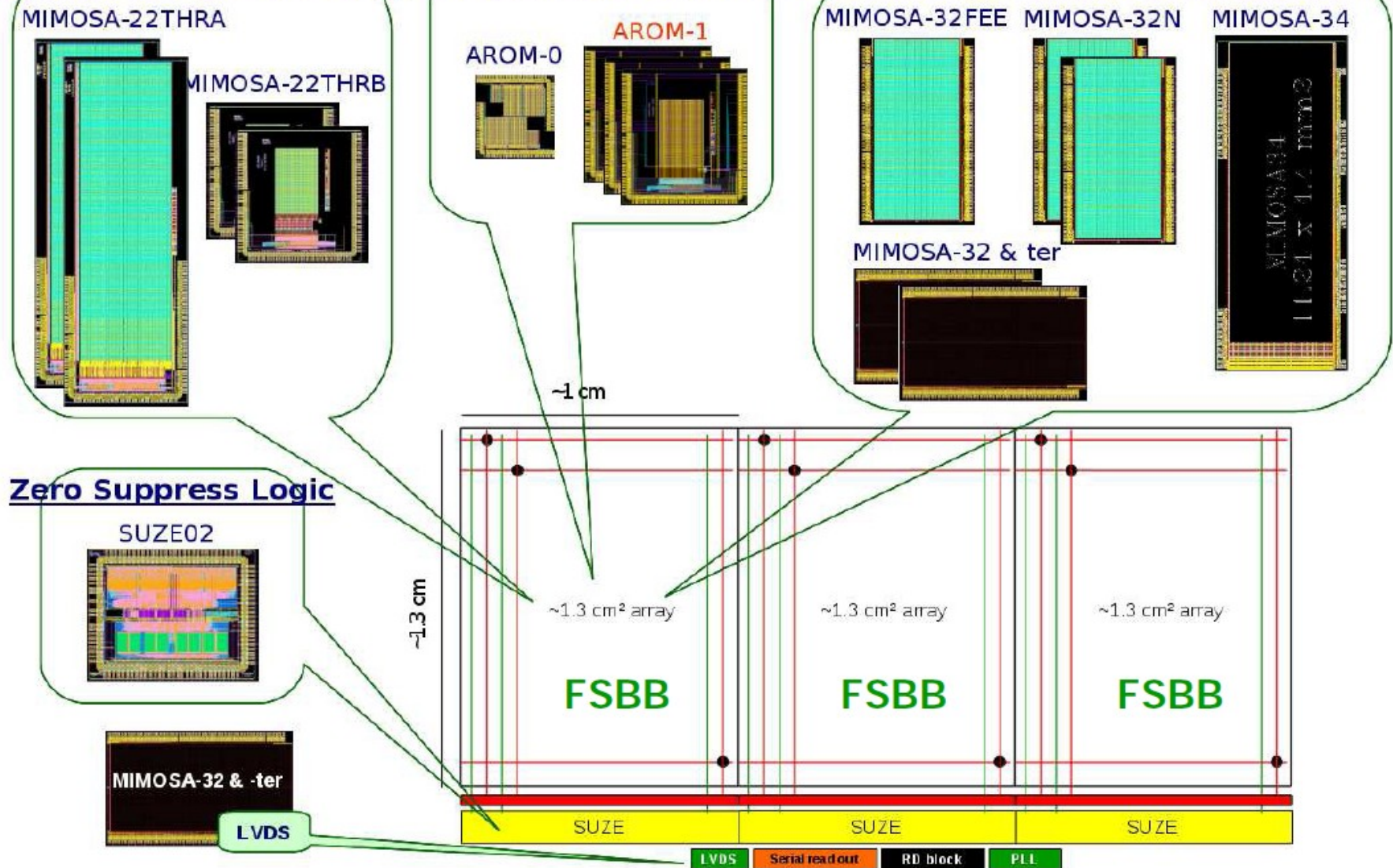
Performances

- $\epsilon_{\text{det}} > 99\%$, $\sigma_{\text{sp}} < 5\mu\text{m}$, fake-rate $< 10^{-5}$
- Slight deterioration after irradiation



Exploring full sensor chain: Prototypes fabricated

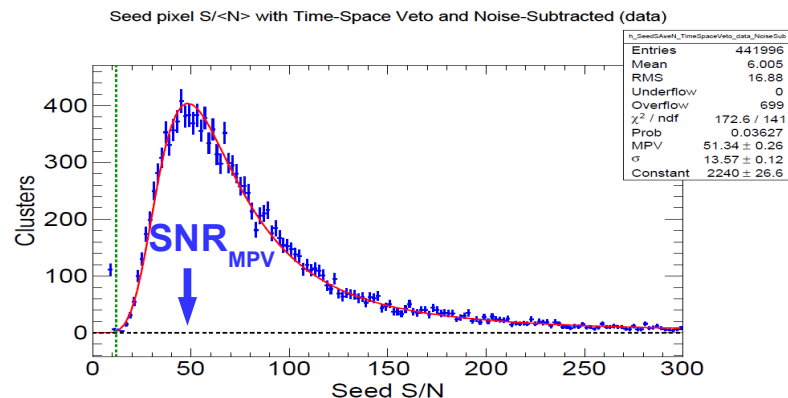
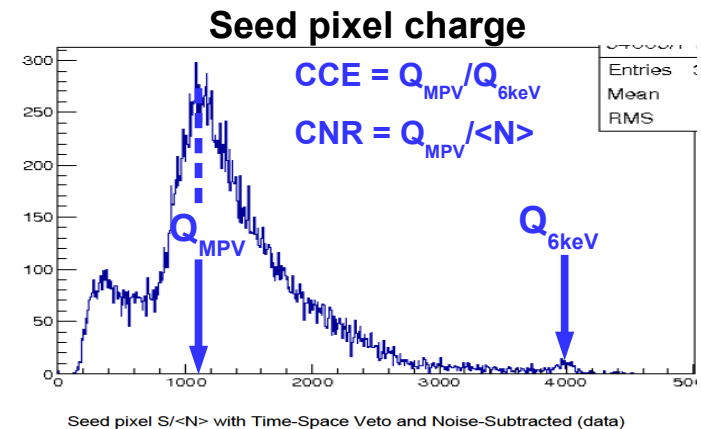
MISTRAL RO Architecture ASTRAL RO Architecture Diode + in-pixel amplification Optimisation



The Testing Probes

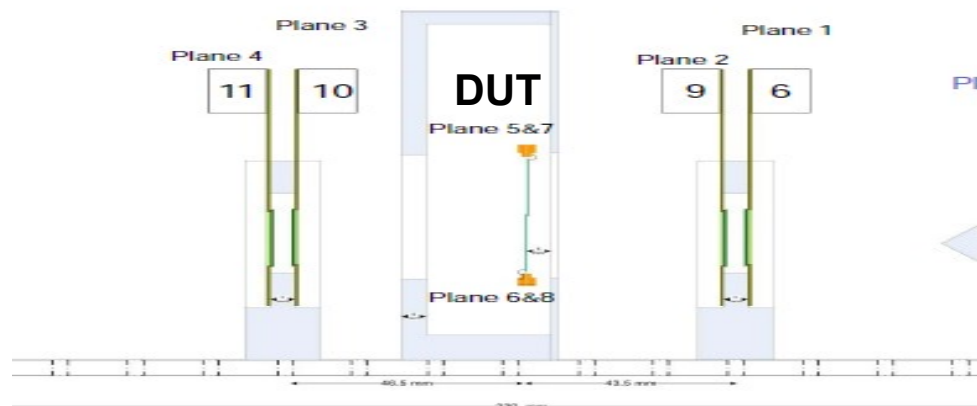
Laboratory tests

- Noise characterization and fake rate
- ^{55}Fe X-ray source
 - ~6keV line
 - Gain, CCE and CNR
- ^{90}Sr β^- source ($Q = 2.28$ MeV)
 - SNR, ϵ_{det} and cluster multiplicity



Test-beam (TB) facilities

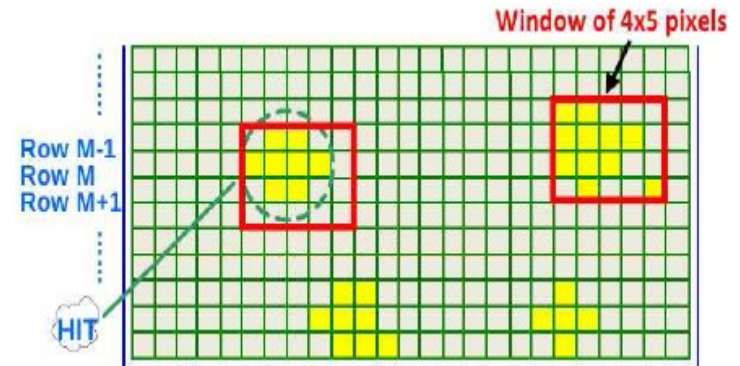
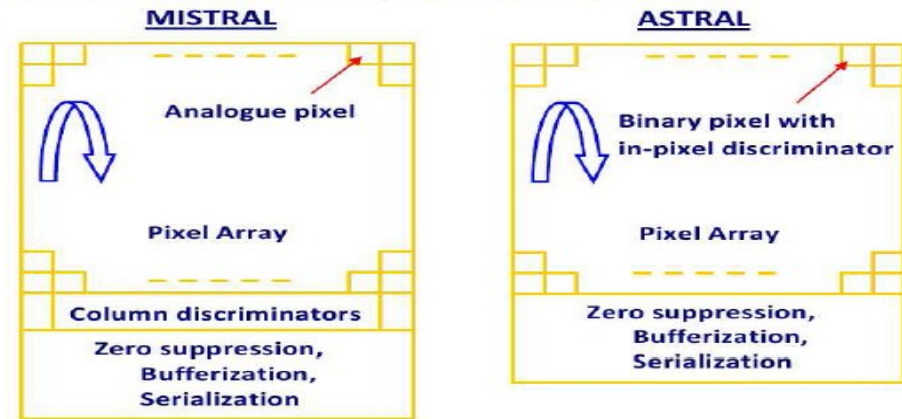
- SPS: ~100 GeV/c π^\pm
- DESY: ~5 GeV/c e^-
- Frascati: ~500 MeV/c e^-
- SNR, ϵ_{det} , cluster multiplicity and σ_{sp}



MISTRAL-O: Synchronous readout

Design addresses 3 issues

- Increasing S/N at pixel-level
 - Sensing node optimization
- ADC @
 - end-of-column \Rightarrow MISTRAL
 - pixel \Rightarrow ASTRAL
- SUZE at chip periphery
 - 2D sparsification algorithm with 4x5 pixels window (evolution from 1D sparsification on ULTIMATE chip)



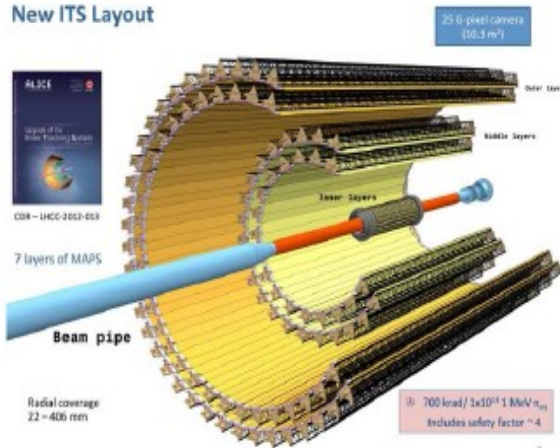
Power vs Speed

- Power:** only the selected rows ($N=1,2,3 \dots$) to be readout
- Speed:** N rows of pixels are readout in ||
 - Integration-time (t_{int}) = frame readout time \Rightarrow

$$t_{int} = \frac{(\text{Row readout time}) \times (\text{No. of Rows})}{N}$$

R&D of CMOS pixel sensors

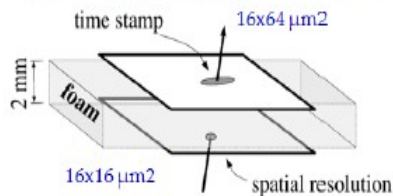
New ITS Layout



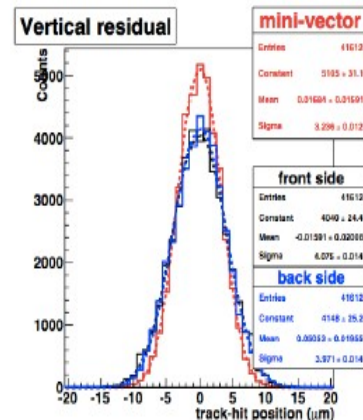
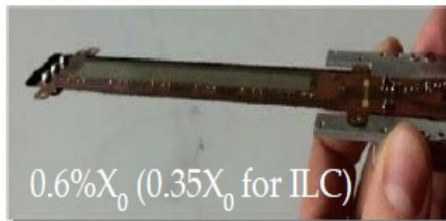
ALICE-ITS = NEW DRIVING APPLICATION OF CPS
based on a better suited (180 nm) CMOS process
(TDR approved by LHCC in March '14)

- ❖ 1st real scale sensor prototype adapted to 10 m² fabricated
 - 1st test results validate architecture in 180 nm technology
 - 2-4 times faster read-out w.r.t. 0.35 μm technology, with up to 60 % power reduction

CPS MAPS: Spatial Resolution and Time Stamping

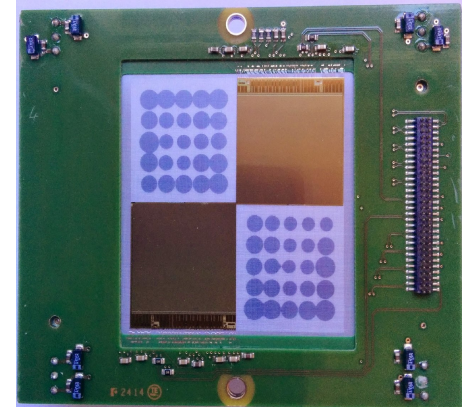


Ultrathin ladder - PLUME



AIDA Telescope

- Big surface and thin reference planes with high spatial resolution
 - Sensing area = 4x3.8cm²
 - Additional plane with high temporal resolution
- ⇒ time stamping



Sensor integration in Ultra Light Devices

- Double sided ladders expected benefits

- Alignment & tracking (pointing)
- Beam background rejection ?
- Material budget, 1 mechanical support
- Redundancy (efficiency)
- Each layer optimized
 - read-out speed vs resolution

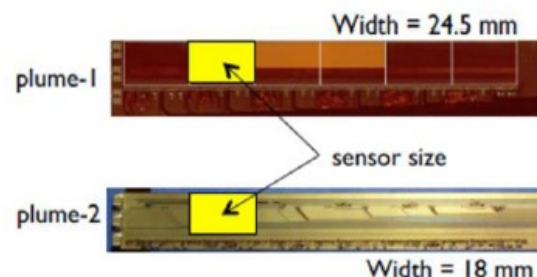
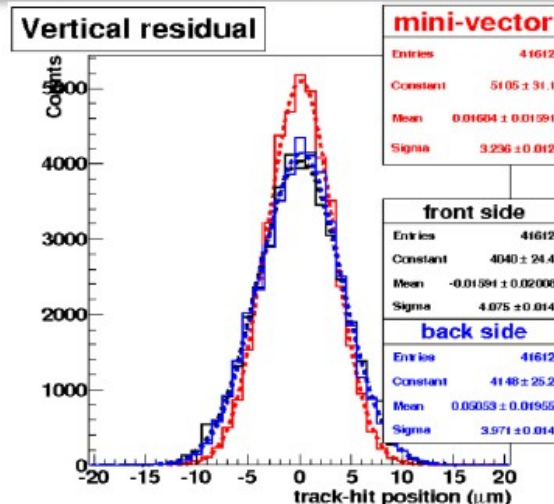
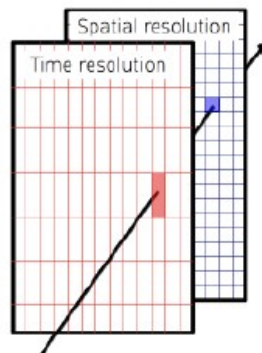
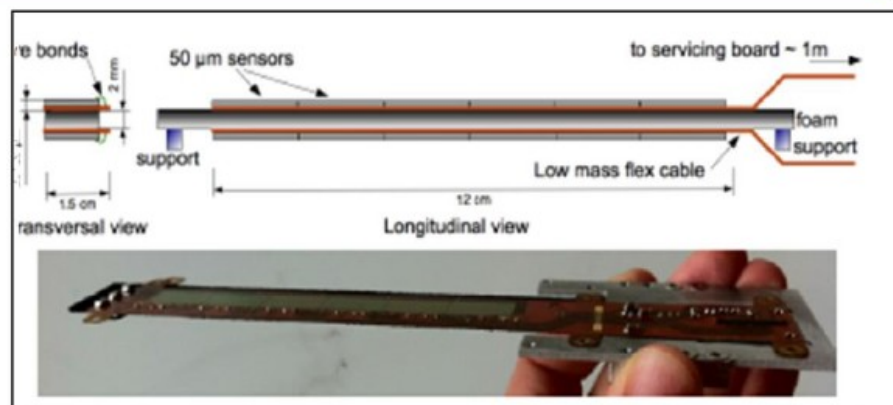
- PLUME coll. (Bristol, DESY, IPHC)

- Plume 01 prototype (<2012)

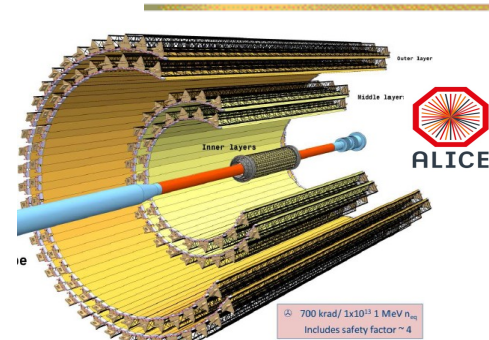
- Fabricated
 - 2 x 6 Mimosa 26 chips
 - 2 mm low density SiC foam
 - Validated in test beam (2011)
 - Operated with air cooling
 - 0.6 % X_0

- Plume 02 prototype

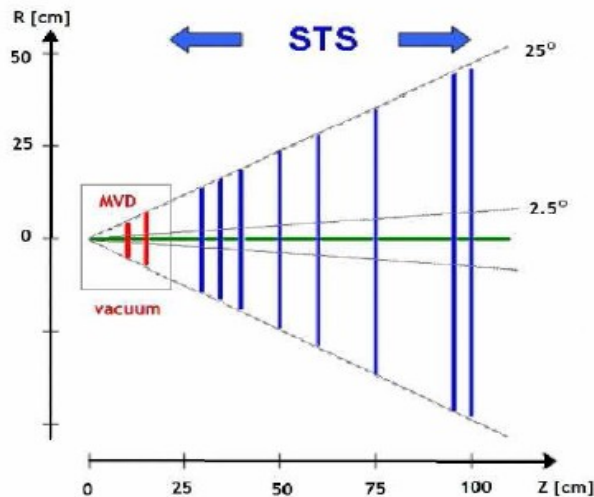
- Under construction (spring 2015)
- Reduced mat. Budget
 - Reduced width (24.5 mm \Rightarrow 18mm)
 - Lighter (alu) flex cable, mechanical support
 - 0.6 % $X_0 \Rightarrow \sim 0.35 \% X_0$ (cross-section)



Next Forthcoming device: CBM Micro-Vertex Detector (MVD)



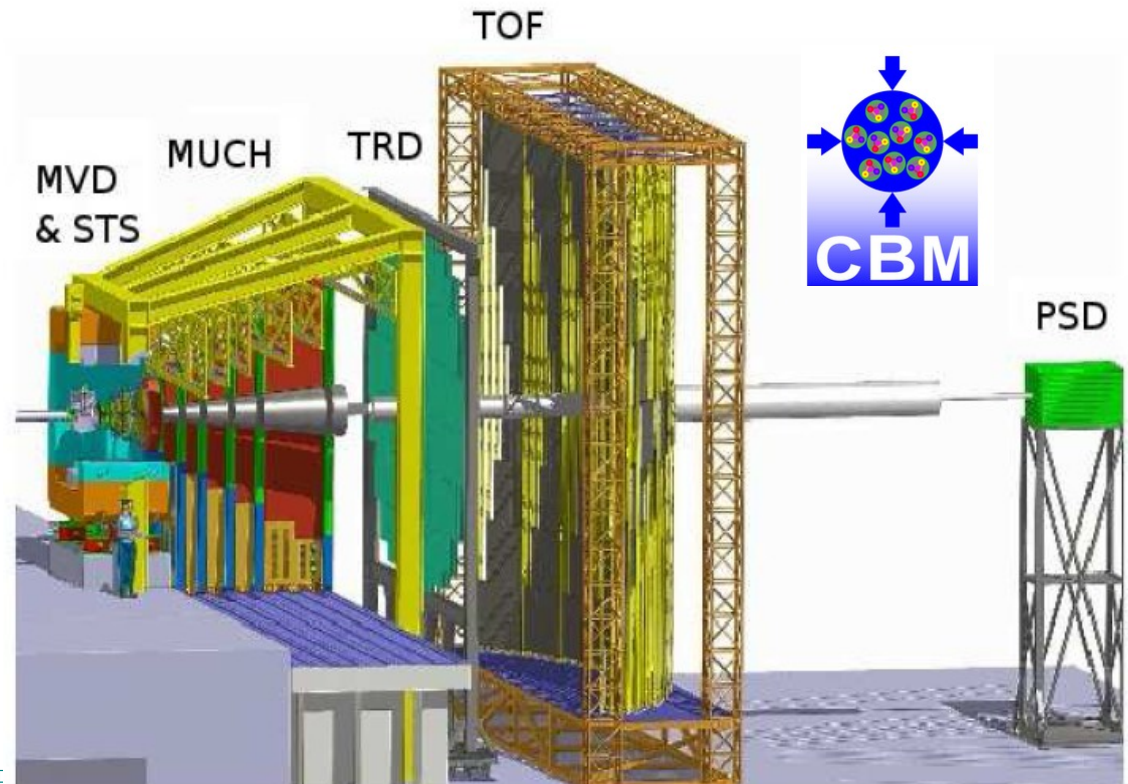
ALICE-ITS 2018/19



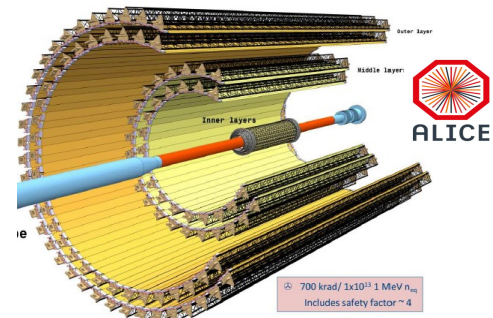
CBM-MVD at FAIR/GSI

3 double-sided stations in vacuum at $T < 0^\circ\text{C}$

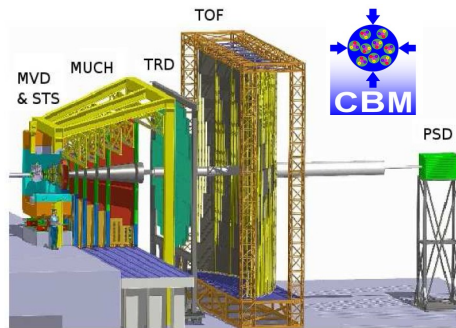
- $\sigma_{sp} \lesssim 5 \mu\text{m}$
- $\sim 0.5 \% X_0 / \text{station}$
- Radiation load: $\gtrsim 10^{14} n_{eq}/\text{cm}^2$



Device under Study: ILC Vertex Detector



ALICE-ITS 2018/19

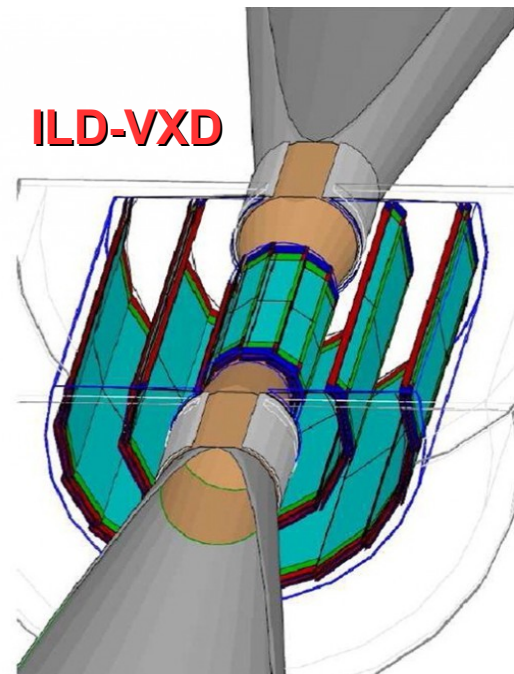
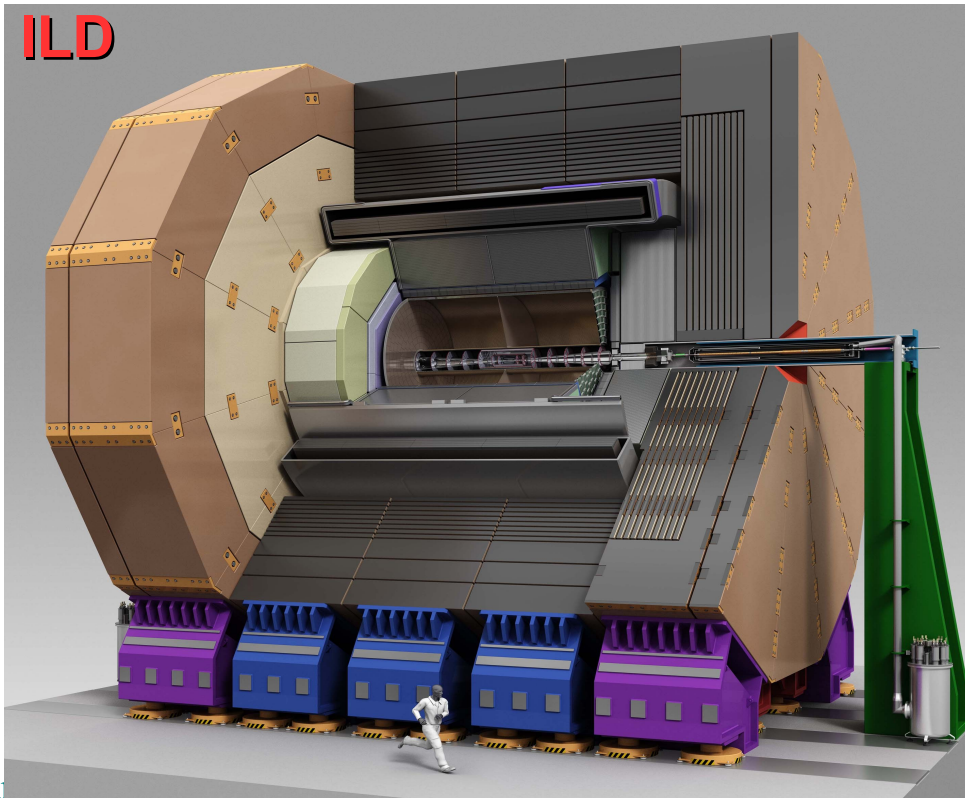


CBM-MVD > 2020

ILD-VXD at ILC

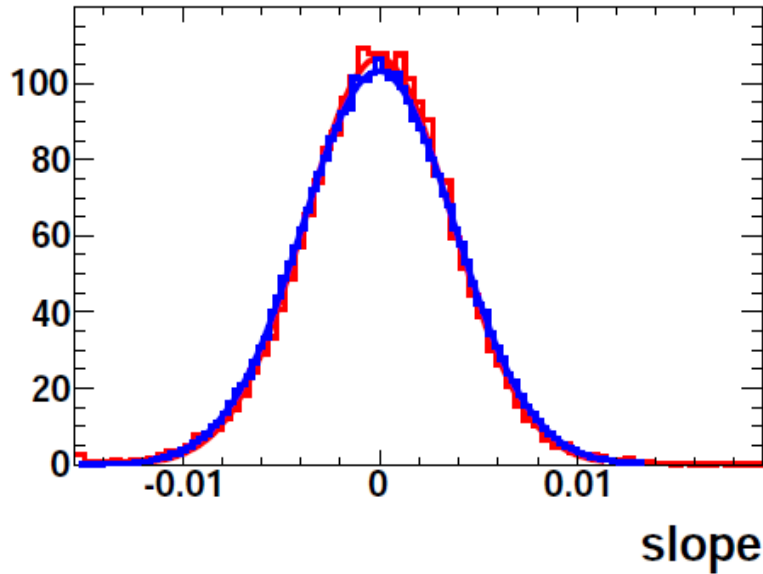
3 double-sided layers

- $\sigma_{sp} \lesssim 3 \mu\text{m}$
- $\sim 0.3 \% X_0 / \text{layer}$
- Radiation load: $O(100) \text{ kRad} + O(10^{11}) n_{eq}/\text{cm}^2 (1\text{yr})$

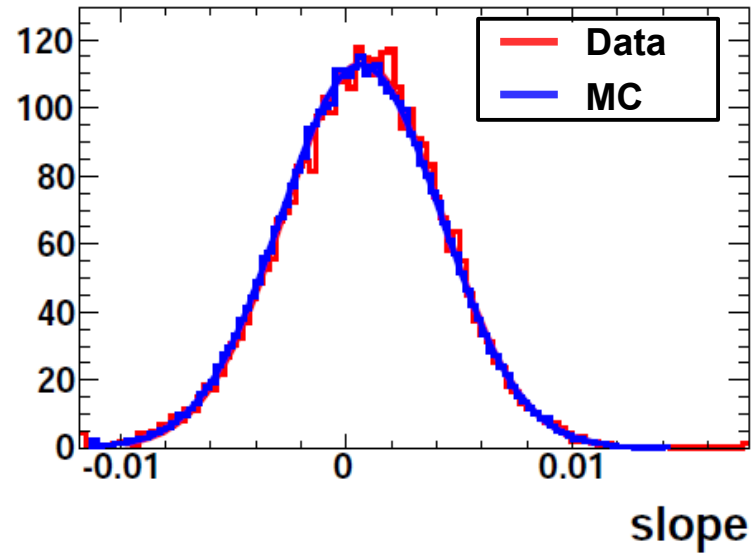


BTF Telescope Simulation: Performances (I)

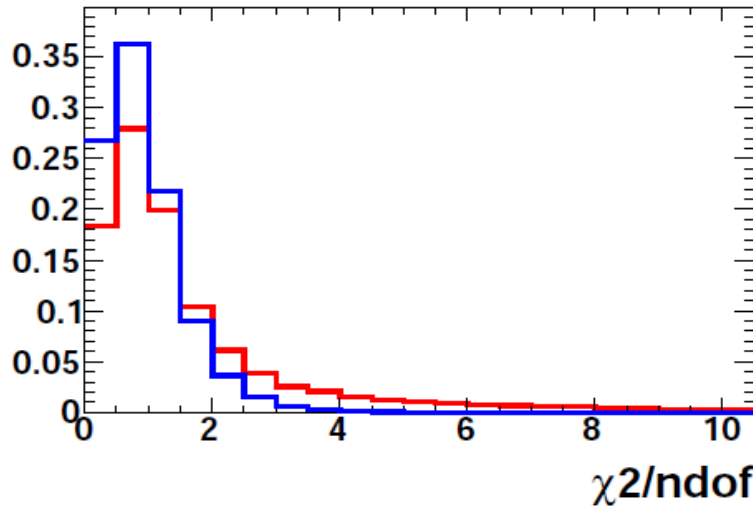
Track slopes $X=f(Z)$



Track slopes $Y=f(Z)$

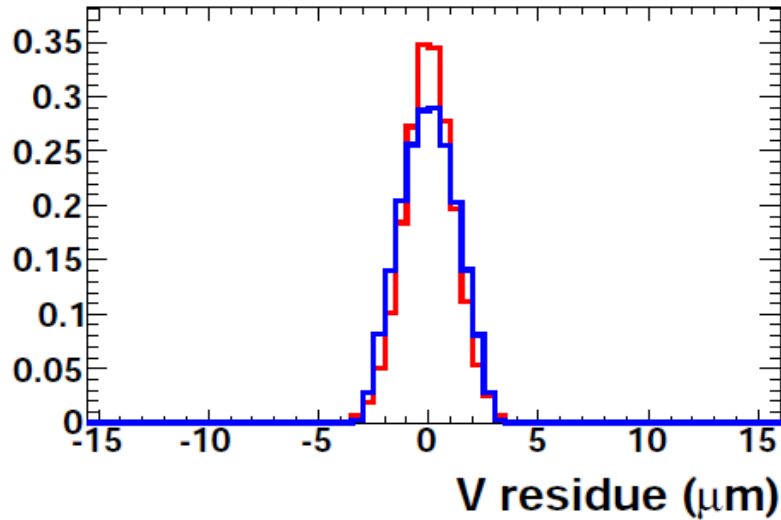


χ^2/ndof of tracks

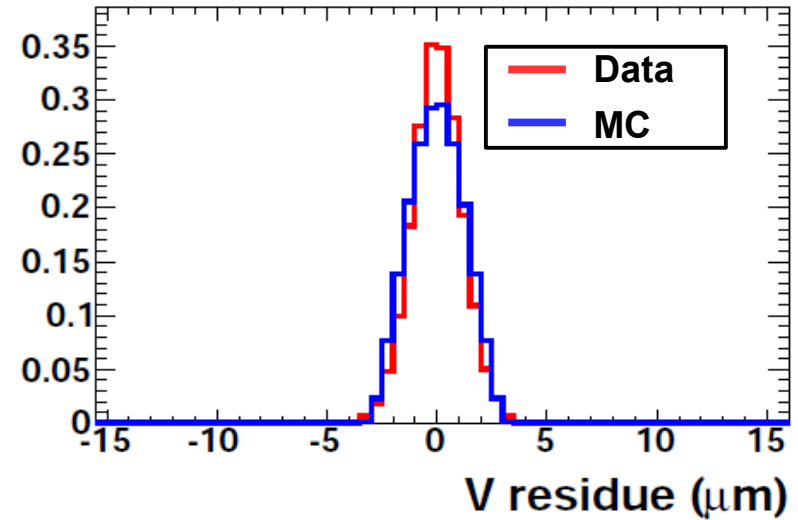


BTF Telescope Simulation: Performances (II)

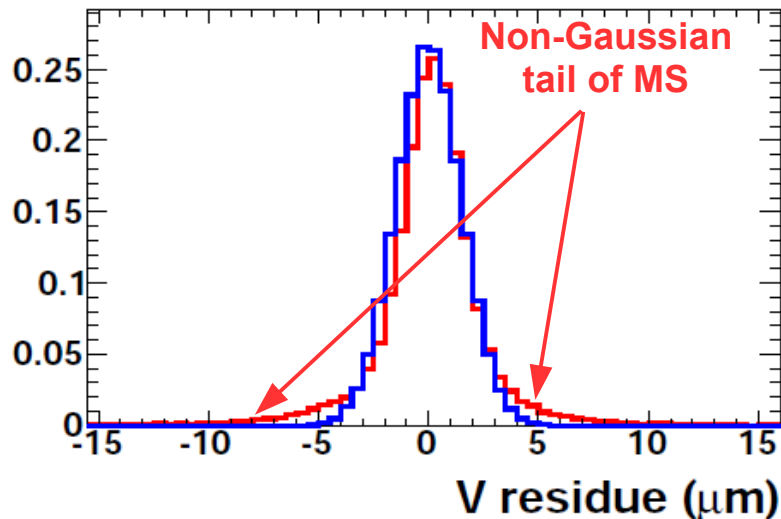
Hit-track vertical residual, 1st Mi18



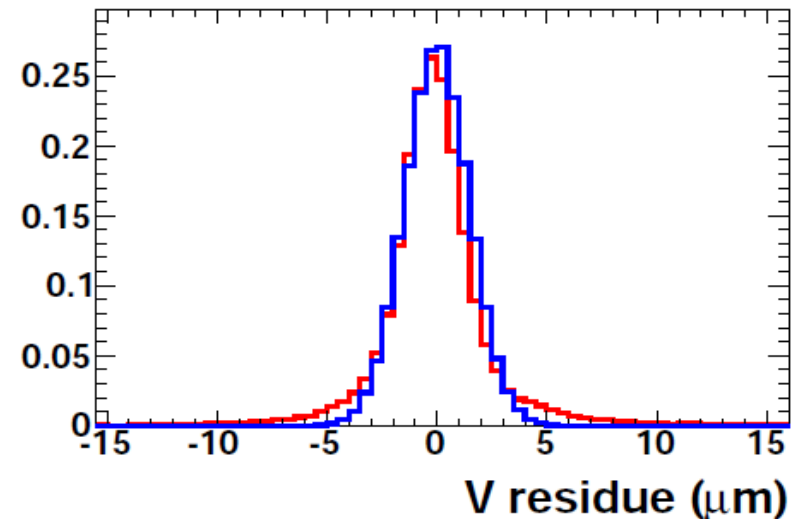
Hit-track vertical residual, 2nd Mi18



Hit-track vertical residual, 3rd Mi18



Hit-track vertical residual, 4th Mi18



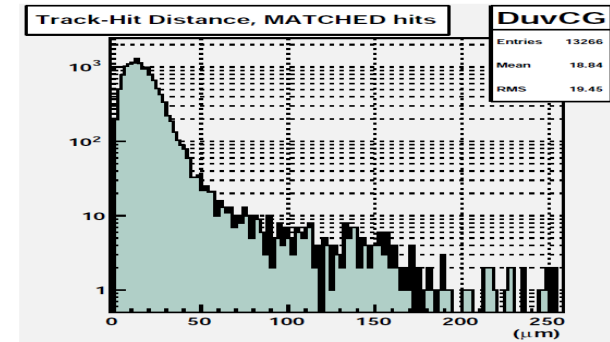
BTF Analysis strategy & Efficiency correction

Analysis strategy

- Reconstruct tracks and extrapolate @ DUT
- Associate DUT hits to track within track-hit distance cut
- Evaluate DUT ϵ_{det} and σ_{sp}

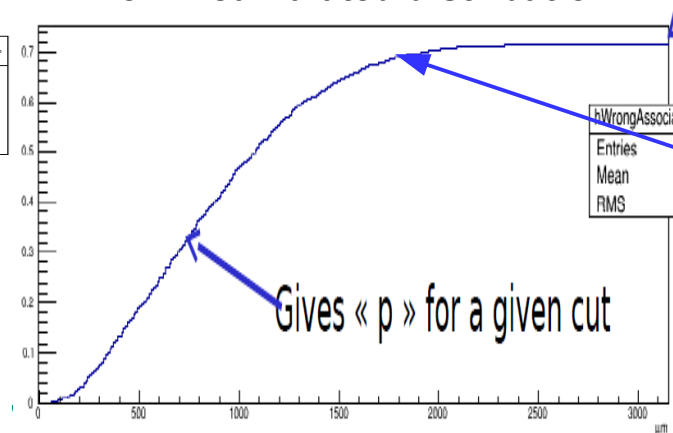
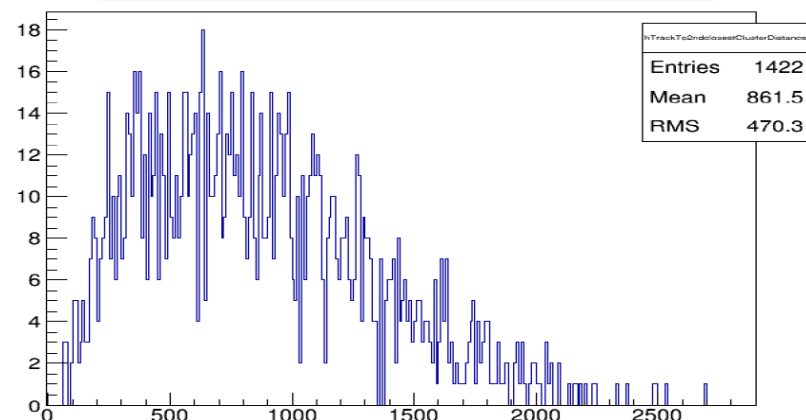
Efficiency Correction: $\epsilon_{\text{det}}^{\text{corr}} = (\epsilon_{\text{det}}^{\text{raw}} - p) / (1 - p)$

- Due to MS non-Gaussian tails some track-hit distance seems quite large (few 100 μm)
 - Enlarging the track-hit distance has 2 consequences on non-efficient events
 - ➔ Increases probability to get a fake hit in this area
 - ➔ Increases probability to associate a real hit from other track
- Method
 - Use efficient events to get the distribution of the 2nd closest hit to the track
 - Use normalized cumulated distribution to estimate p



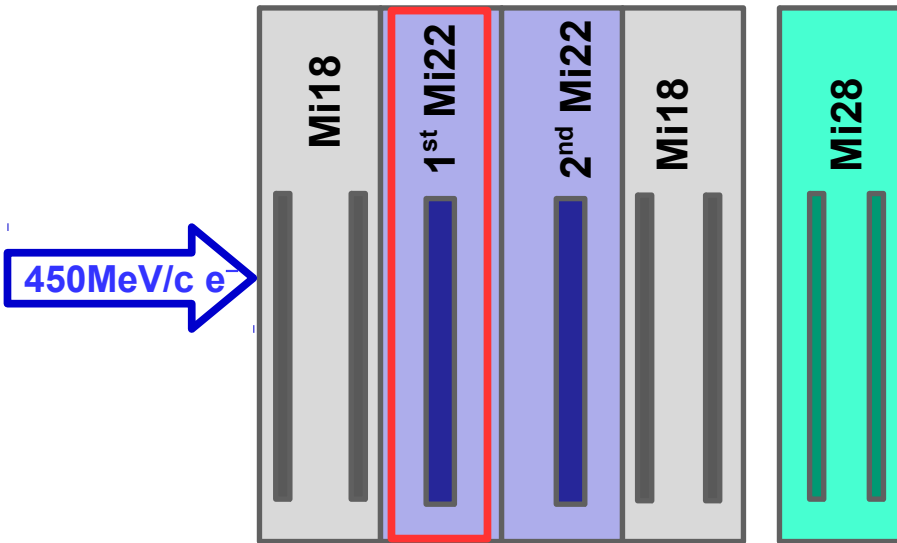
Track - hit distance of the 2nd closest hit

Norm. cumulated distribution



Doesn't saturate to 1
because some events
have only one hit

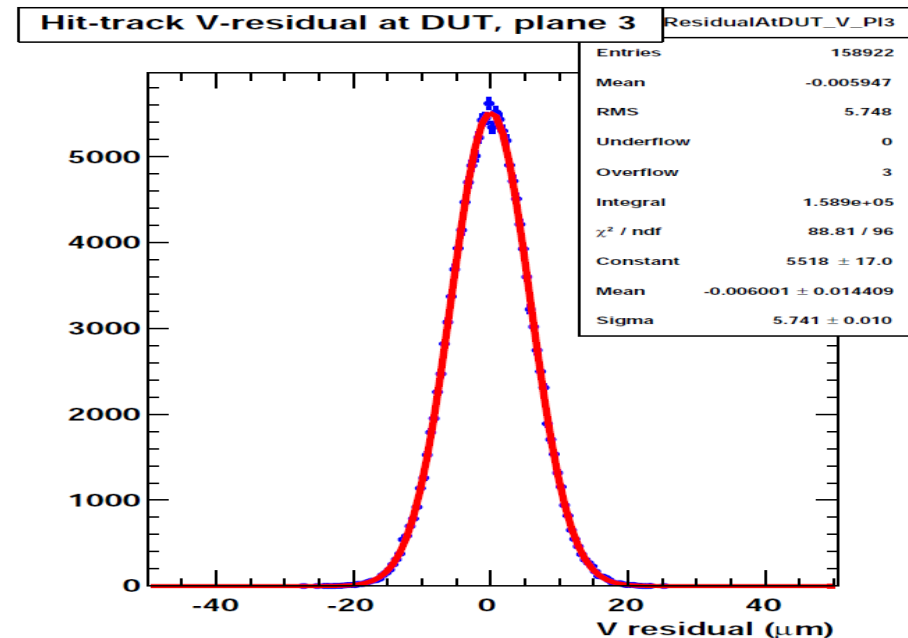
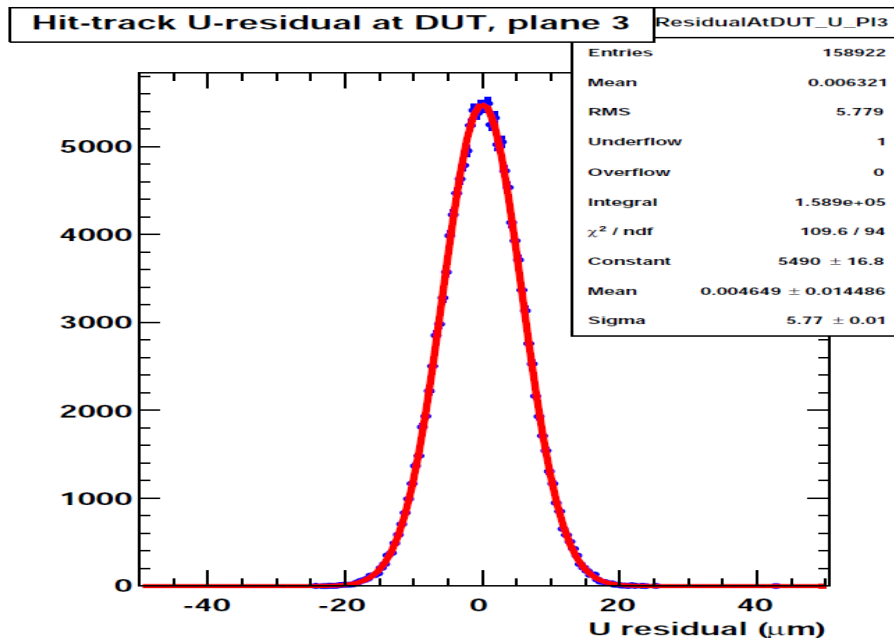
BTF Telescope Simulation: σ_{Tel} @ 1st DUT position



Telescope resolution @ 1st DUT position
(both DUTs supposed thinned to 50 μm)

$$\sigma_{\text{Tel}} = (5.77 \pm 0.01_{\text{stat}} \pm 0.20_{\text{syst}}) \mu\text{m}$$

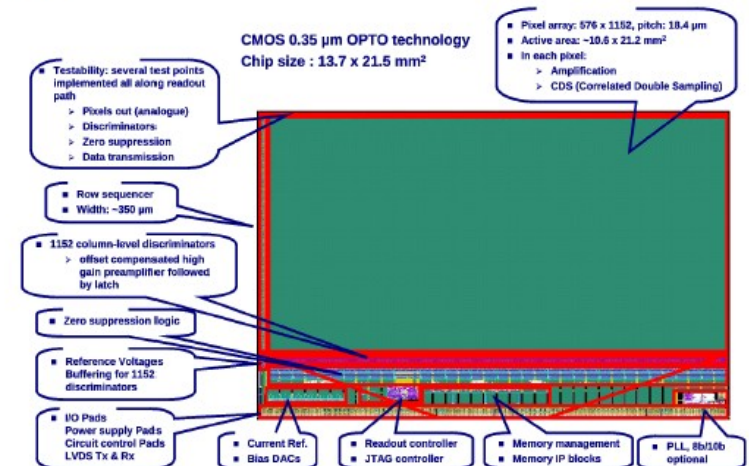
Telescope resolution confirmed
with Geant3 based simulation



CMOS Pixel Sensors: Established Architecture

- Main characteristics of MIMOSA-26 sensor equipping EUDET BT :

- 0.35 μm process with high-resistivity epitaxial layer
(coll. with IRFU/Saclay)
- column // architecture with in-pixel amplification (cDS)
and end-of-column discrimination, followed by \emptyset
- binary charge encoding
- active area: 1152 columns of 576 pixels ($21.2 \times 10.6 \text{ mm}^2$)
- pitch: 18.4 $\mu m \rightarrow \sim 0.7$ million pixels
 - ▷ charge sharing $\Rightarrow \sigma_{sp} \sim 3\text{-}3.5 \mu m$
- $t_{r.o.} \lesssim 100 \mu s$ ($\sim 10^4$ frames/s)
 - \rightarrow suited to $> 10^6 \text{ part./cm}^2/\text{s}$
- JTAG programmable
- rolling shutter architecture
 - \Rightarrow full sensitive area dissipation $\cong 1$ row
 - ▷ $\sim 250 \text{ mW/cm}^2$ power consumption (fct of N_{col})
- thinned to 50 μm (yield $\sim 90 \%$)

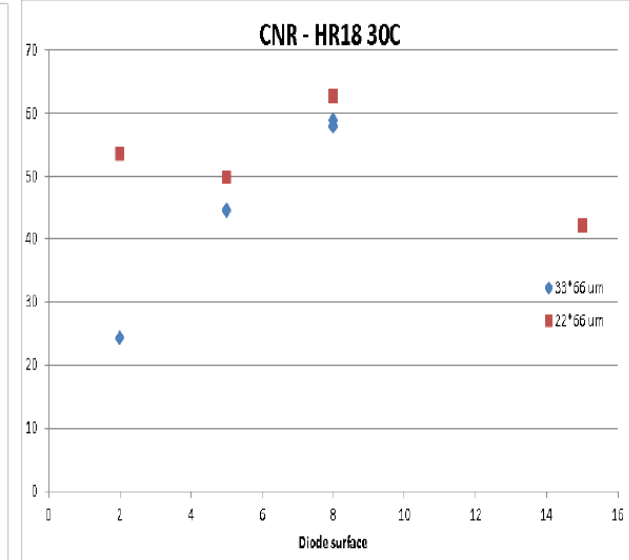
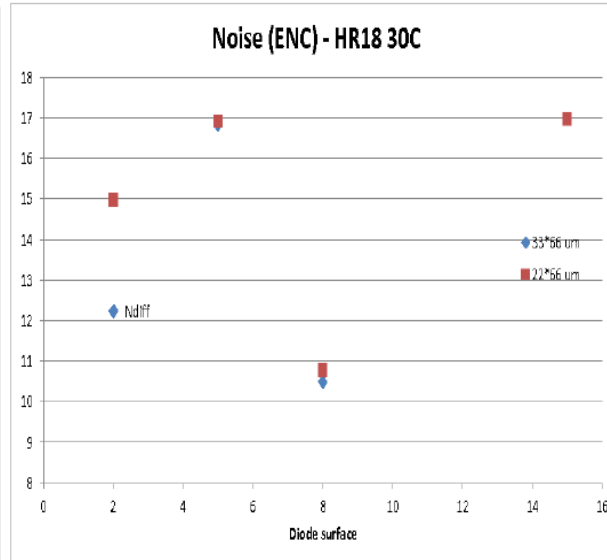
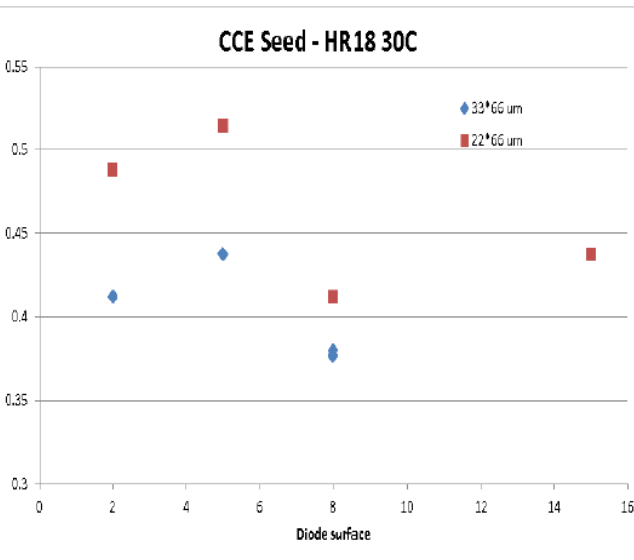


- Various applications : VD demonstrators, NA63, NA61, FIRST, oncotherapy, dosimetry, ...

⁵⁵Fe source: CCE/Noise/CNR vs diode for large pixels

- CCE, TN and CNR vs sensing node for large pixels with HR18 epi-layer

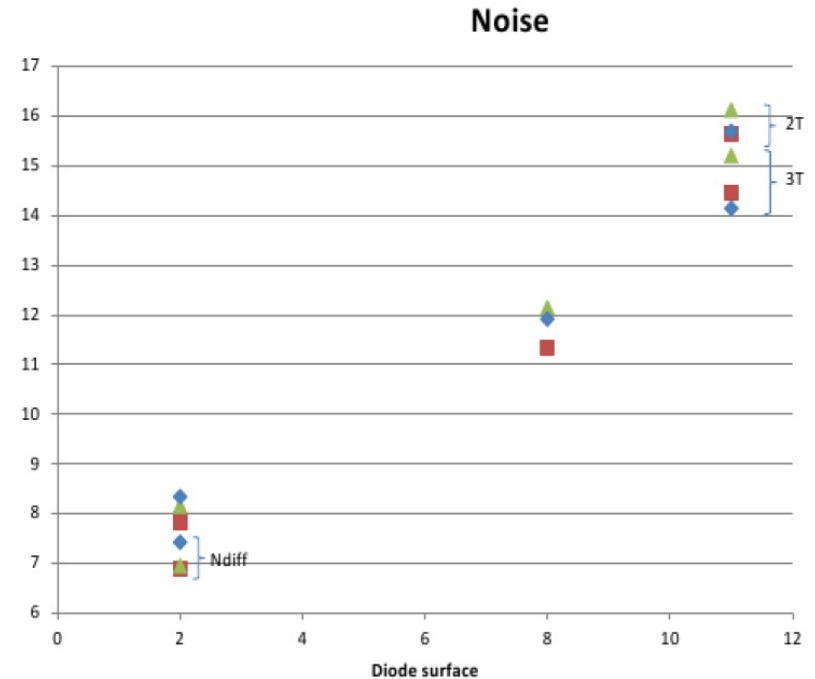
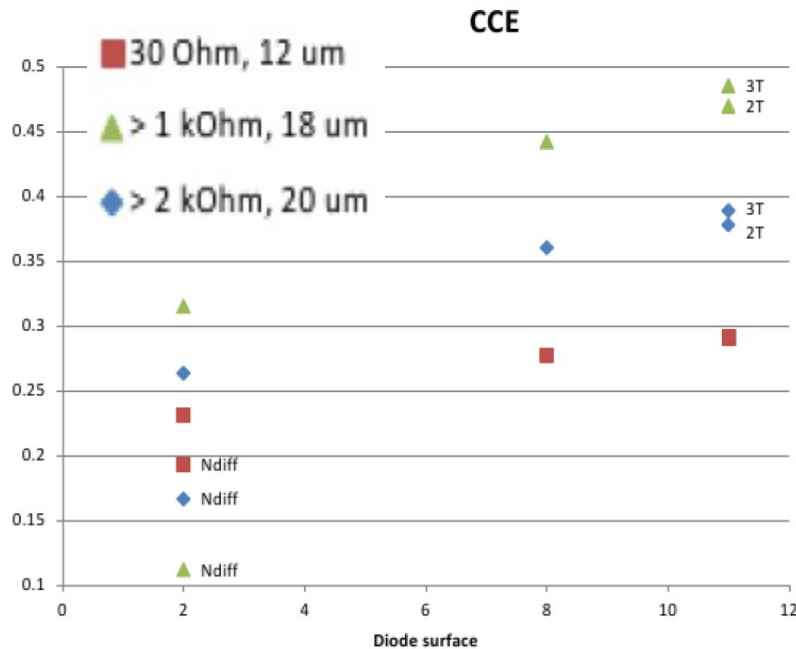
◆ 33*66 μm
■ 22*66 μm



- Good to excellent CCE, even for small sensing diodes or for 33x66 μm^2 pixels
- TN $\sim 17/11$ e^- ENC for single 10.9/8 μm^2 sensing diodes
- TN $\sim 17/15$ e^- ENC for pairs of 5/2 μm^2 sensing diodes
- High CNR: up to ~ 60 for 8 μm^2 sensing diodes
- Pixel detection performances fully satisfactory \Rightarrow confirmation from beam test (see next slide)

⁵⁵Fe source: CCE & Noise vs diode for small pixels

- CCE and TN for $22 \times 33 \mu\text{m}^2$ pixels for different diode dimensions (footprint $10.9 \mu\text{m}^2$)

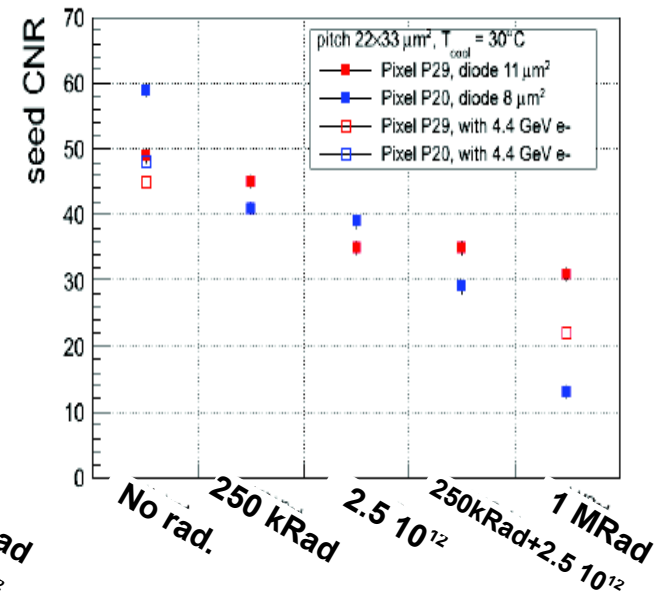
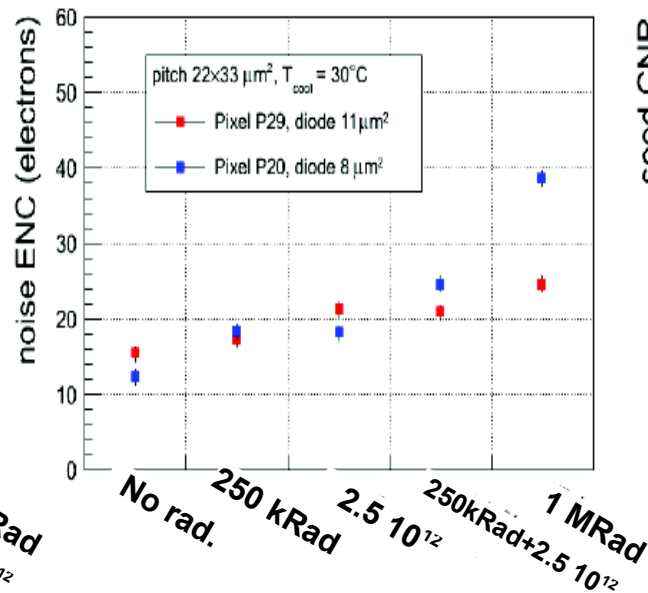
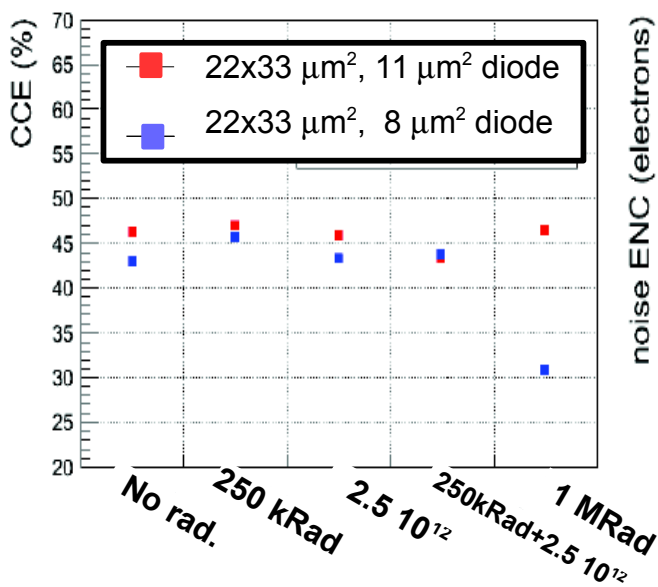


- CCE is highest for HR18 epi-layer
- Weak dependence of CCE with diode dimensions \Rightarrow around 30% for $2 \mu\text{m}^2$
- Nearly linear variation of TN with diode dimensions
 $\Rightarrow 8 \rightarrow 16 \text{ e}^- \text{ ENC}$ for diode $2 \rightarrow 10.9 \mu\text{m}^2$
- Small sending diode with $> 10 \mu\text{m}^2$ footprint attractive in terms of CCE

^{55}Fe source: radiation tolerance for $22 \times 33 \mu\text{m}^2$ pixels

MIMOSA-34:

- $22 \times 33 \mu\text{m}^2$ pixels with diode of 8 and $10.9 \mu\text{m}^2$: TN and CCE/CNR @ $T = 30^\circ\text{C}$ from ^{55}Fe source for different irradiations
- Comparison when possible of CNR and SNR from 4.4 GeV e^- TB (DESY)
- **Comments:**
 - Small diode more sensitive to TID
 - TID impacts both CCE and TN
 - CNR of $10.9 \mu\text{m}^2$ diode pixel exceeds 20 (MPV) after 250 kRad + $2.5 \times 10^{12} n_{\text{eq}}/\text{cm}^2$



MIMOSA-34: sensing node impact for small pixels

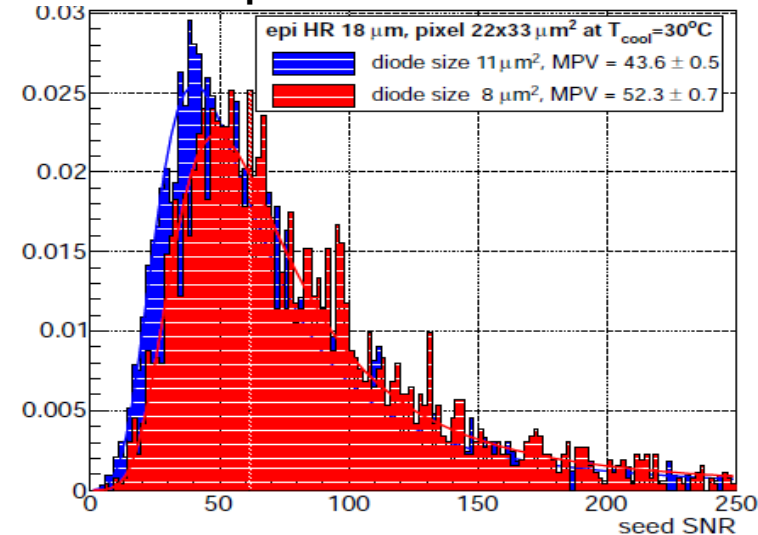
■ DESY BT Set-up (August 2013):

- 2BT: 8xSi-strips & 6xMIMOSA-26 (120 μm thick)
- $\sim 4.4 \text{ GeV/c } e^-$ beam

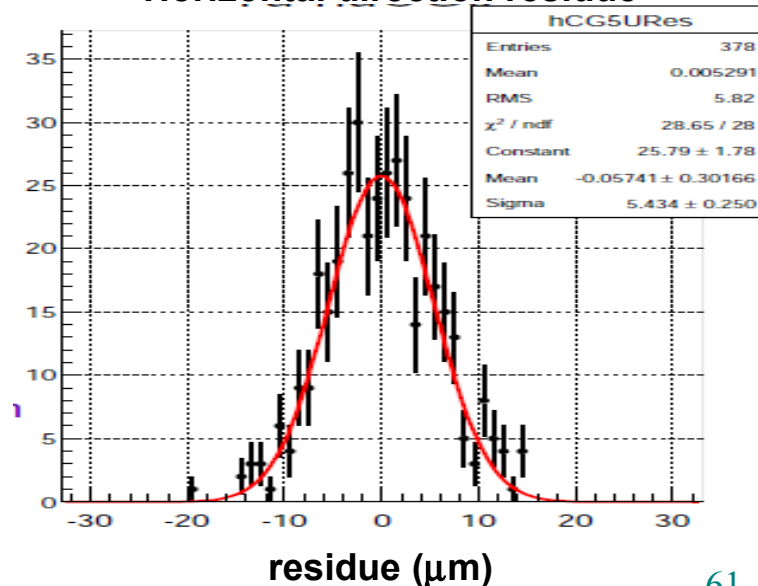
■ MIMOSA-34: 22x33 μm^2 pixels @ $T = 30^\circ\text{C}$

- **Sensing node impact (HR18)**
- Sub-arrays: P-29 10.9/10.9 μm^2 diode/footprint
P-20 8.0/10.9 μm^2 diode/footprint
- 8 μm^2 diode features $\sim 20\%$ higher SNR (MPV)
 \Rightarrow slightly higher ϵ_{det} (both $> 99\%$)
- $Q_{\text{clus}} \sim 1350/1500 e^-$ for 8/10.9 μm^2 diode
 \Rightarrow marginal charge loss
- Binary residue: 5-5.5 $\mu\text{m} \Rightarrow \sigma_{\text{sp}} < 5 \mu\text{m}$

Seed pixel SNR distribution



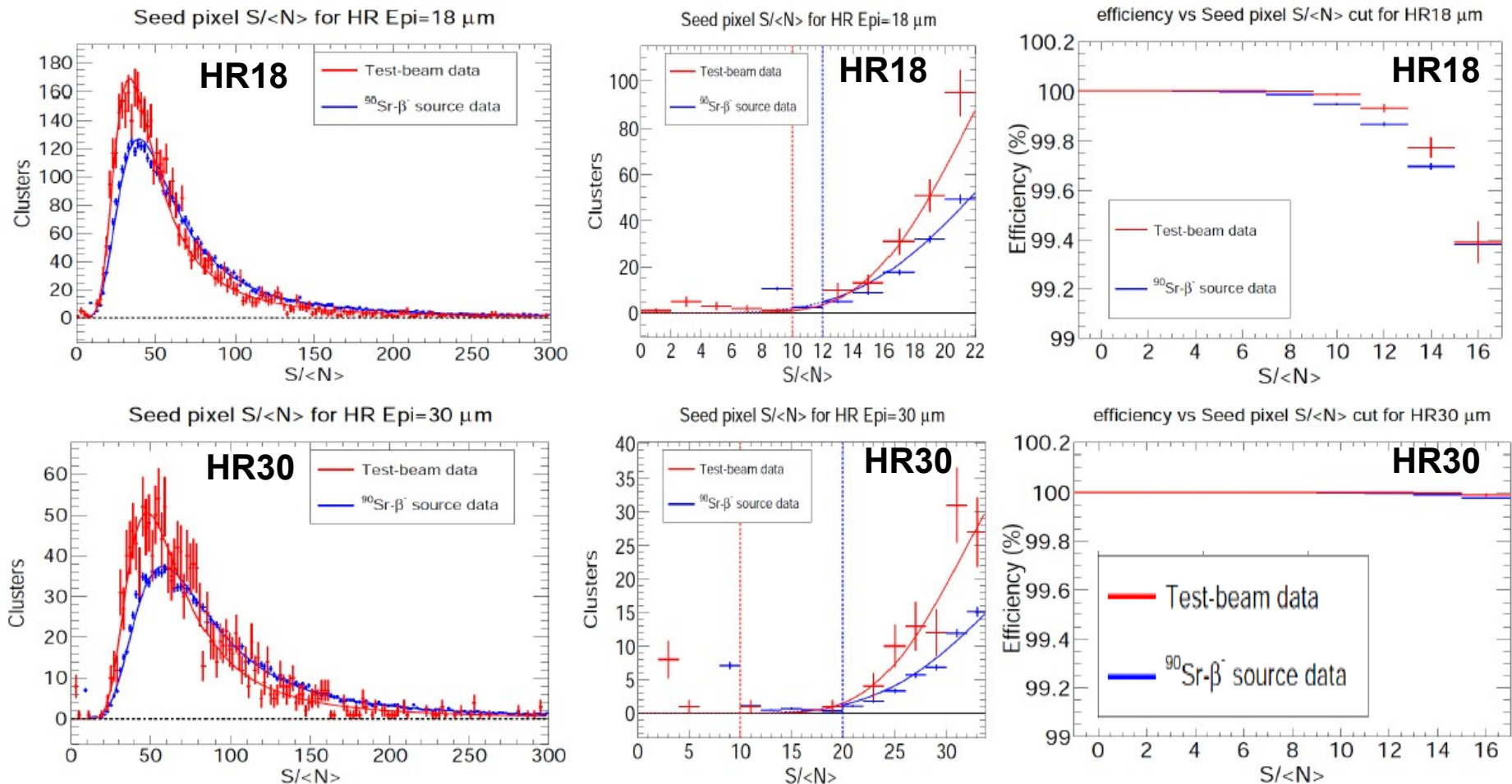
Horizontal direction residue



β^- (^{90}Sr) source vs 4.4 GeV e^- (DESY)

MIMOSA-34:

- β^- (^{90}Sr) vs 4.4 GeV e^- for $22 \times 66 \mu\text{m}^2$ pixels: SNR & ε_{det} for HR18/HR30
- Conclusion:** lab test with β^- (^{90}Sr) source allow estimating ε_{det}

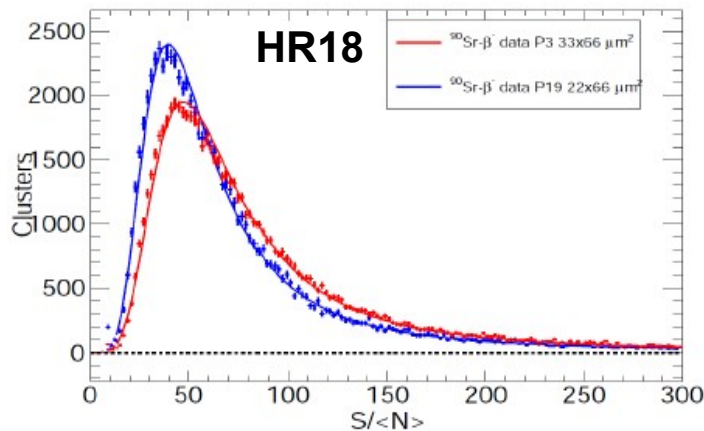


From 22x66 to 33x66 μm^2 pixels

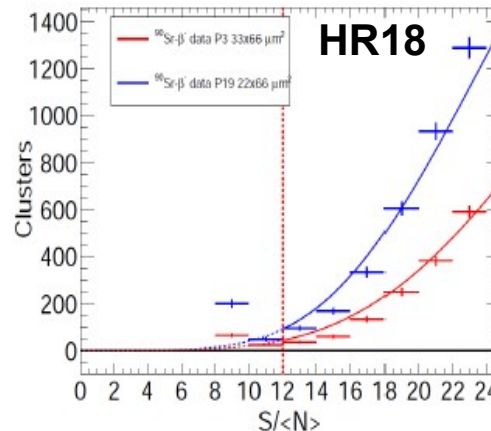
MIMOSA-34:

- 22x66 vs 33x66 μm^2 pixels: SNR & ϵ_{det} with β^- (^{90}Sr) for HR18/HR30
- Comment:** 33x66 μm^2 (8/15 μm^2 diode/footprint) pixels exhibit high SNR \Rightarrow high ϵ_{det}

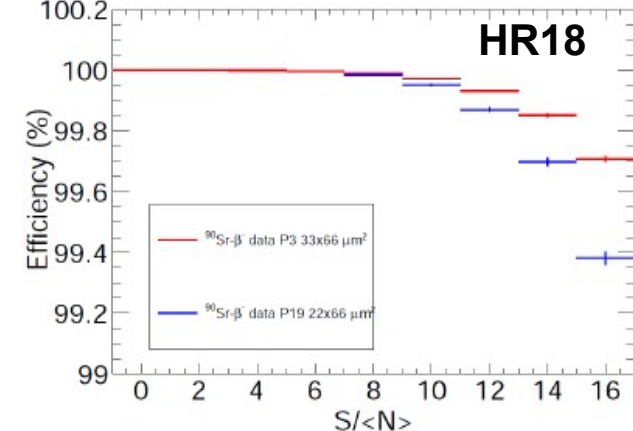
Seed pixel $S/\langle N \rangle$ for HR Epi=18 μm



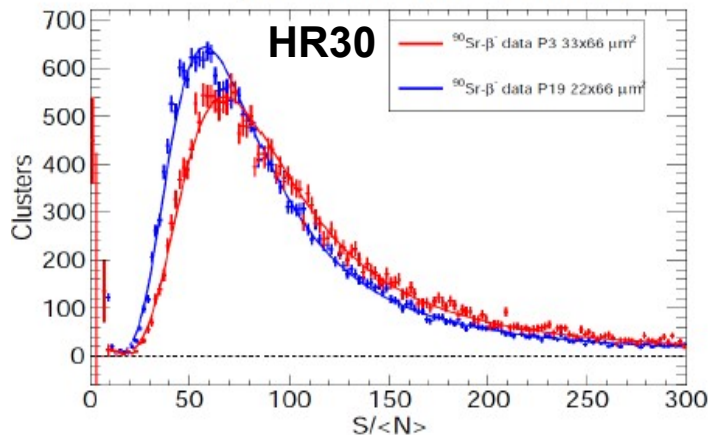
Seed pixel $S/\langle N \rangle$ for HR Epi=18 μm



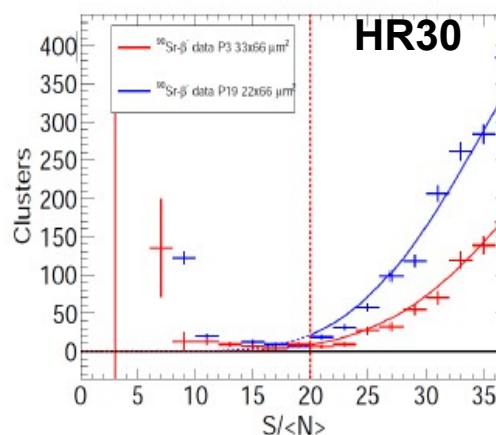
efficiency vs Seed pixel $S/\langle N \rangle$ cut for HR18 μm



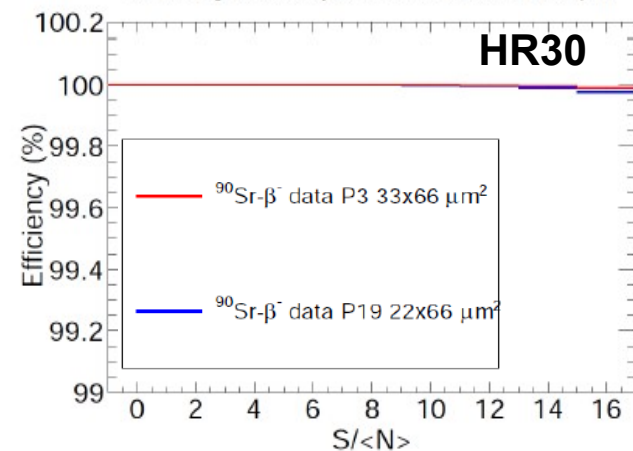
Seed pixel $S/\langle N \rangle$ for HR Epi=30 μm



Seed pixel $S/\langle N \rangle$ for HR Epi=30 μm



efficiency vs Seed pixel $S/\langle N \rangle$ cut for HR30 μm

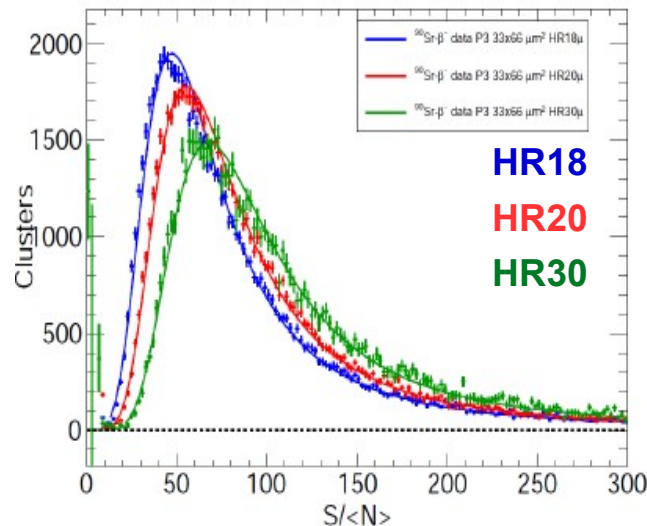


33x66 μm^2 pixels vs epitaxial-layer

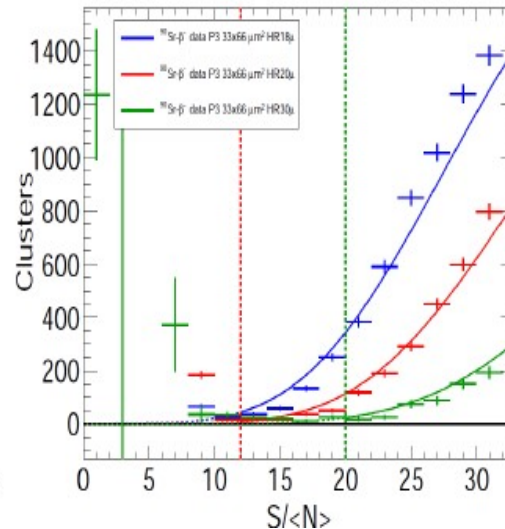
MIMOSA-34:

- 33x66 μm^2 pixels (8/15 μm^2 diode/footprint): SNR & ϵ_{det} with β^- (^{90}Sr) for HR 18,20,30
- Comments:**
 - Single 8/15 μm^2 diode/footprint provides high SNR despite large pixel (low sensing node density)
 - HR30 epi-layers gives high SNR (MPV ~ 70) from β^- (^{90}Sr)
 \Rightarrow pretty high ϵ_{det} for high SNR cut (e.g. 10)
 - Expected spatial resolution for 33x66 μm^2 pixels: $\sigma_{\text{sp}} \approx 10\mu\text{m}$

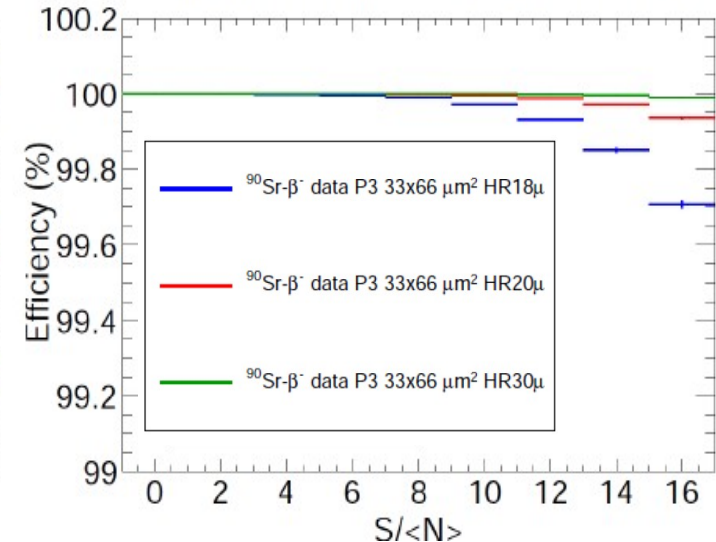
Seed pixel S/<N> for different HR Epi-layers



Seed pixel S/<N> for different HR Epi-layers



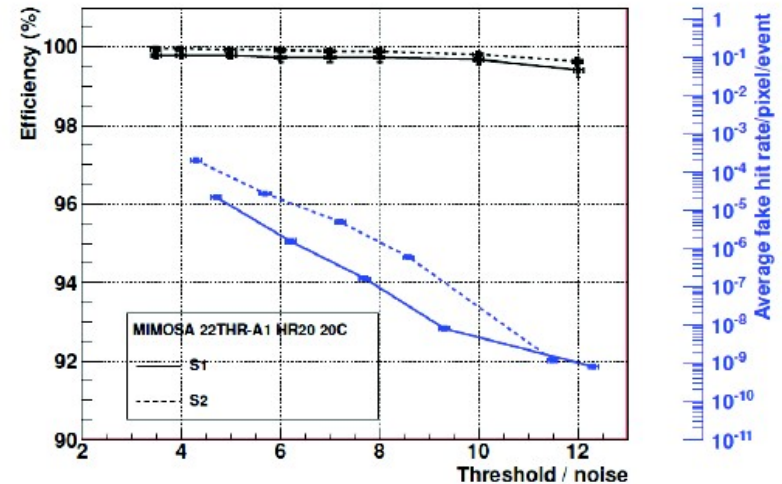
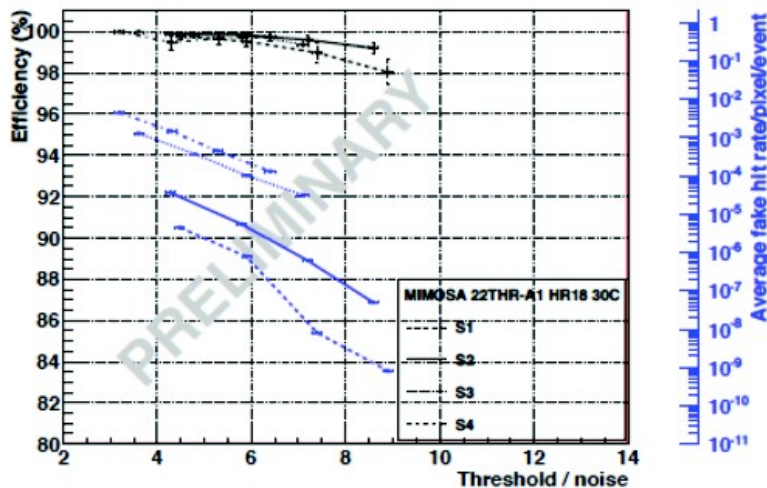
efficiency vs Seed pixel S/<N> cut for HR18 μm





Det. Efficiency & Fake rate

- Measured from 128 columns ended with discriminators: MIMOSA-22THRa1

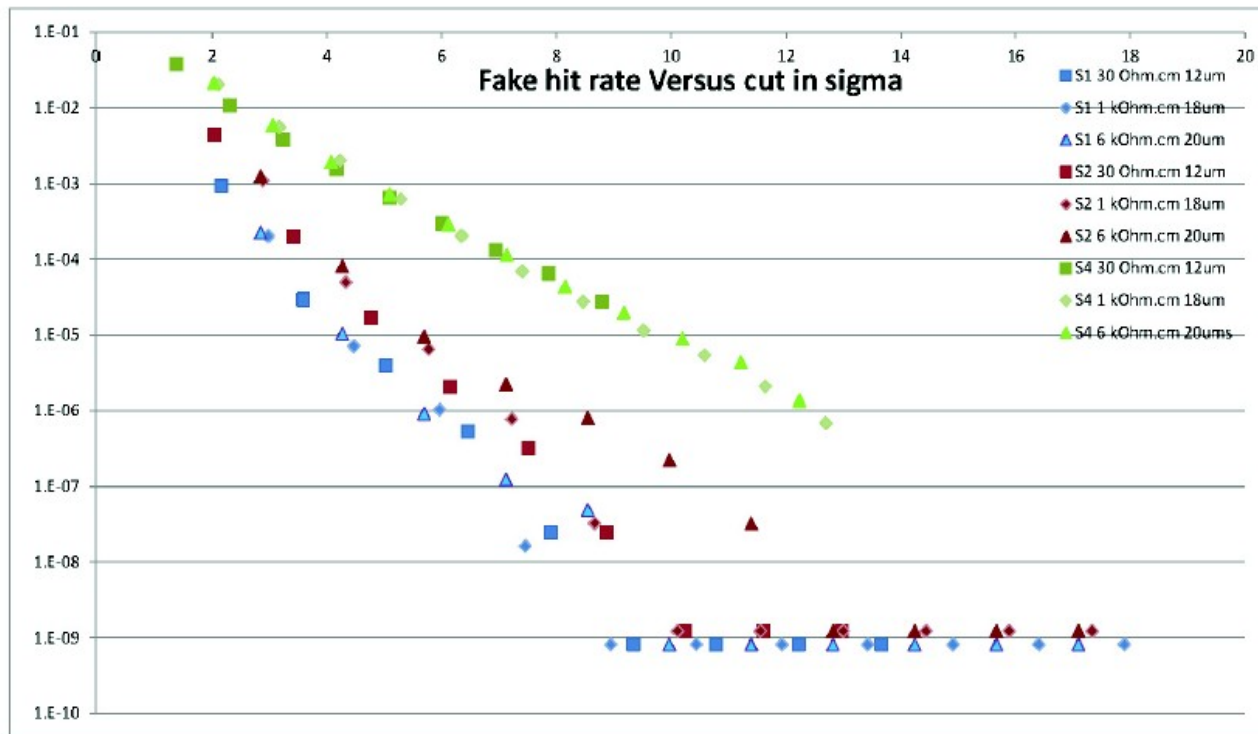


- For threshold within 5 to >10 times the <noise>
 - Efficiency > 99.5 %
 - Fake hit rate $\lesssim O(10^{-5})$

- S1 = T gate: $2 \times 0.36 \mu\text{m}^2$
- S2 = T gate: $1 \times 0.36 \mu\text{m}^2$
- S3 = T gate: $1 \times 0.18 \mu\text{m}^2$ (small diode)
- S4 = T gate: $1 \times 0.18 \mu\text{m}^2$



MISTRAL-like: fake rate



Input transistor gate

- S1 = $2 \times 0.36 \mu\text{m}^2$
- S2 = $1 \times 0.36 \mu\text{m}^2$
- S3 = $1 \times 0.18 \mu\text{m}^2$ (small diode)
- S4 = $1 \times 0.18 \mu\text{m}^2$

Enlarged input transistor gate:

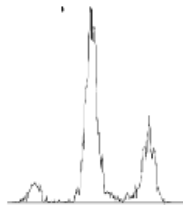
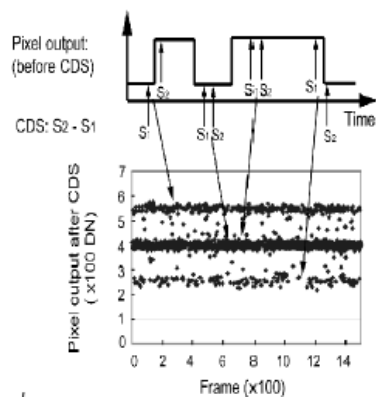
➔ Effective mitigation of fake rate due to noisy pixels

- STEPS VALIDATED IN 2012 :

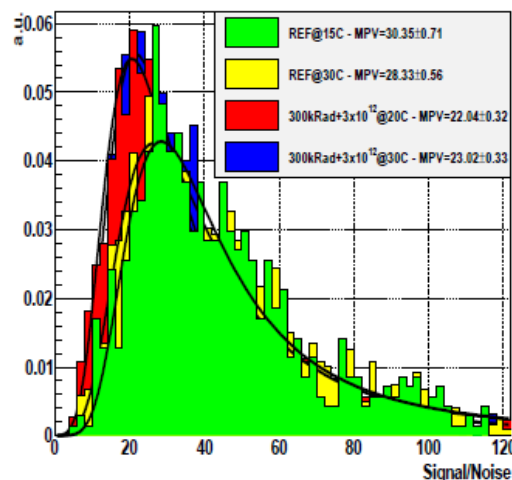
- ✳ Several in-pixel amplifier variants lead to satisfactory SNR & det. eff. ($20 \times 20 \mu m^2$) incl. after 1 Mrad & $10^{13} n_{eq}/cm^2$ at $30^\circ C$
- ✳ Results pres. at VCI-2013 (J. Baudot)

- CALL FOR IMPROVEMENT :

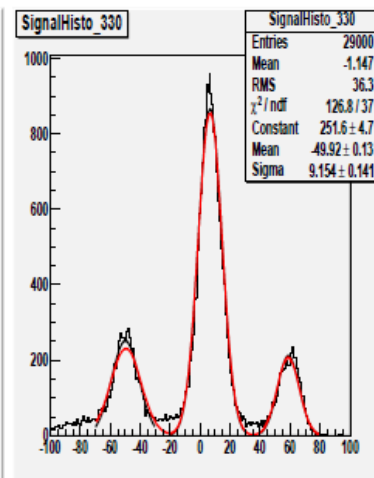
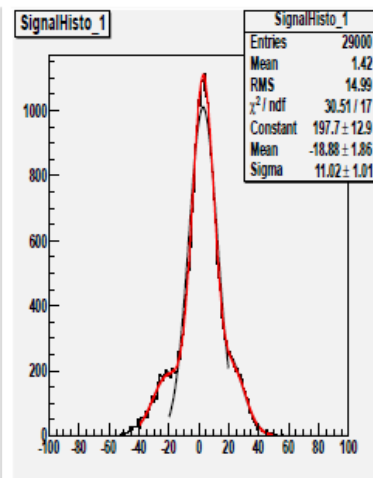
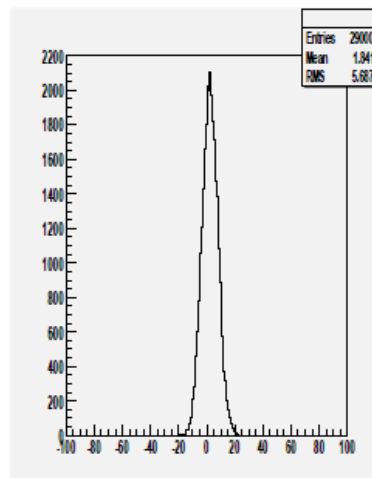
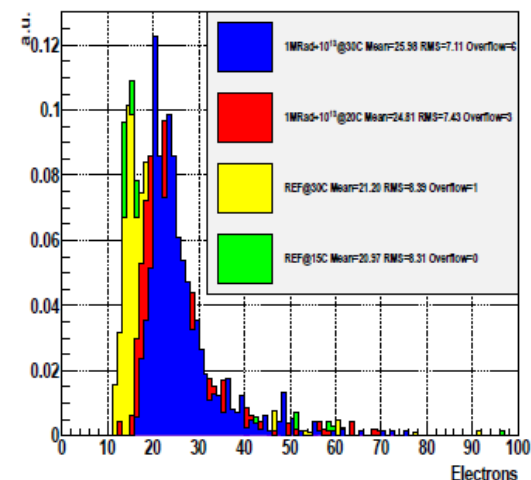
- ✳ Pixel circuitry noise :
tail due few noisy pixels
→ attributed to RTS noise
⇒ required optimising T geometries



Signal/Noise ratio for P25

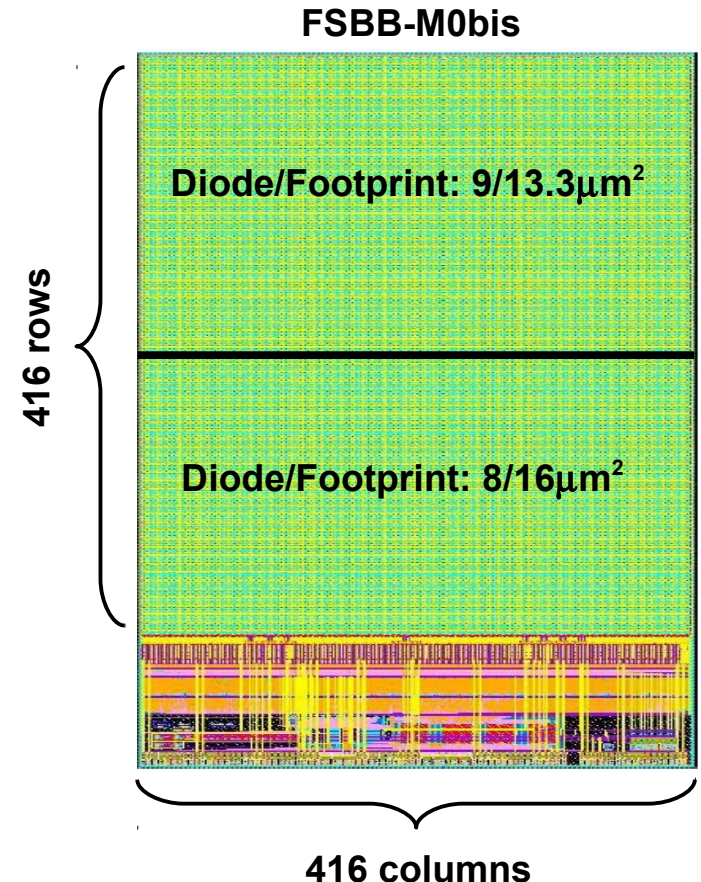


Noise for P25



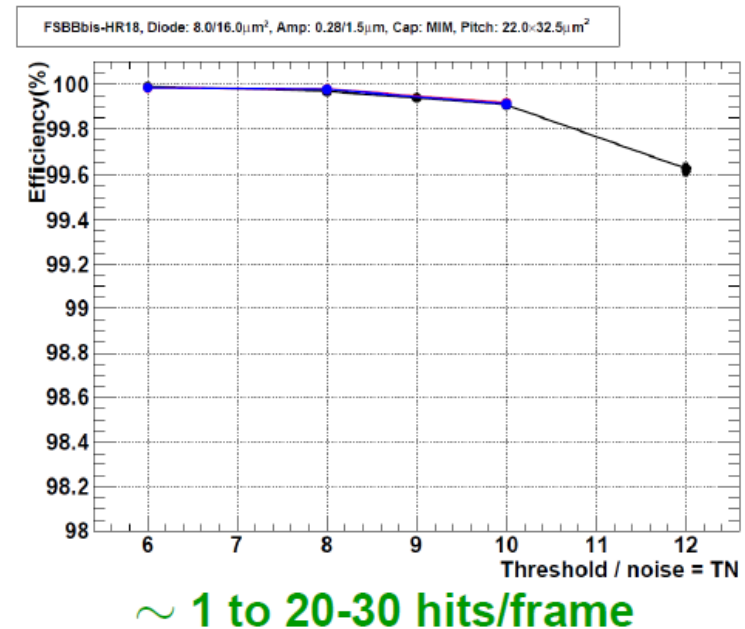
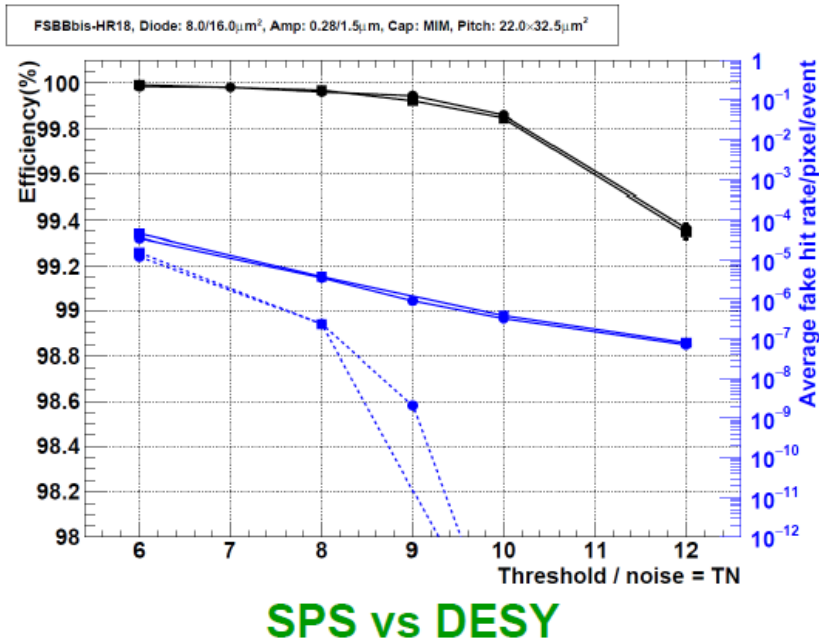
FSBB-M0bis main features

- TJsc-0.18 CIS process, HR ($\sim 1\text{--}2\text{k}\Omega\text{cm}$) 18/25/30 μm epitaxy, thinned to 50 μm
- Staggered pixel: 22x32.5 μm^2 including pre-amplification and clamping with 6 metal layers (ML)
- **416x416 = 173k** of col. x row of pixels ended by discriminator (8-cols with analogue output)
- Double-row readout at 160MHz clock frequency \Rightarrow **40 μs integration time**
- **On-chip 3-stage sparsification: SUZE-02** (different from MISTRAL-0, SUZE-03)
- 4 Memories of 512x32 bits
- 2 output nodes at 320Mbits/s (used only one for TB)
- Integrated JTAG and regulators
- Sensitive area is 13.7 x 9.0 mm $\sim 1.2\text{cm}^2$
- **Improvements w.r.t FSBB-M0 \Rightarrow shortcomings solved**
 - Mitigation of cross coupling effects
 \Rightarrow **now capable of operating full matrix**
 - Bit transmission: bit inversion at discriminator output
- **Two sensing node variations in same chip**
 - (NMOS T_{input} Pre-Amp W/L = 1.5/0.28 μm)
 - Diode/Footprint: 8/16 μm^2
 - Diode/Footprint: 9/13.3 μm^2



Main FSBB-M0 Detection Performances (2/3)

- Study of detection efficiency stability :
 - * Difference between SPS (120 GeV pions) & DESY (4.5 GeV electrons)
 - * Effect of occupancy : from ~ 1 hit/frame to ~ 25 hits/frame



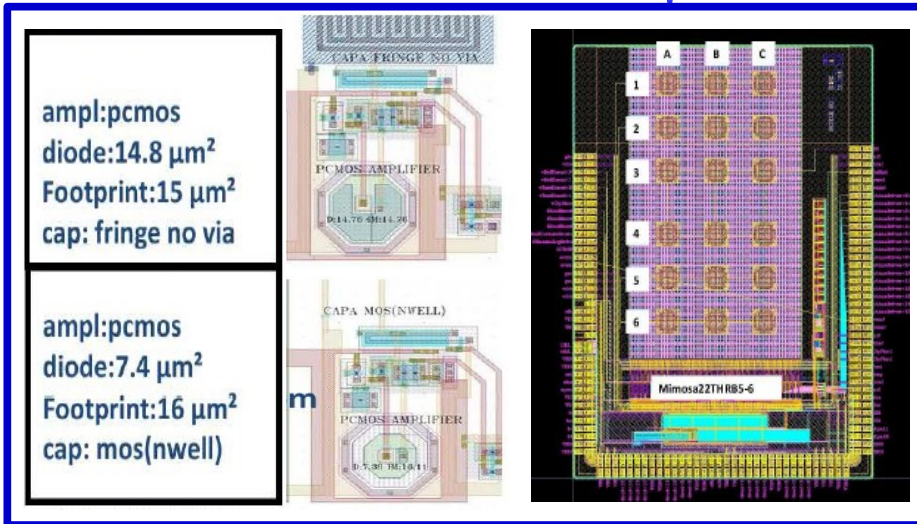
\Rightarrow No variation observed

MIMOSA-22THRb6/7: characteristics

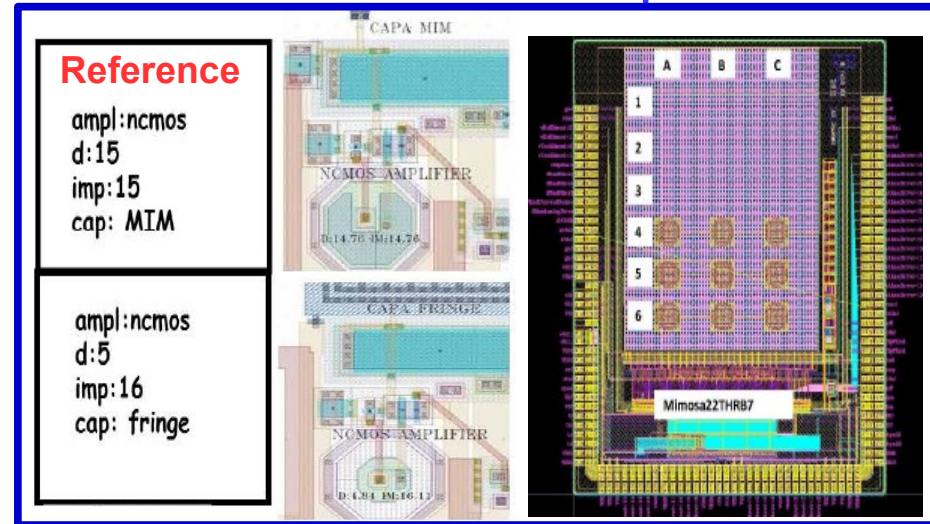
Design features

- 64x64 pixel array (staggered): 56 columns ended with discri. and 8 with analog output
- Readout $\approx 5\mu\text{s}$ (100MHz clock)
- Epitaxial layer: HR18

Mi22-THRB6: $36 \times 62.5\mu\text{m}^2$



Mi22-THRB7: $39 \times 50.8\mu\text{m}^2$



Purpose of the chip

- Validate pads over pixels
- Validate in-pixel circuitry concentrated on $\approx 3\text{ML}$ \Rightarrow modified clamping capacitor
- Validate large pixel performances w.r.t. TDR requirements on layers 3 – 6

\Rightarrow **MISTRAL-O**

Reminder of lab results: Individual pixel response to ^{55}Fe X-rays

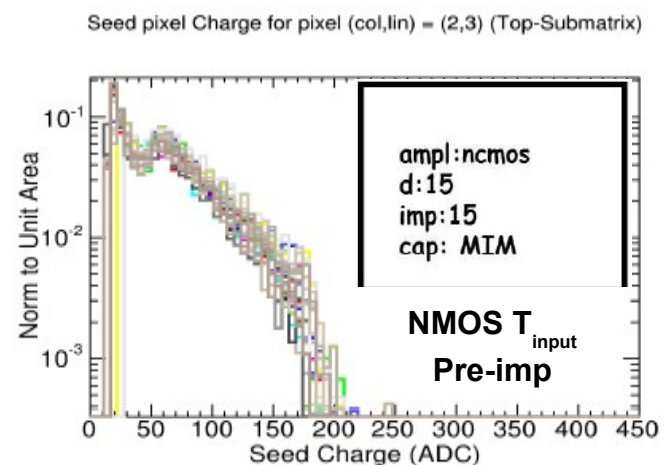
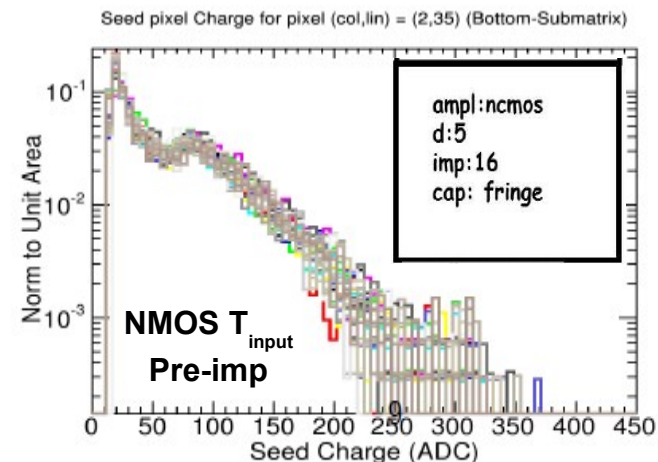
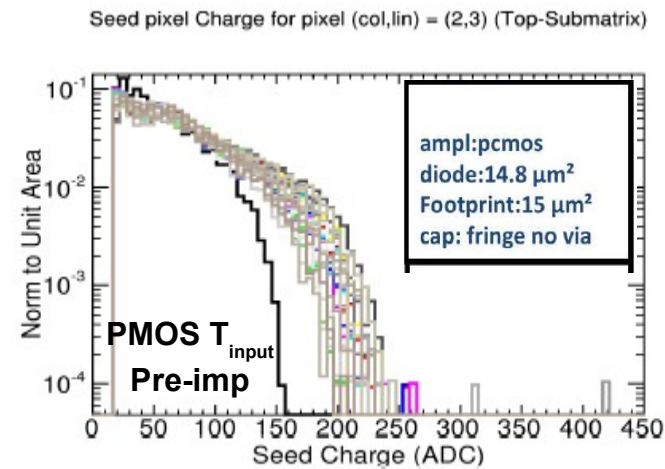
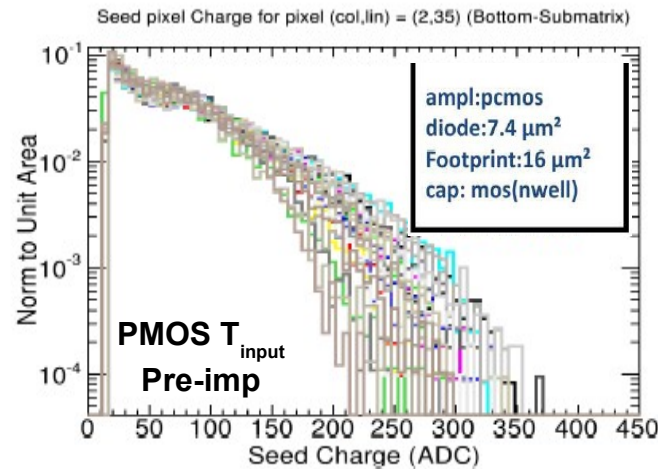
- Mi22THRb7 has a gain quite uniform
- Mi22THRb6 shows gain dispersion among pixels \Rightarrow were not sure about the effect on ε_{det}

- MIMOSA-22THRb6

analog outputs

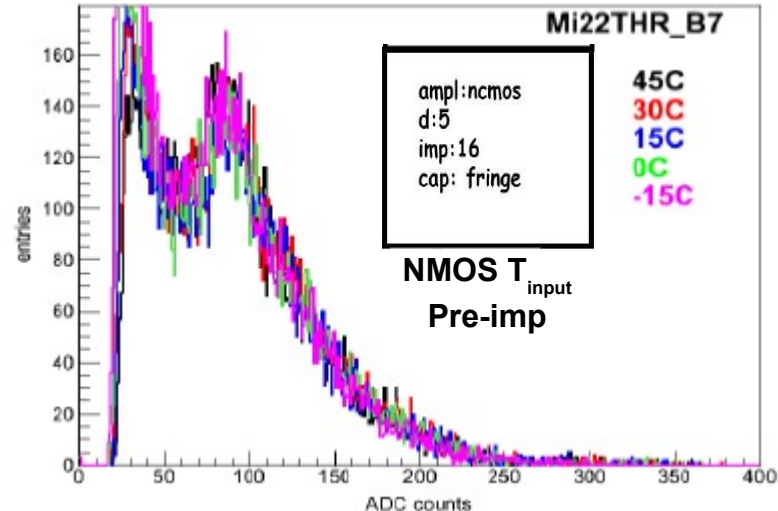
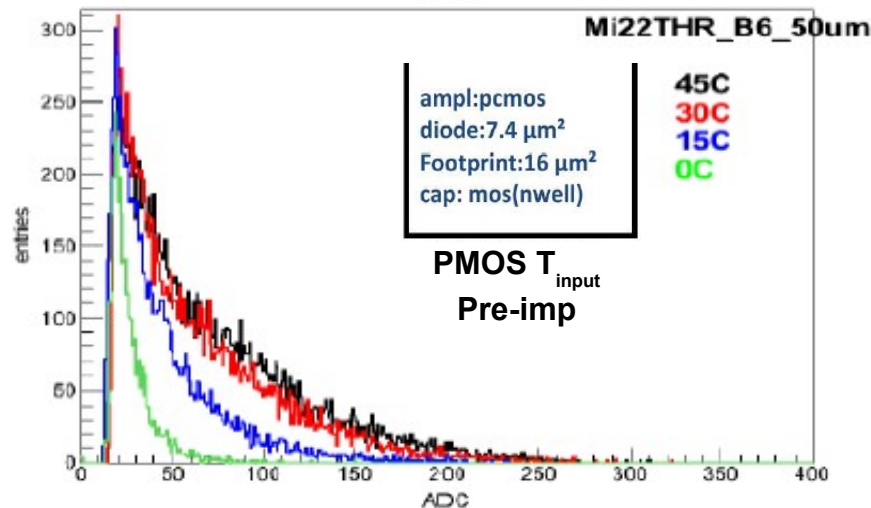
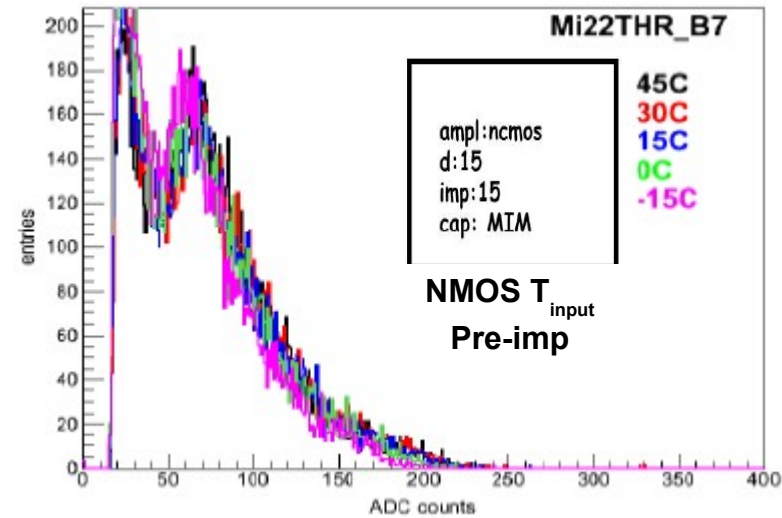
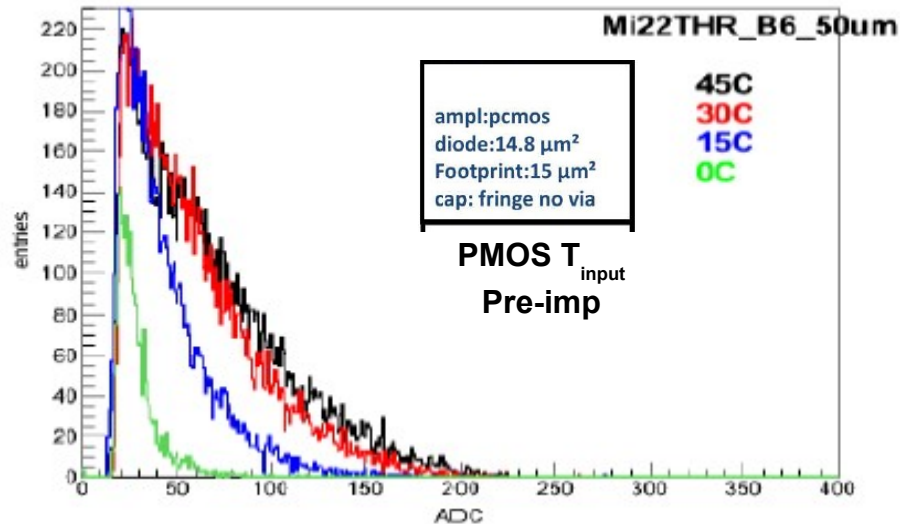
- MIMOSA-22THRb7

analog outputs



Reminder of lab results: Temp. dependence of pixels to ^{55}Fe X-rays

- Mi22THRb7 has quite stable response vs T
- Mi22THRb6 shows a significant dependence with T: $\nearrow T \Rightarrow \nearrow \text{gain}$



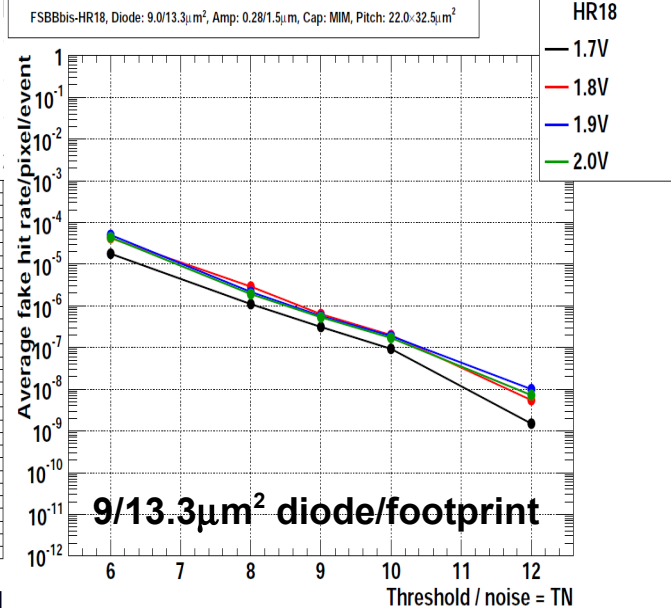
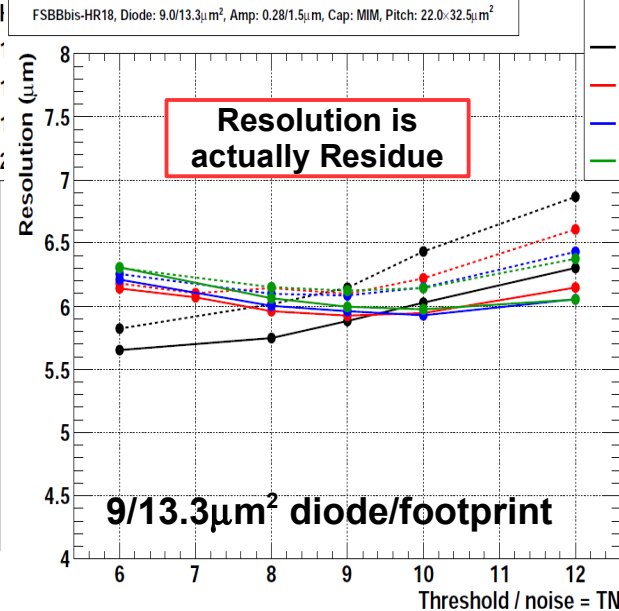
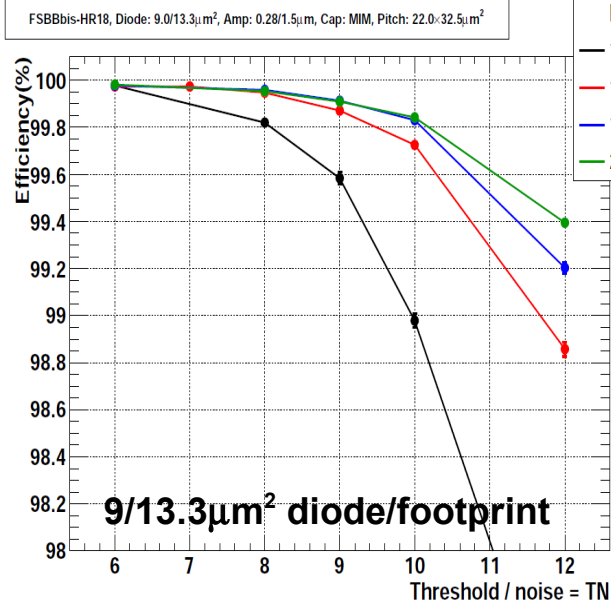
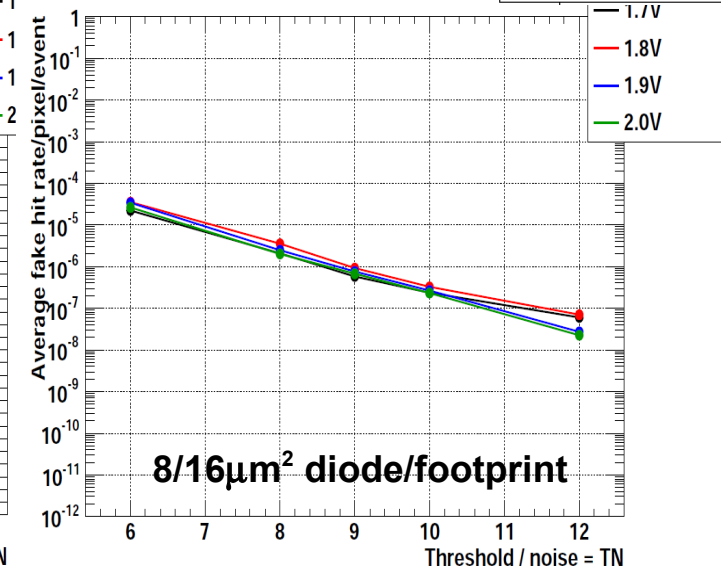
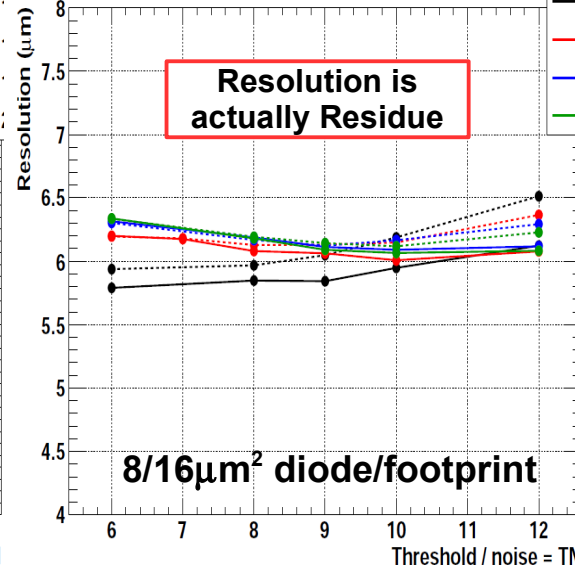
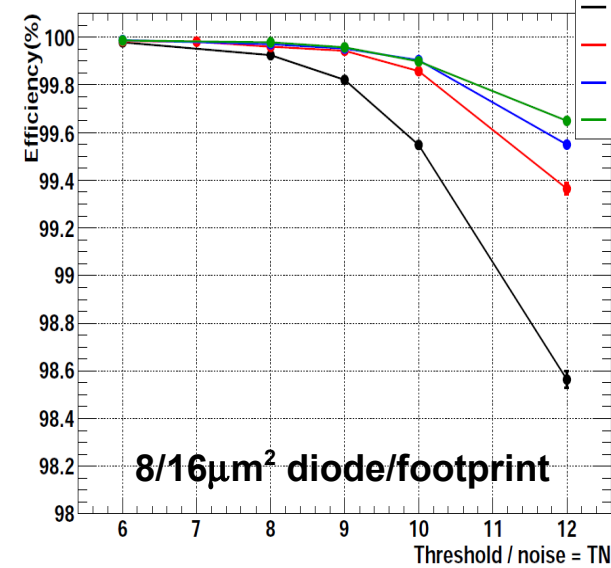
FSBB-M0bis-HR18: Robustness w.r.t VDD/VDA

HR18
— 1.7V
— 1.8V
— 1.9V
— 2.0V

FSBBbis-HR18, Diode: $8.0/16.0\mu\text{m}^2$, Amp: $0.28/1.5\mu\text{m}$, Cap: MIM, Pitch: $22.0\times 32.5\mu\text{m}^2$

FSBBbis-HR18, Diode: $8.0/16.0\mu\text{m}^2$, Amp: $0.28/1.5\mu\text{m}$, Cap: MIM, Pitch: $22.0\times 32.5\mu\text{m}^2$

FSBBbis-HR18, Diode: $8.0/16.0\mu\text{m}^2$, Amp: $0.28/1.5\mu\text{m}$, Cap: MIM, Pitch: $22.0\times 32.5\mu\text{m}^2$



Hot pixel masking effect on ϵ_{det} & σ_{sp} : Motivation

■ Reducing I_{pix}

- Increases ϵ_{det} \Rightarrow dramatical effect for highly irradiated sensors ☺
- Increases fake rate \Rightarrow factor of 10 increase for highly irradiated sensors ☹
- Masking procedure can be a good strategy for highly irradiated sensors
 \Rightarrow can reduce fake rate by $\sim 1 - 2$ orders of magnitude depending masking fraction

■ It is then important to study the effect of masking on ϵ_{det} & σ_{sp}

- Masking will cut away some single pixel clusters
- ϵ_{det} relative reduction should be prop. to (masking fraction) x (fraction mult. = 1 clusters)
 - Should be a marginal effect due to sizeable pixel cluster multiplicity of FSBB
 - $\Delta\epsilon_{\text{det}}$ vs (fraction mult. = 1 clusters) should be linearly related
- σ_{sp} should get marginally degraded due to loss of hit position information of masked pixels

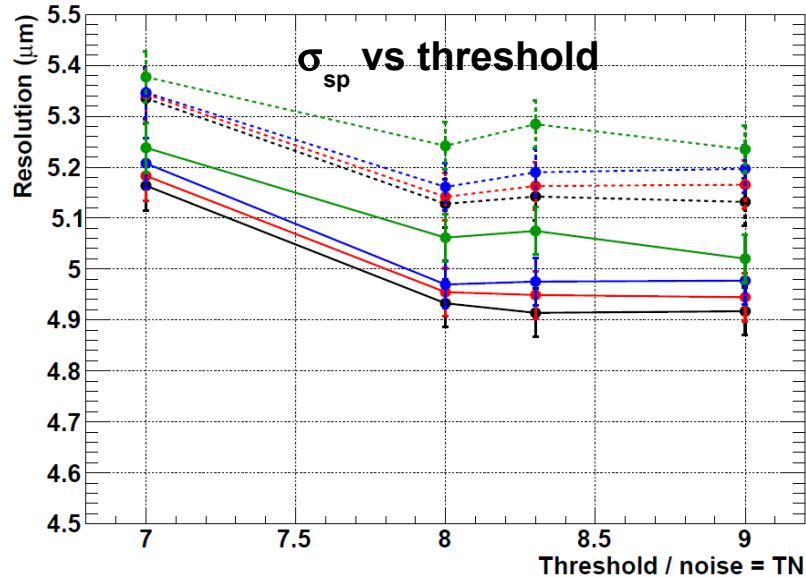
■ Tested the above hypothesis on different sensors and varied configurations

- Non-irradiated sensors @ nominal configuration
- Highly irradiated sensor ($1.6\text{MRad} + 10^{13}n_{\text{eq}}(\text{MeV})/\text{cm}^2$) for $I_{\text{pix}} = 30$ & 50 (nominal) μA

Hot pixel masking effect on ϵ_{det} & σ_{sp} : Results (I)

— Masking 0.00%
 — Masking 0.50%
 — Masking 1.00%
 — Masking 2.00%

FSBBbis-HR18, Diode: 8.0/16.0 μm^2 , Amp: 0.28/1.5 μm , Cap: MIM, Pitch: 22.0 \times 32.5 μm^2



Example:

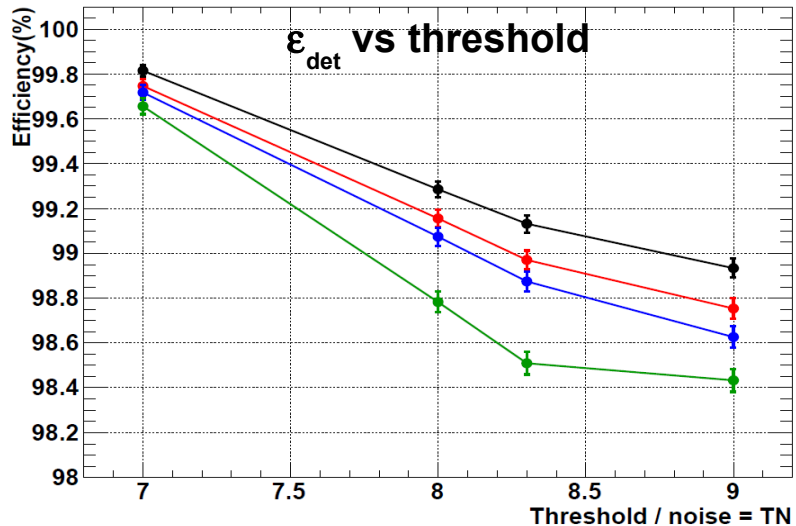
Irradiated sensor 1.6MRad + $10^{13} \text{n}_{\text{eq}}/\text{cm}^2$

Diode/Footprint: 8/16 μm^2

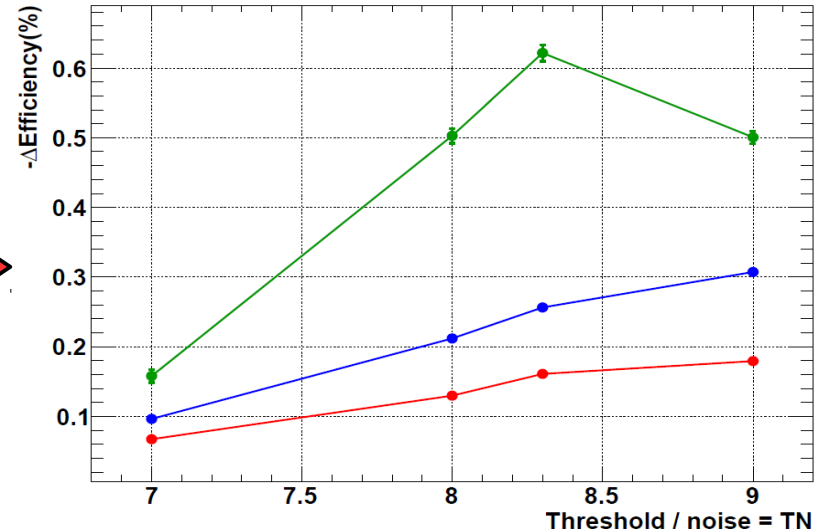
- Marginal increase of σ_{sp}
- Small reduction of ϵ_{det}

\Rightarrow quite smaller than masking fraction

FSBBbis-HR18, Diode: 8.0/16.0 μm^2 , Amp: 0.28/1.5 μm , Cap: MIM, Pitch: 22.0 \times 32.5 μm^2

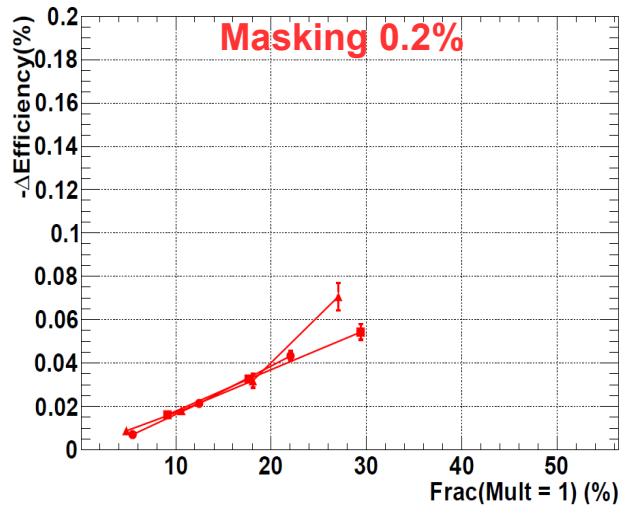


$-\Delta\epsilon_{\text{det}}$ (w.r.t 0% masking) vs threshold

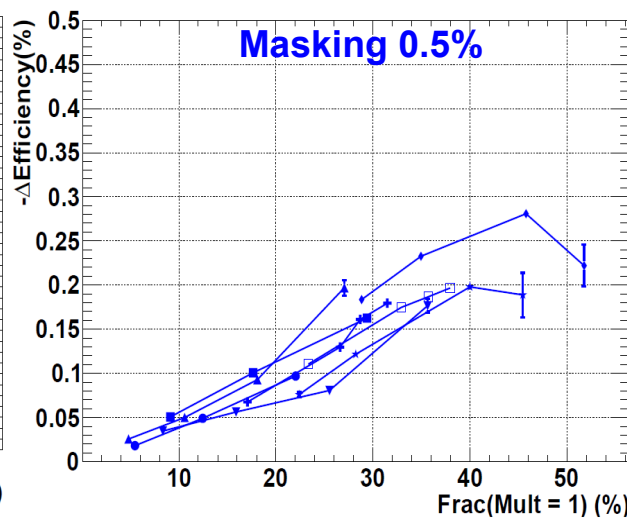


Hot pixel masking effect on ϵ_{det} & σ_{sp} : Results (II)

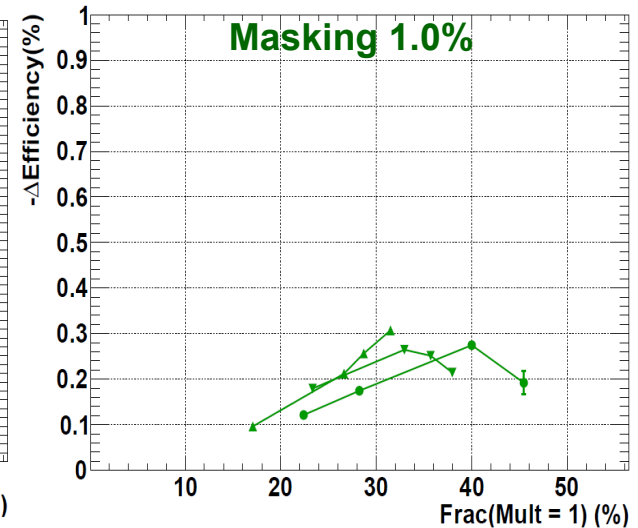
-ΔEfficiency vs Frac(Mult = 1) 0.2% Masking



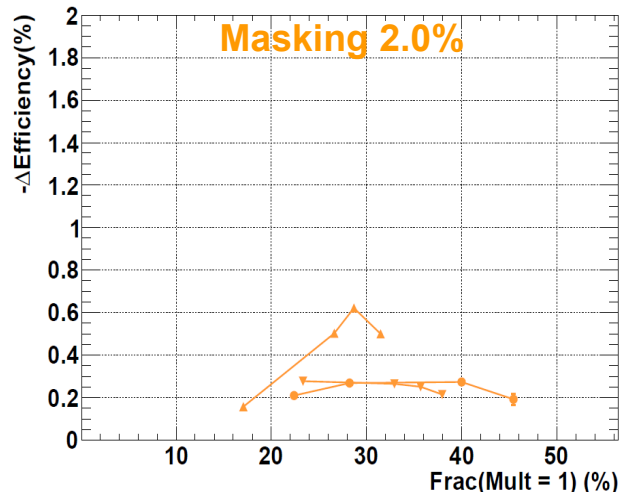
-ΔEfficiency vs Frac(Mult = 1) 0.5% Masking



-ΔEfficiency vs Frac(Mult = 1) 1.0% Masking



-ΔEfficiency vs Frac(Mult = 1) 2.0% Masking

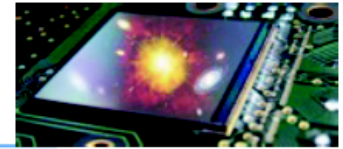


$-\Delta\epsilon_{\text{det}}$ vs fraction mult = 1 clusters (Frac(Mult = 1))

- Different markers in a plot correspond to the different sensors and configurations studied
- $-\Delta\epsilon_{\text{det}}$ values quite smaller than masking fraction in full Frac(Mult=1) (threshold)
- Nearly linear correlation between $-\Delta\epsilon_{\text{det}}$ & Frac(Mult=1)

⇒ Useful to predict efficiency reduction for a given masking fraction and threshold

Motivation for depleted CPS

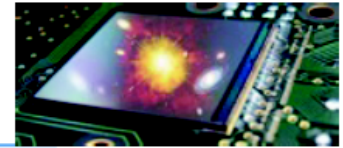


- High energy physics trend
 - Tolerate high non-ionizing part. Fluences $10^{15} n_{eq}/cm^2$ (tracker / vertex)
 - Integration time $\ll \mu s$
- X-rays detection
 - Require thickness (Beer-Lambert attenuation law)
 - Require equivalent collection properties all over epi-layer
- Fully depleting the sensitive layer is a key
 - However situation different / sensors for hybrid-systems (CERN-RD50)
 - ➔ Same substrate embed sensitive and first amplification layer



- Open questions
 - Which structure to enforce depletion?
 - Depth & uniformity on chip area
 - impact on in-pixel treatment μ -circuits?
 - Noise, transistor behavior

Way 1: High Voltage



■ Experiments

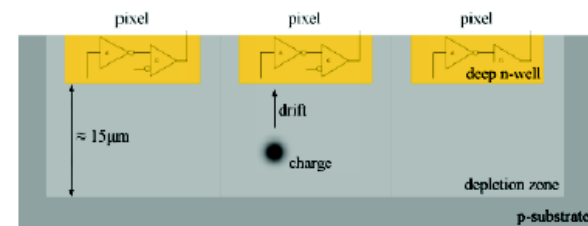
- ATLAS, $\mu 2e$, CLIC
- Groups in Bonn, CERN, Genève, Heidelberg, Karlsruhe, Marseille...
- new collab. → CERN-RD53

■ Concept

- Low resistivity (10-20 $\Omega \cdot \text{cm}$)
 ⇒ **High Voltage** applied few 10s V
- HV-compliant CMOS technologies

■ HV-CMOS

- Depleted depth demonstrated
 5 to 15 μm with 60-70V
- Fast amplification $\sim 1 \mu\text{s}$
- Only 30% signal loss after $10^{15} n_{\text{eq}}/\text{cm}^2$

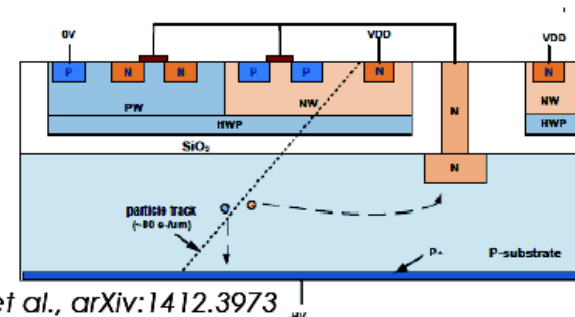


S.Feigl et al., PoS (TIPP2014) 280

■ HV-SOI

! Prototypes area 10 mm²

- Depleted depth demonstrated
 40-50 μm with 150-200 V
- Hint of tolerance beyond $10^{14} n_{\text{eq}}/\text{cm}^2$



T.Hemperek et al., arXiv:1412.3973

Way 2: High Resistivity



■ Experiments

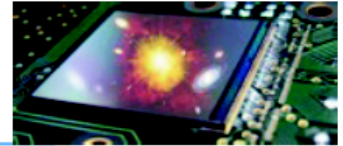
- ALICE, CBM
- soft X-rays detection
- Groups in Bonn, CERN, RAL, Strasbourg

■ Concept

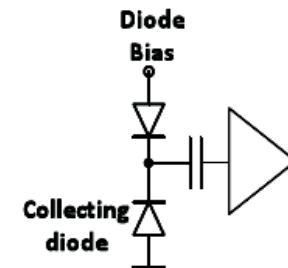
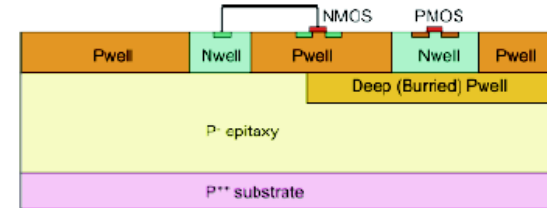
- High Resistivity thin epi-layer
➡ moderate voltage $\lesssim 10$ V

➡ See next slides for IPHC developments

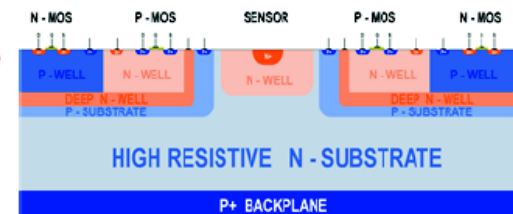
Depleted-CPS prototypes



- 2 Technologies explored
- Tower Jazz 0.18 μm \rightarrow Pegasus-1/2
 - Various sensitive layers
 - epi with $>1 \text{ k}\Omega \cdot \text{cm}$, 18, 30, 40 μm thick
 - Czochralski substrate-thick
 - Main architecture tested
 - Analogue readout with 10 μs integration time
 - Collection node AC-coupled to amplifier
 - Small matrix: 32 columns x 56 rows
 - Pixel size 25x25 μm^2



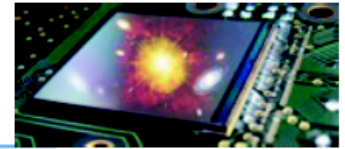
- EPC-ESPROSS 0.15 μm \rightarrow MIMOSA-33
 - high resistivity 50 μm thinned + passivated substrate
 - Main architecture tested
 - Analogue read-out with 11 μs integration time
 - Back-side biasing through IP structure
 - Small matrix: 8 columns x 44 rows
 - Pixel size 25x25 μm^2



M. Havranek et al., JINST 10 (2015) 02, P02013

Ready for back-side illumination !

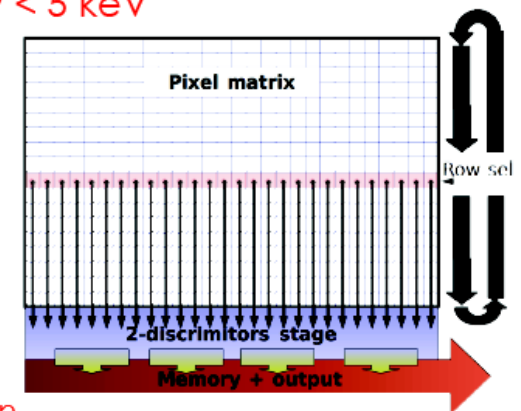
Ongoing prototypes design



- Submission to Tower-Jazz 0.18 μm technology (June 2015)

- MIMOSA - 22 SX

- Forerunner of sensors dedicated to X-rays with energy $< 5 \text{ keV}$
 - Pixel pitch $\leq 25 \times 25 \mu\text{m}^2$ and $\approx 10^4$ photons/pixel/sec
- Developed with the detector group of SOLEIL
- "Not so small" matrix: $5.6 \times 4.4 \text{ mm}^2$
- combine :
 - AC coupled collection diode from PEGASUS
 - read-out architecture developed for ALICE
- Binary output:
 - From 2 discriminators/column \rightarrow energy window selection
 - Photons detected individually \rightarrow counting & spatial resolution

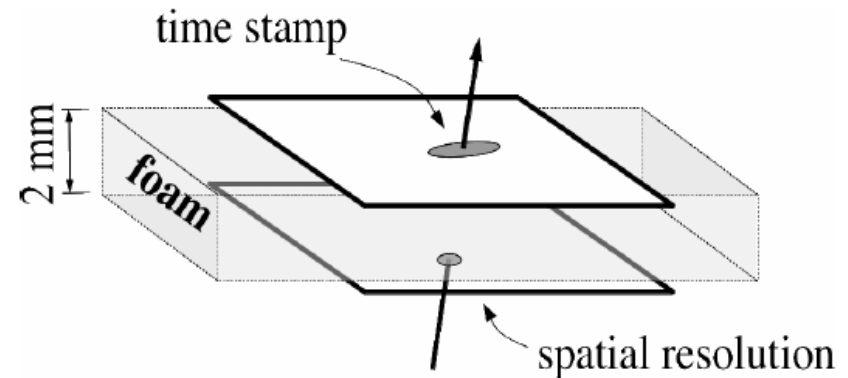


- Small analogue prototype

- Faster amplification \rightarrow target 10^6 photons/pixel/sec
- Mitigation of noise

ILD - VXD Concept Addressed

- Two types of CMOS Pixel Sensors :
 - Inner layers : Priority to read-out speed & spatial resolution
 - Outer layers : Priority to power consumption and good resolution
- Inner layers : $\sim 300 \text{ cm}^2$
 - L1 : small pixels with end-of-column binary charge encoding $\mapsto \lesssim 3 \mu\text{m}$
 - $\Rightarrow 20 \times 14 \mu\text{m}^2$ with 2-row read-out : $\lesssim 40 \mu\text{s}$
 - $\Rightarrow 17 \times 17 \mu\text{m}^2$ with 1-row read-out : $60 \mu\text{s}$
 - \hookrightarrow 2-row read-out : $30 \mu\text{s}$ (tbc)
 - L2 : elongated pixels with in-pixel binary charge encoding $\mapsto \sim 5 \mu\text{m}$
 - $\Rightarrow 22 \times 33 \mu\text{m}^2$ with 2-row read-out : $\sim 8 \mu\text{s}$
 - $\Rightarrow 22 \times 33 \mu\text{m}^2$ with 4-row (tbc) read-out : $\sim 4 \mu\text{s}$
- Outer layers : $\sim 3000 \text{ cm}^2$
 - L3-6 : large pixels with end-of-col 3-4 bit ADCs
 - $35 \times 35 \mu\text{m}^2$ pixels : $\lesssim 4 \mu\text{m}$ & $120 \mu\text{s}$
 - $25 \times 50 \mu\text{m}^2$ pixels : $\lesssim 4 \mu\text{m}$ & $80 \mu\text{s}$



Processes Suited to the R&D

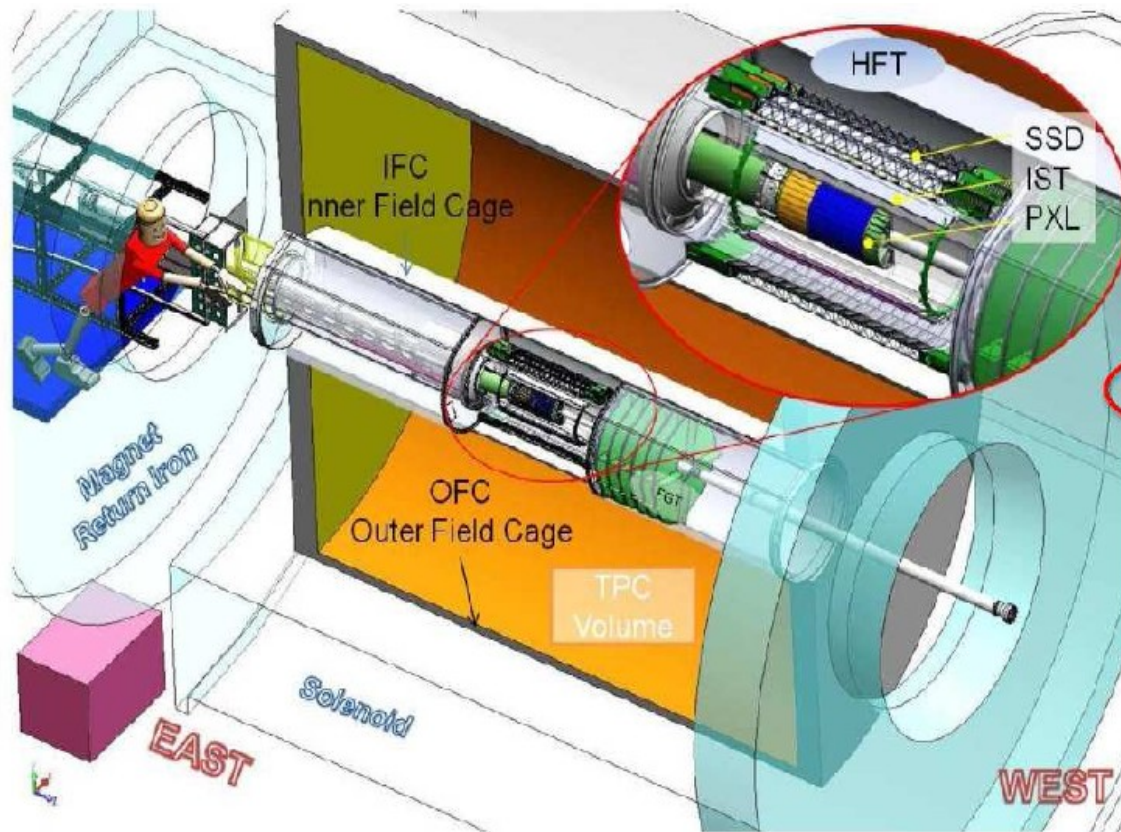
- SPECIFIC ASPECTS OF TOWER 0.18 μm CIS PROCESS : **established contact**
 - access to various starting materials (incl. in MPW)
 - designing details well known by the designers and testing crews
- COMPARISON TO L-FOUNDRY (INFO. TBC) : **used by HL-LHC R&D groups**

Process	Feature Size	Supply Voltage	Number of ML	Type	Comments
Tower-SC	180 nm	1.8 V (3.3 V)	6	4-well	
L-Foundry	150 nm	1.8 V (3.3 V)	8	4-well	110 nm : 1.2 V

Process	min. area	MPW runs cost	duration	MLM runs area	cost
Tower-SC	5x5 mm ²	37,500 USD	\gtrsim 4.5 months	none	
L-Foundry	???	???	???	11x11 mm ²	60-80 kE

Process	thickness	Starting Material resistivity	source	availability	Comments
Tower-SC	18-40 μm or more	$\sim 1 - 10 \text{ k}\Omega \cdot cm$	internal & external	MPW, ER	
L-Foundry	??	High-Res	internal only ?	MLM, ER	

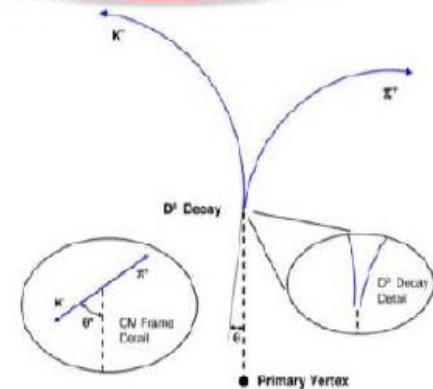
PXL in STAR Inner Detector Upgrades



TPC – Time Projection Chamber
(main tracking detector in STAR)

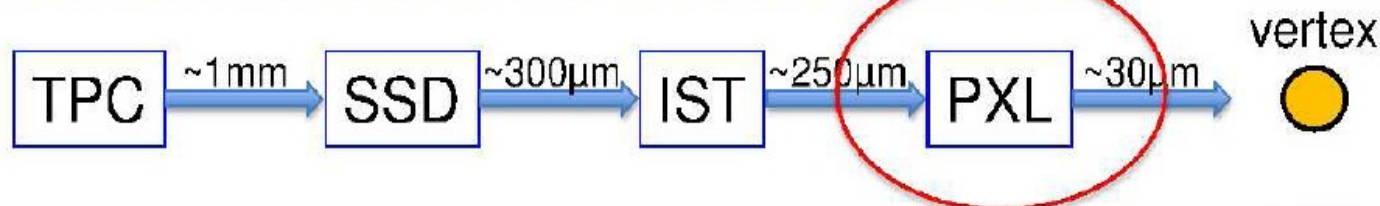
HFT – Heavy Flavor Tracker

- SSD – Silicon Strip Detector
 - $r = 22 \text{ cm}$
- IST – Inner Silicon Tracker
 - $r = 14 \text{ cm}$
- PXL – Pixel Detector
 - $r = 2.8, 8 \text{ cm}$



Direct topological reconstruction of
Charm – displaced vertices

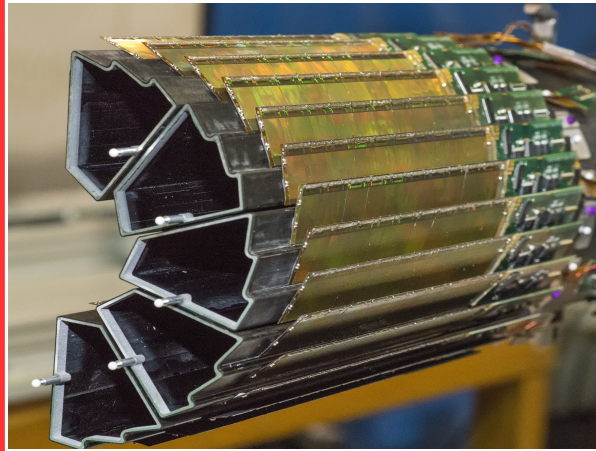
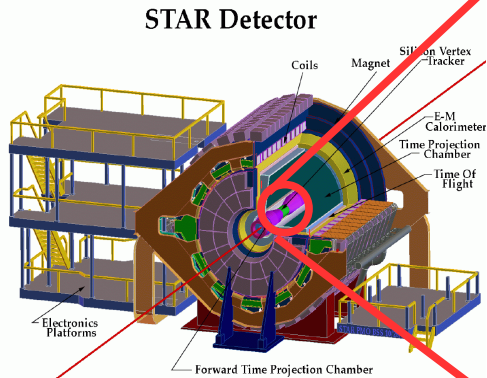
We track inward from the TPC with graded resolution:



L. Greiner
(CPIX-14)

CPS State-of-the-Art in operation: STAR-PXL detector

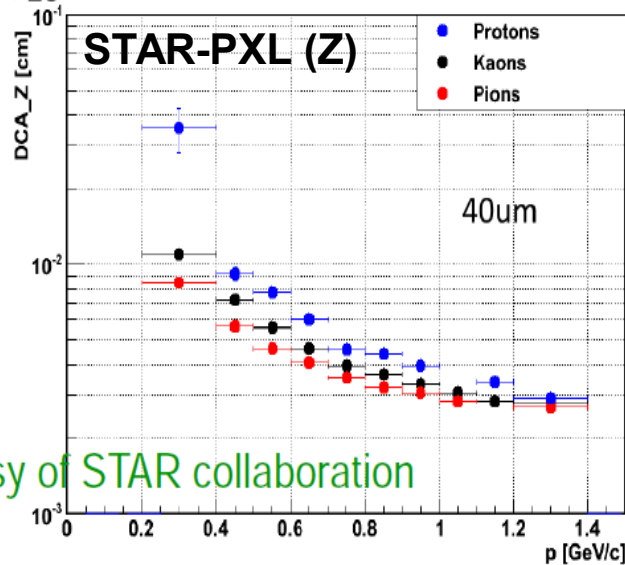
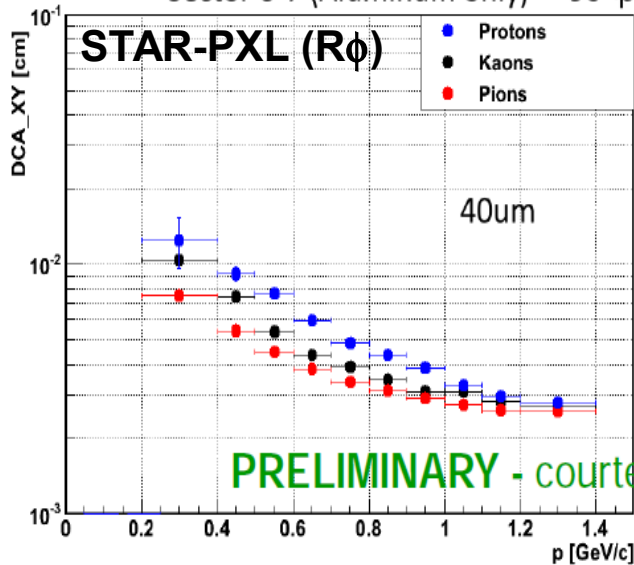
STAR-PXL @ RHIC: 1st CPS @ collider experiment !



STAR-PXL HALF-BARREL

- 2 layers @ $r = 2.8, 8$ cm
- 20 ladders (10 sensors) ($0.37\% X_0$)
 - 200 sensors $\Rightarrow 180 \times 10^6$ pixels
- Air flow cooling: $T < 35^\circ\text{C}$

Sector 6-7 (Aluminum only) $-90 < \phi < -20$

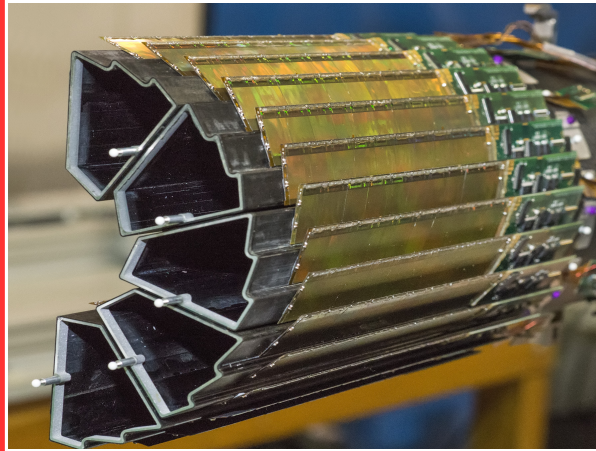
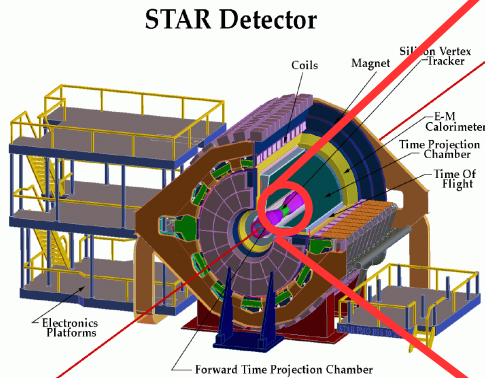


Several Physics-runs

- 1st run Mar-Jun 2014
- 2nd run Jan-Jun 2015
- Measured $\sigma_{ip}(p_T)$ matching requirements ($\sim 40 \mu\text{m}$ @ 600 MeV/c for π^\pm/K^\pm)
- Getting prepared for 3rd run (Jan. 2016)

CPS State-of-the-Art in operation: STAR-PXL detector

STAR-PXL @ RHIC: 1st CPS @ a collider experiment !



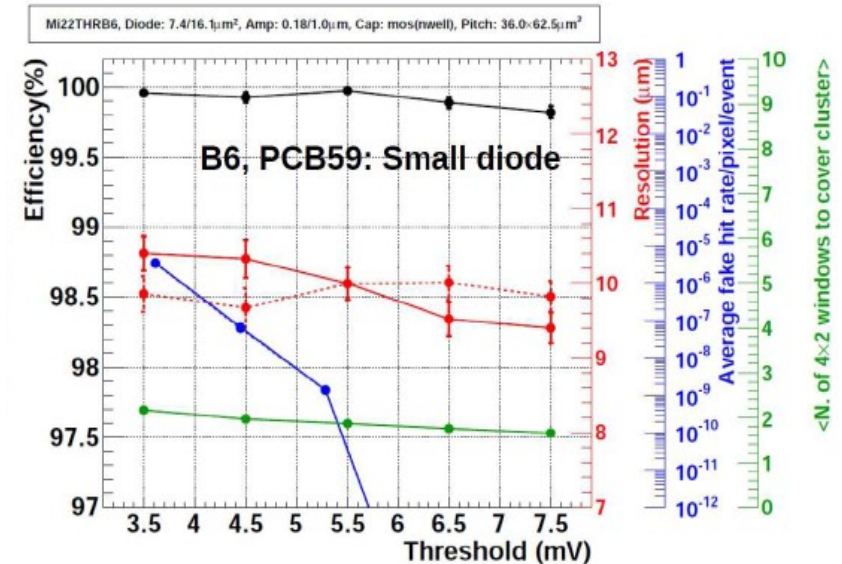
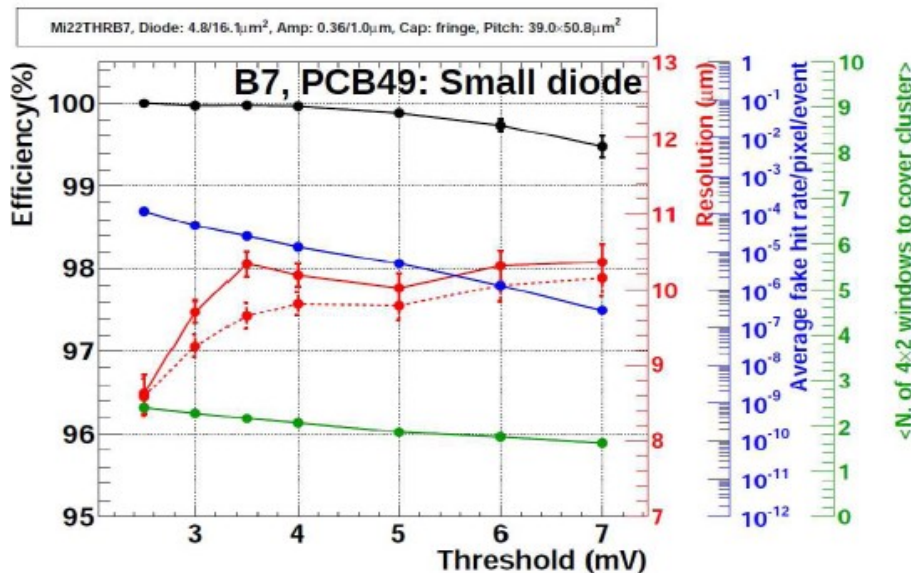
STAR-PXL HALF-BARREL

- 2 layers @ $r = 2.8, 8 \text{ cm}$
- 20 ladders (10 sensors) ($0.37\% X_0$)
⇒ 180M pixels
- Air flow cooling: $T < 35^\circ\text{C}$



Main MIMOSA-22THRb detection performances (1/2)

Pixel type	Pixel dim.	Diode/Footprint	Pre-Amp T.	Clamping capa.	Integ. time
MIMOSA-22THR b7	39 μm x 50.8 μm	5/16 μm^2	N-MOS	MOS (N-well)	5 μs
MIMOSA-22THR b6	36 μm x 62.5 μm	7/16 μm^2	P-MOS	fringe (metal layers)	5 μs

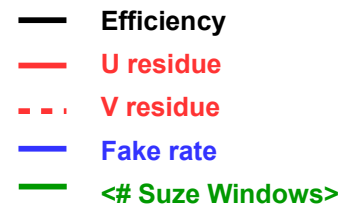


Excellent detection performances for both chip variations

- $\epsilon_{\text{det}} > 99\%$ & $\sigma_{\text{sp}} \sim 10 \mu\text{m}$ (as expected)

P-MOS vs N-MOS Pre-Amplify input transistor

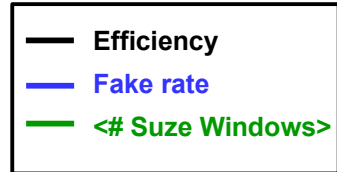
- P-MOS:** less RTS noise, higher gain and sensing node voltage
- N-MOS:** better pixel response uniformity, less T-dependency and maturity (STAR-PXL)



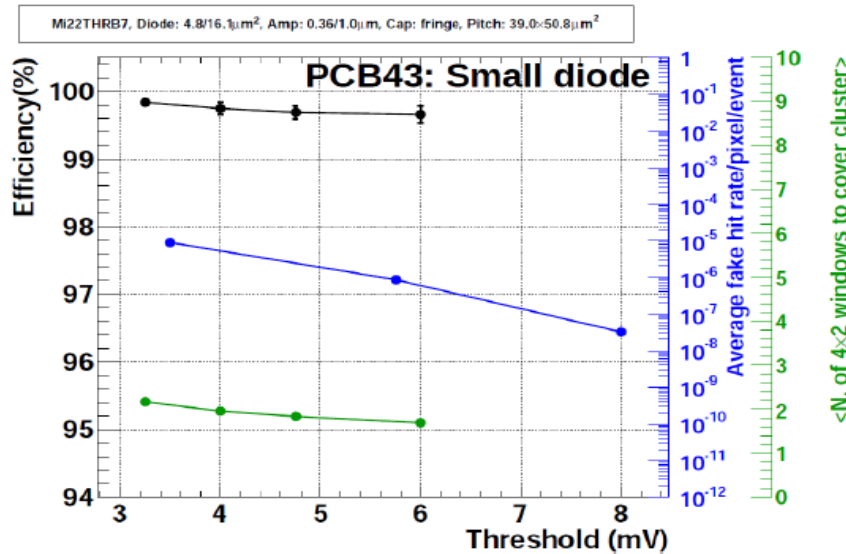
Main MIMOSA-22THRb detection performances (2/2)

Study of rad. tolerance @ $T \gtrsim 30^\circ\text{C}$: loads relevant to ALICE-ITS outer layers

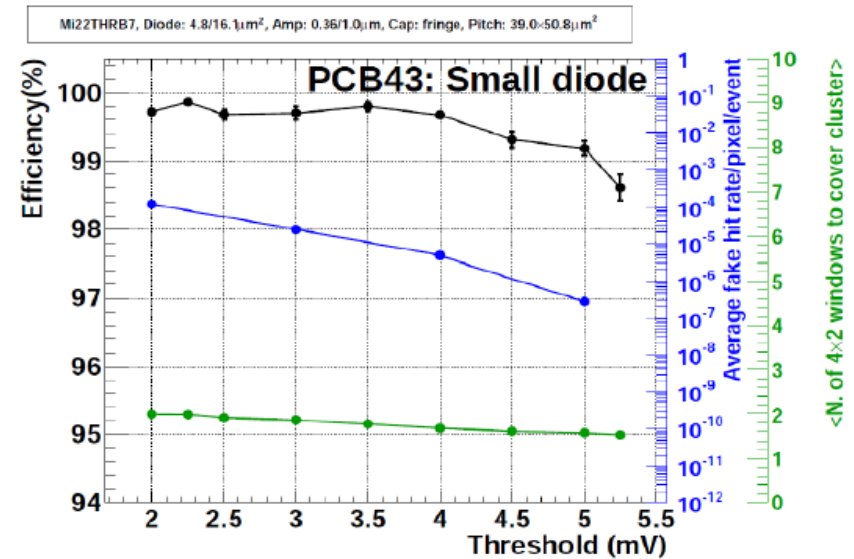
- Load:** up to 150 kRad $\oplus 1.5 \times 10^{12} n_{\text{eq}}/\text{cm}^2$



MIMOSA-22THRb7 (N-MOS Pre-Amp input transistor)



50 kRad $\oplus 5 \times 10^{11} n_{\text{eq}}/\text{cm}^2$



150 kRad $\oplus 1.5 \times 10^{12} n_{\text{eq}}/\text{cm}^2$

Good detection performances after irradiation

Validation of large pixel design for the outer layers of the ALICE-ITS!